Abstract

LEE, SEUNG GEOL. Assessment of Metrics in Color Spaces. (Under the supervision of Dr. Renzo Shamey)

The perceptibility and acceptability of small color differences ($\Delta E^* < 5$) were investigated using 66 textile-based color difference pairs around a CIE blue color center. Samples were polyester fabrics dyed with disperse dyes under well-controlled dyeing procedures and using precise recipe prediction methods. Each pair was assessed three times by 26 observers in three separate repetitions using gray scale and a total of 5148 assessments were obtained. A standard viewing booth was used with uniform gray surrounding corresponding to $L^*=74$. This resulted in minimizing the crispening effect due to the large lightness difference between the surround and the samples, all of which had an L^* value of approximately 35. A third-degree polynomial equation was used to convert gray scale ratings to visual differences (DV). SAS statistical analysis showed over-fitting of data when a fourth-degree polynomial equation is used at 95% confidence level. However, it was shown that a third-degree polynomial fitting was satisfactory. Third-degree polynomial fitting equations were obtained using CIELAB, CIE94(1:1:1), CMC(1:1), and CIEDE2000(1:1:1), respectively, and the results were found to be very similar for all equations. Inter and intra-group variability was assessed using paired t-test and PF/3, and the results indicated observer training through repeat assessments.

The performance of color difference formulae was evaluated using a correlation coefficient (r) and PF/3 at two lightness weights (K_L or *l*) of 1 and 2.

Correlation coefficients of 0.91, 0.92 were obtained for CIEDE2000 at K_L of 1 and 2, respectively indicating that CIEDE2000 gives the best performance amongst the color difference equations examined. Using PF/3, the BFD equation was found to give the best results at both lightness scales giving values of 37.46, and 42.46, respectively. PF/3 results also indicate that at K_L = 2, CIEDE2000 gives the worst performance amongst equations examined. In addition, results based on correlation coefficient and PF/3 evaluation do not match well especially at lightness scale of 2. The optimal K_L was also obtained for various color difference formulae using a range of K_L values within 0.2-3.0 and with an interval of 0.1. Using PF/3 as a metric the best formula performance was obtained when K_L or l was set to 0.99, 1.04, 1.21, and 1.33 for CIEDE2000 (K_L:K_C:K_H), BFD(l:c), CMC(l:c), and CIE94(K_L:K_C:K_H) formulae, respectively.

The best-fit ellipsoid equation in the CIELAB color space was obtained for the Lee-Shamey Blue dataset developed in this study. This ellipsoid was compared with ellipsoids optimized to the RIT-DuPont dataset. The ellipses based on Lee-Shamey blue dataset have the smallest ratio of axes in the CIE a*b* as well as CIE a*L* and b*L* planes (2.73, 1.16, and 1.58, respectively), with an area of (0.93, 0.45, and 0.78, respectively). The dataset was also converted to CIExyY coordinates for comparison with other published data. In the chromaticity-discrimination ellipse, the ellipse based on Lee-Shamey Blue dataset has the smallest ratio of axes (4.27) as well as area (0.08) among the ellipses obtained from RIT-DuPont, Witt, and BFD datasets.

Assessment of Metrics in Color Spaces

By

Seung Geol Lee

A thesis submitted to the Graduate Faculty of

North Carolina State University

in partial fulfillment of the requirements for the

Degree of Master of Science in

Textile Chemistry

Raleigh, NC

2007

Approved By:

Dr. Renzo Shamey	**Dr. Warren J. Jasper**
(Chair of Advisory Committee)	(Co-Chair of Advisory Committee)
Dr. David Hinks	**Dr. Larry K. Norris**

Biography

Seung Geol Lee was born on October 07, 1978 in Pusan, Republic of Korea. He received his Bachelor of Science in Textile Engineering, and Bachelor of Home Economics in Clothing & Textiles with Summa Cum Laude from Pusan National University in August 2004. In Fall 2005, he joined the College of Textiles at North Carolina State University as a Masters student in the Textile Chemistry program.

Acknowledgements

The author would like to thank Dr. Renzo Shamey, Chairman of his advisory committee, for his advice, support, and guidance throughout this study. It was his confidence in the author and continuous encouragement that made this work possible. Dr. Warren J. Jasper, Co-Chairman of his advisory committee, contributed much to the author's understanding of geometrical mathematics and MATLAB programming. Appreciation is also extended to Dr. David Hinks and Dr. Larry K. Norris, members of the advisory committee, for their valuable advice, suggestions, and encouragement.

The author would also like to thank Prof. Rolf Kuehni for his valuable comments, Miss Lina M. Cárdenas for her help with statistical analysis of the dataset and the design of large gray scale and sample mount, Mr. Matthew Farrell for his help with dyeing procedure, and Mr. Byoung Don Kong for his help with mathematical programming. The author is also grateful to all observers who willingly participated in visual assessments. The author would also like to thank the National Textile Center, USA, for providing financial support for this project.

Finally, thanks to all members of my family, especially my parents, Sangjoon and Youngsuk, and my wife Junghyun and my daughter (to be born in June 2007), for their continued love, support and encouragement throughout this study.

Table of Contents

List of Tables

List of Figures

I. Literature Review

1. Introduction to Color

1.1. Definition of Color

Color is what we see and perceive. It may be defined as the result of light interacting with an object and subsequently detected by a human visual system. Interactions between light and an object include reflection, scattering, transmission, absorption, refraction and interference. Color is defined by the Webster's dictionary as[1]:

"Any of manifold phenomena of light (as red, brown, pink, gray, green, blue, and white) or of visual sensation or perception that enables one to differentiate objects even though the objects may appear otherwise identical (as in size, form, or texture)"

The interaction of light with objects is detected by the human eyes and processed by the brain[2]. This procedure is very complex, entirely subjective and not fully understood. It is clear, however, that the understanding of color requires the study of a variety of scientific domains including physics, chemistry, physiology, mathematics, and psychology.

1.2. Perception of Color

The physical stimulus from a light source hitting an object, and detected by the human visual system, i.e. the eye and the brain, is perceived as color, as shown

in Figure 1. This results from a series of photochemical and electrochemical reactions in the visual system.

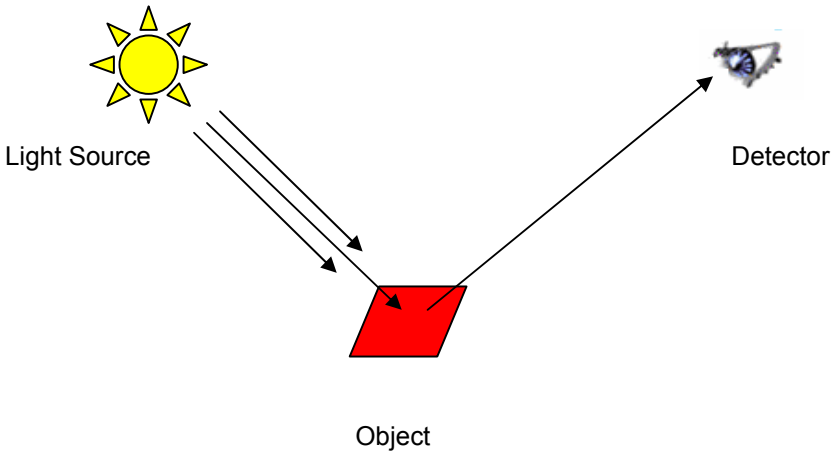

Figure 1. The interaction of a light source, an object, and a detector.

Light hitting the eye is focused on the retina, which is on the back-side of the eye ball, as shown in Figure 2. The retina is a thin layer of neural cells that converts light into neural impulses, as shown in Figure 3. The retina is made of several neuronal layers. Light hits the photoreceptors, i.e. cones and rods, present in the retina and they in turn produce photochemical signals. These signals are passed through horizontal cells, bipolar cells, and ganglion cells, respectively. They are thus transformed to particular patterns and sent to the brain through the optic nerves.

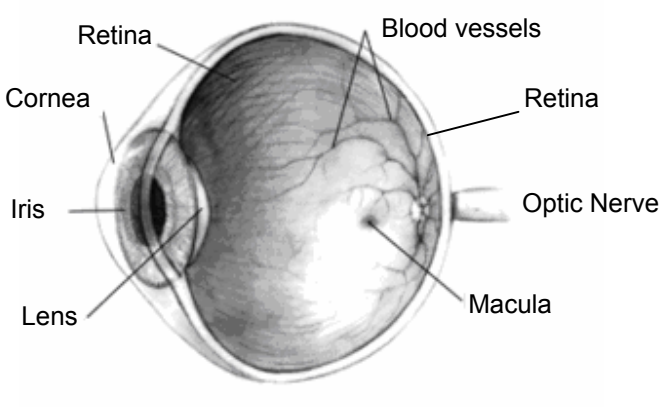

Figure 2. Human eye cross-sectional view[3].

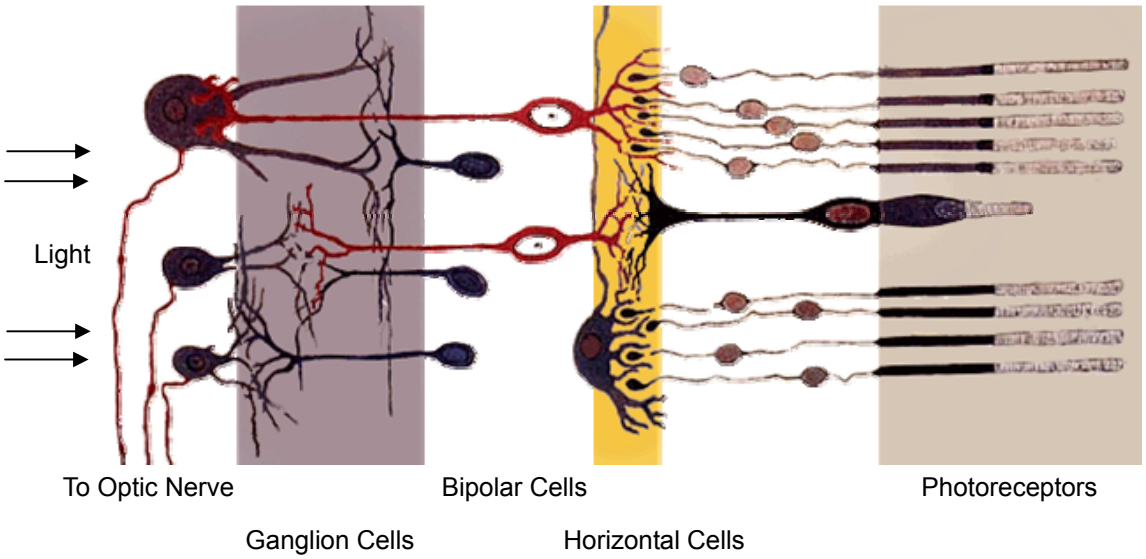

Figure 3. Axial organization of retina[4].

The retina contains photoreceptor cells known as rods and cones that respond to light. The cones respond to bright light, resulting in high visual acuity, and color vision. The rods respond to dim light and yield low visual acuity, and are responsible for monochromatic vision. There are three kinds of cones which typically respond to 3 different wavelength regions:

- L (Long) type cone responds to yellowish-green light or long wavelengths.
- M (Medium) type cone responds to bluish-green light or medium wavelengths.
- S (Short) type cone responds to bluish-violet light or short wavelengths.

They have peak wavelengths at 564 nm, 534 nm, and 420 nm, respectively. In case of rods, the maximum peak wavelength is at 498 nm as shown in Figure 4.

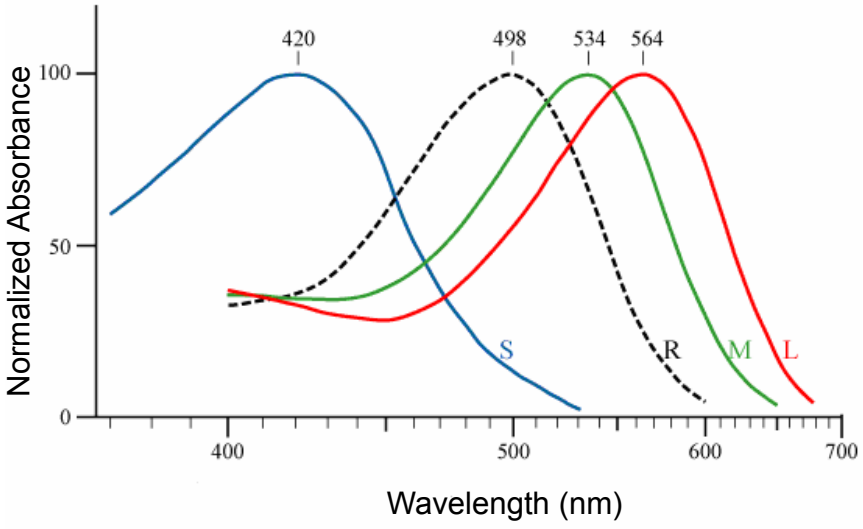

Figure 4. Spectral absorption curves of the cone and rod cells[5].

1.3. Color Control*: Why is it important?*

Color may be described by numbers in the color industry. The use of mathematical notation and effective modeling brings several merits. It allows for instant color communication, accurate reproduction of colors, increases confidence in color matching, and precise quality control of products. The ultimate goal of color control is to develop an accurate and precise integrated color control system that

can be easily implemented throughout the industrial manufacturing complex[6-7]. Any mathematical assessment of color must effectively model, at the least, the three basic variables discussed previously, the light source, reflectance of the object, and the observer. Hence, the basis of color measurement is founded in trichromatic theory.

2. Trichromatic Colorimetry

2.1. Color Matching Laws

Newton was the first scientist who conducted detailed color matching experiments with light[8]. For instance, he found that white light can be produced by mixing only yellow and blue wavelengths. Color measurement, also referred to as colorimetry, is fundamentally based on additive mixing, as shown in Figure 5. In theory any color stimuli can be matched with a set of colored lights known as primary colors which are Red (R), Green (G), and Blue (B), according to additive mixing laws, as shown in Figure 6.

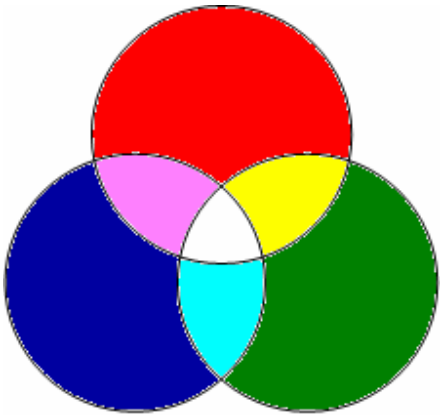

Figure 5. Additive color mixing with red, green, and blue primaries.

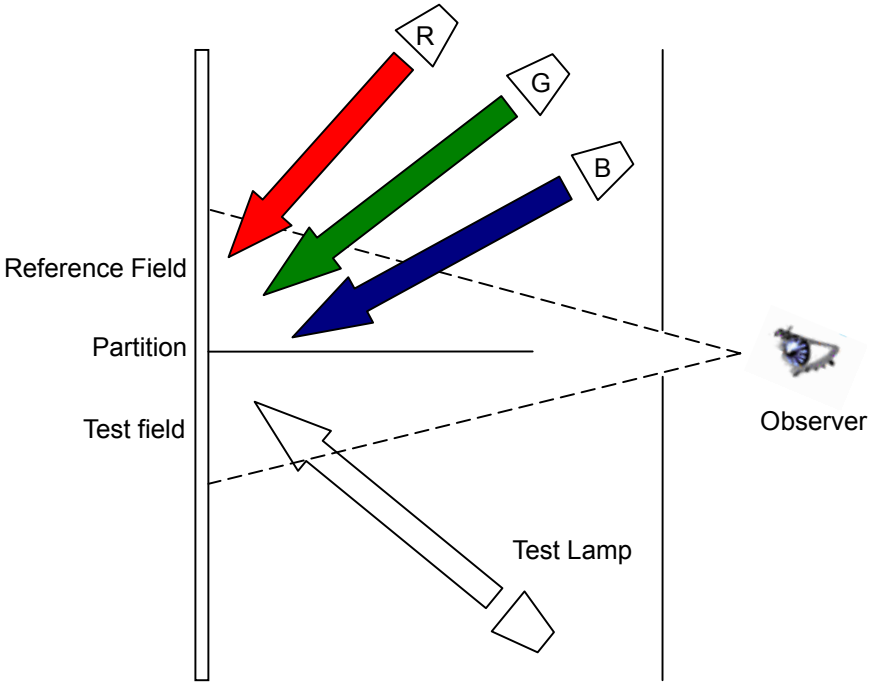

Figure 6. A simple color matching device with red, green, and blue primaries.

These additive mixtures follow four fundamental color matching laws[9-11]:

If A ≡ B, then B ≡ A: Symmetry Law (1)

If A ≡ B and B ≡ C, then A ≡ C: Transitivity Law (2)

If A ≡ B, then αA ≡ αB: Proportionality Law (3)

If A ≡ B and C ≡ D, then (A + C) ≡ (B + D) and

(A + D) ≡ (B + C): Additivity Law (4)

Where

A, B, C, and D are color stimuli;

α is any positive factor altering the radiant power of the color stimulus, and ≡ means 'visually matches'.

These laws are often summarized by the Grassman's laws shown below:

$$c[C] \equiv r[R] + g[G] + b[B] \quad (5)$$

Where,

[R], [G], and [B] are three primary lights,

[C] is the test light,

c, r, g, and b are the amounts of color stimuli used to match the test light.

2.2. Commission Internationale de l'Eclairage (CIE)

The Commission Internationale de l'Eclairage (CIE), or the International Commission of Illumination, is a more than 80 year old organization, which develops science and technology for the standardization of light and lighting and related fields, and publishes technical reports to enable the effective reproduction of color. In the field of light and color, many international standards depend on CIE recommendations.

2.3. Tristimulus Values

The CIE developed a mathematical method of describing the color of a sample based on the trichromacy theory[9,12]. They introduced three numbers known as tristimulus values, X, Y, and Z, to define color in a three-dimensional space. Equations 6–9 show the relationship between tristimulus values and the three constituent components of color. These are the observer, defined by the color matching functions (x, y, z), object, specified by its spectral reflectance properties (R_λ) and the light source, given as the spectral power distribution of a standard illuminant (S_λ). The constant, k, in Equation 10 is a normalizing constant and $\Delta\lambda$

is the measurement wavelength interval.

$$X = k\sum_{\lambda} S_{\lambda} R_{\lambda} \bar{x}_{\lambda} \Delta\lambda \tag{6}$$

$$Y = k\sum_{\lambda} S_{\lambda} R_{\lambda} \bar{y}_{\lambda} \Delta\lambda \tag{7}$$

$$Z = k\sum_{\lambda} S_{\lambda} R_{\lambda} \bar{z}_{\lambda} \Delta\lambda \tag{8}$$

$$k = \frac{100}{\sum_{\lambda} S_{\lambda} \bar{y}_{\lambda} \Delta\lambda} \tag{9}$$

Tristimulus values define the amounts of a set of primaries and are used to define a color match for a given colors stimulus.

2.4. CIE Standard Observer

As already shown the calculation of tristimulus values depends on the definition of the observer component. Human perception of color is subjective and cannot be easily included in the calculation of a definite color parameter. In order to solve this problem a standard was defined to adequately represent average normal color vision. This standard vision was defined as the CIE Standard Observer in 1931. In the development of standard observer CIE employed observers with normal color vision and light adapted conditions to typical levels of illumination.

2.4.1. The 1924 CIE Standard Photopic Observer

During the beginning of the twentieth century, the fact that two different wavelengths of light of equal radiant power often had very different brightness was

noticed. This means physical measurements of the power of a light source correlated poorly with the perceived brightness of the source. A brightness sensitivity is derived based on performing flicker photometry known as brightness matching or heterochromatic brightness matching for each wavelength of the spectrum in comparison to results at a reference wavelength (such as 555nm). In 1924, the CIE adopted Gibson and Tyndall's visibility curve, V_λ function, as known today as the CIE standard photometric observer[13].

The brightness of a source is calculated by multiplying its spectral radiance by the V_λ function, wavelength by wavelength, followed by summation, and finally multiplying by a normalized constant. This photometric calculation is used extensively to define the level of illumination and other photometric properties[14].

2.4.2. The 1931 CIE Standard Colorimetric Observer

Guild and Wright in England measured the color matching functions of a small number of color normal observers[15, 16]. Both experiments employed the same viewing conditions; a bipartite field subtending a 2 degree visual angle that was surrounded by darkness. The selected primaries to provide excellent repeatability when building visual colorimeters had peaks at 435.8 nm, 546.1 nm, and 700 nm, respectively. This set of color matching functions is represented by $\bar{r}_\lambda$, $\bar{g}_\lambda$, and $\bar{b}_\lambda$ and defines tristimulus values of the spectrum colors for this particular set of primaries. However, $\bar{r}_\lambda$, $\bar{g}_\lambda$, and $\bar{b}_\lambda$ color matching functions obtained from average observers had both positive and negative values as shown in Figure 7. This greatly increases the complexity of subsequent calculation.

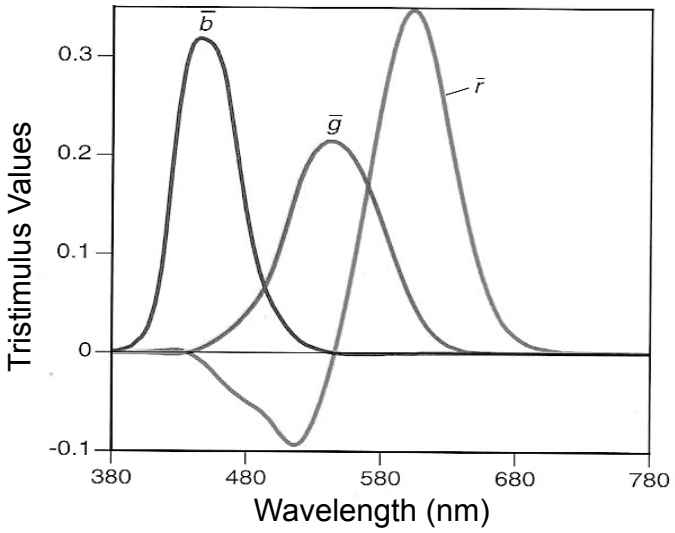

Figure 7. Original $\bar{r}_\lambda$, $\bar{g}_\lambda$, and $\bar{b}_\lambda$ color matching functions containing both positive and negative tristimulus values[15].

This concern was alleviated by a new set of primaries such that their color matching functions were all positive, and where one of the color matching functions would be the 1924 CIE standard photometric observer function, V_c. The spectral luminous efficiency function, V_λ is related to luminous flux P_v and radiant flux P_e using the following relationship:

$$P_{\upsilon,\lambda} = 683 \int_{380}^{780} P_{e,\lambda} V(\lambda) d\lambda$$

The factor 683 is the approximate figure required to convert the watts of radiant flux into lumens of light and has the units of lm W^{-1}.

The transformed system is called the X, Y, and Z system with color matching functions represented by $\bar{x}_\lambda$, $\bar{y}_\lambda$, and $\bar{z}_{\lambda,}$as shown in Figure 8.

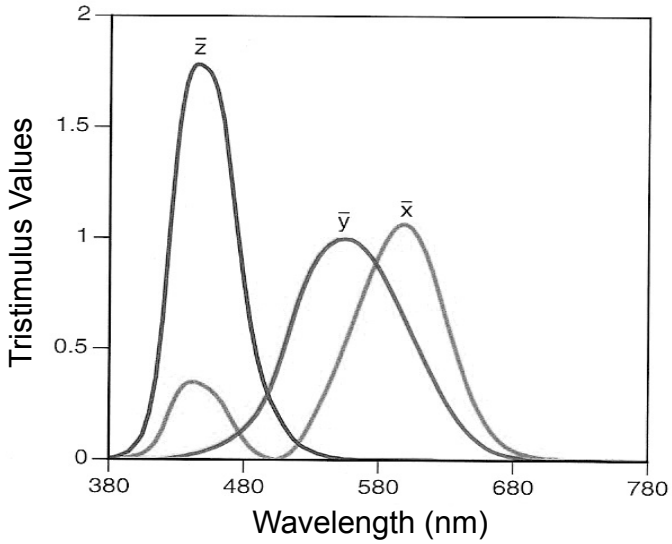

Figure 8. The transformed $\bar{r}_\lambda$, $\bar{g}_\lambda$, and $\bar{b}_\lambda$ color matching functions[17].

This system is the 1931 CIE 2 degree standard observer and is intended to represent the color matching results of the average human population having normal color vision using a 2 degree field of view[18].

2.4.3. The 1964 CIE Supplementary Standard Colorimetric Observer

The experiments for the 1931 CIE standard observer were performed with a small angle that included only the fovea of the retina, which is located in the center of the macula region of the retina. The fovea covers about a 2 degree field of view and does not contain rods, the resulting color matching functions should be equally applicable for colors viewed at typical levels of illumination. There are a number of applications in which stimuli subtend a much larger visual angle, so the 2 degree standard observer is not sufficient for all applications. The CIE adopted and combined two additional datasets from Stiles and Burch, and Speranskaya who

measured the color matching functions of a total of 50 observers using a 10 degree field of view. The average of these color matching functions was standardized as the 1964 CIE supplementary standard colorimetric observer[19, 20]. The 1964 CIE standard observer is denoted as $\bar{x}_{10\lambda}$, $\bar{y}_{10\lambda}$, and $\bar{z}_{10\lambda}$.

2.4.4. The CIE Standard Deviate Observer

Standard deviate observer was developed from the CIE standard observer functions. The CIE standard observers are based on the average response of a small number of observers. Thus, a real observer may not be exactly represented by either of the CIE standard observer functions. In 1989, the standard deviate observer, developed by the CIE, was designed to represent the difference of the variability among the observers[21-23]. It was derived from singular value decomposition using 20 of Stiles' 49 observers using a 10 degree visual field[19]. The decomposition method gave four sets of deviation functions[24]. The first set of deviation functions, shown in Figure 9 and Equations 10-12, in conjunction with a CIE standard colorimetric observer (either 1931 or 1964), is used to define the color-matching functions of the standard deviate observer.

$$\bar{x}_{dev}(\lambda) = \bar{x}(\lambda) + \Delta\bar{x}_i(\lambda) \quad (10)$$

$$\bar{y}_{dev}(\lambda) = \bar{y}(\lambda) + \Delta\bar{y}_i(\lambda) \quad (11)$$

$$\bar{z}_{dev}(\lambda) = \bar{z}(\lambda) + \Delta\bar{z}_i(\lambda) \quad (12)$$

where

$\bar{x}_{dev}(\lambda)$, $\bar{y}_{dev}(\lambda)$, and $\bar{z}_{dev}(\lambda)$ are the standard deviate observer color matching functions, $\Delta\bar{x}_i(\lambda)$, $\Delta\bar{y}_i(\lambda)$, and $\Delta\bar{z}_i(\lambda)$ are the first deviation functions, obtained from decomposition of Stiles' experimental results, and, $\bar{x}(\lambda)$, $\bar{y}(\lambda)$, and $\bar{z}(\lambda)$ are a CIE standard colorimetric observer color-matching function.

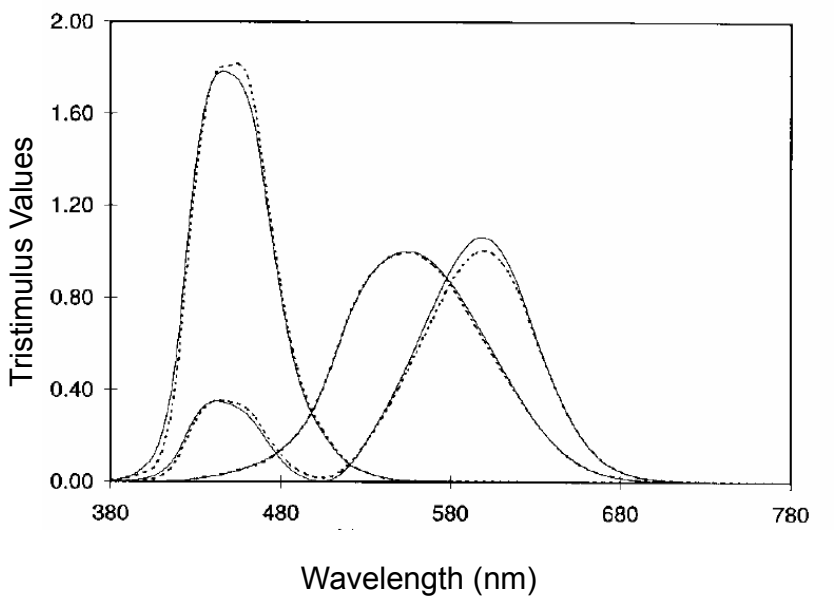

Figure 9. CIE standard deviate observer (dashed lines), and 1931 CIE standard colorimetric observer color-matching functions (solid lines)[24].

The standard deviate observer can be used to calculate confidence limits about any tristimulus specification where these limits represent variability among observers. This is also used to calculate an index of observer metamerism. It is also possible to predict changes in color with changes in observer responses based on the set of confidence limits.

2.5. Light Sources

Light sources may be precisely characterized by the exact distribution of the power emitted in the visible spectrum. The most important source of light is daylight, and this has many phases with different spectral power distributions. Also, there are many artificial sources, such as incandescent and fluorescent, also with different spectral power distributions.

2.5.1. Thermal Radiators

Light sources are based on physical emitters of radiant energy, e.g. a lamp and the sun. Thermal radiators emit light as a function of wavelength. An ideal thermal radiator is Planckian or Black body radiator. Planckian or Black body radiator is a theoretical body with a spectral radiant excitance at temperature T per unit wavelength interval given by Equations 13-15 and shown in Figure 10.

$$M_e = \frac{c_1}{\lambda^5\left(e^{c_2/T\lambda} - 1\right)} \quad \left(W \cdot m^{-3}\right) \tag{13}$$

$$c_1 = 2\pi c^2 h = 3.74183 \times 10^{-16} \quad (W \cdot m^2) \tag{14}$$

$$c_2 = hc/k = 1.458786 \times 10^{-2} \quad (m \cdot K) \tag{15}$$

Where,

c is the velocity of light in vacuum, $2.99792458 \times 10^8 \quad \left(m \cdot s^{-1}\right)$;

h is the Planck constant, $6.626176 \times 10^{-34} \quad \left(J \cdot s\right)$;

k is the Boltzmann constant, $1.380662 \times 10^{-23} \quad \left(J \cdot K^{-1}\right)$.

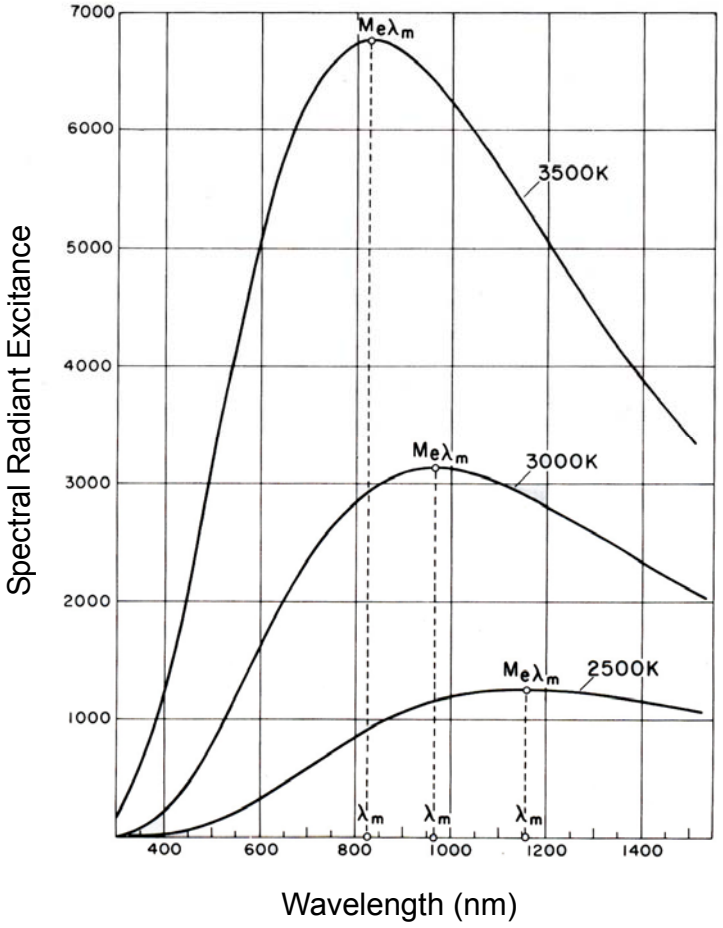

Figure 10. Spectral power distributions of radiant excitance of a blackbody radiator with color temperature of 2500K, 3000K, and 3500K, representing a maximum radiant excitance at wavelength equal to 1160, 965, and 830 nm[25].

2.5.2. Relative Spectral Power Distribution

Relative spectral power distribution is a normalized distribution typically specified in a 10nm interval and centered at the specified wavelength. Spectral sources and illuminant spectral power distributions are usually normalized at 560 nm as shown by Equation 16 and Figure 11.

$$S_\lambda = \frac{E_\lambda}{E\ at\ 560nm} \tag{16}$$

where,

E is spectral irradiance ($W \cdot m^{-2}$); irradiance is the radiant flux incident per unit area[26].

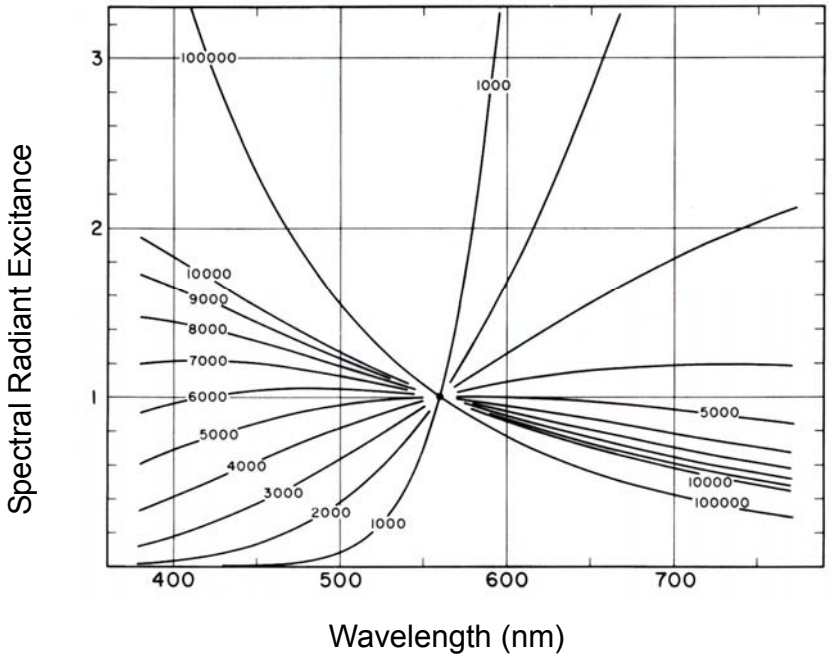

Figure 11. Relative spectral distributions of radiant excitance of a black body radiator at different color temperatures T(K). All lines are normalized at 560nm[25].

2.5.3. Color Temperature

Color temperature (T_C) is a characteristic of visible light that has important applications in all fields related to color in which the light source is specified. The color temperature of a light source is determined by comparing its hue with a theoretical, heated black-body radiator. The Kelvin temperature at which the

heated black-body radiator matches the hue of the light source is that source's color temperature, and it is directly related to Planck's law of black body radiation.

2.5.4. Correlated Color Temperature

Correlated color temperature is the temperature, usually expressed in Kelvin, of the Planckian radiator that would emit light of the chromaticity most closely resembling that of the light from the source[27].

2.5.5. CIE Standard Illuminants

The CIE defined a set of spectral radiant power distributions known as CIE standard illuminants. These datasets intended to represent some of the most common CIE standard illuminants and are briefly described in the following sections.

2.5.5.1. CIE Standard Illuminant A

CIE standard illuminant A has the profile of a color temperature at 2856 K. It is used to represent the spectral power distribution of a typical incandescent tungsten filament lamp. The spectral power distribution of CIE standard illuminant A is shown in Figure 12.

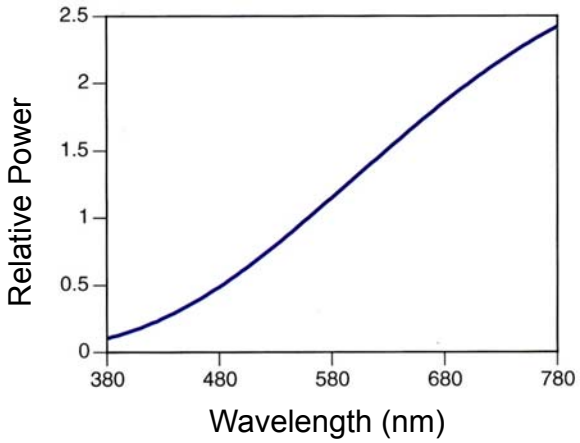

Figure 12. Spectral power distribution of CIE standard illuminant A[28].

2.5.5.2. CIE Standard Illuminant B

CIE standard illuminant B is intended to represent noon sunlight at a color temperature of 4878 K.

2.5.5.3. CIE Standard Illuminant C

CIE standard illuminant C is based on filtering illuminant A. CIE standard Illuminant C is intended to represent average daylight of north sky from an overcast sky at a color temperature of 6774K. Due to inadequate representation of the UV component of light in illuminants B and C they are no longer recommended for use.

2.5.5.4. CIE Standard Illuminant D

The D series of illuminants were constructed to represent natural daylight. Illuminant D65 represents a phase of natural daylight at a color temperature of 6504K and is used in textile industry. Illuminant D50 represents daylight at a color

temperature of 5000K and is used in the graphic arts industry. Illuminant D75 represents cold indoor daylight lighting. Spectral power distribution of CIE standard illuminant C, D50, and D65 are as shown in Figure 13.

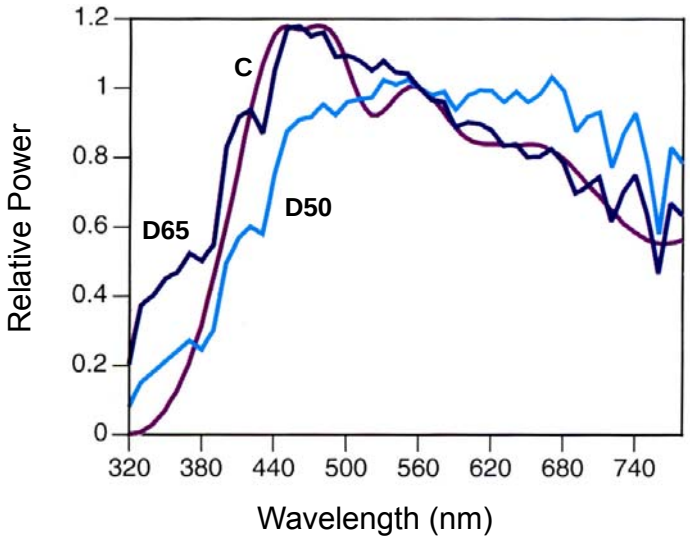

Figure 13. Spectral power distribution of CIE standard illuminant C, D50, and D65[28].

2.5.5.5. CIE Standard Illuminant F

The F series of illuminants are constructed to represent various types of fluorescent lighting. Illuminant F2 represents cool white fluorescent. Illuminant F11 represents narrow-band fluorescent. Illuminant F7 and F8 are representative of daylight fluorescent lamps and are often used as approximations of D65 and D50, respectively. Spectral power distributions of CIE standard illuminant F2 and F11, and F7 and F8 are shown in Figures 14 and 15, respectively.

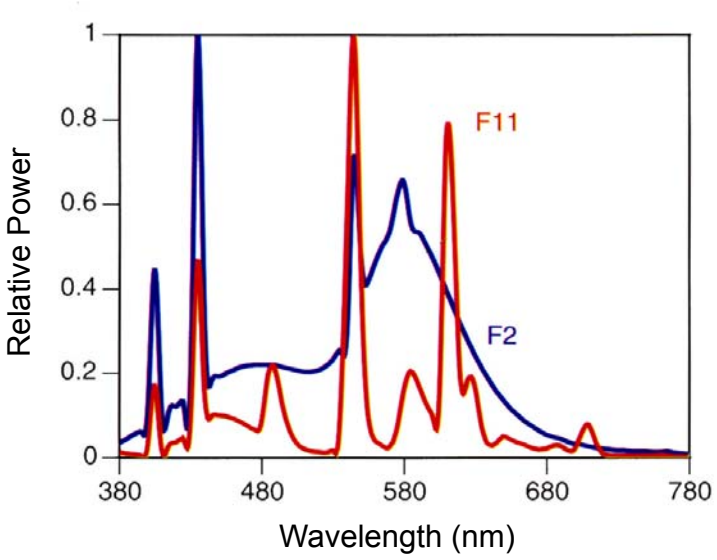

Figure 14. Spectral power distribution of CIE standard illuminant F2 and F11[28].

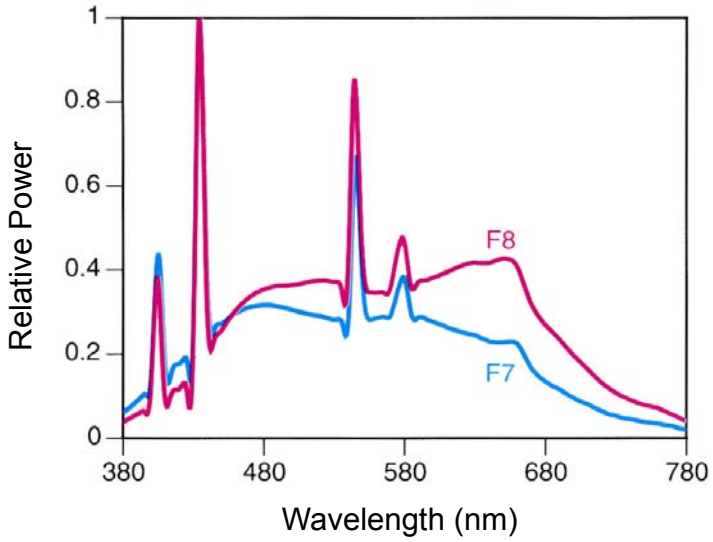

Figure 15. Spectral power distribution of CIE standard illuminant F7 and F8[28].

2.6. Interactions of Light with Objects

Observers perceive color of opaque materials by detecting light which is

reflected from them. In addition to some surface reflections, light may also be refracted, when it meets the surface of an object. The refracted light which penetrates an object undergoes absorption and scattering, giving rise to the overall color appearance of an object. The simple interaction of processes is shown in Figure 16.

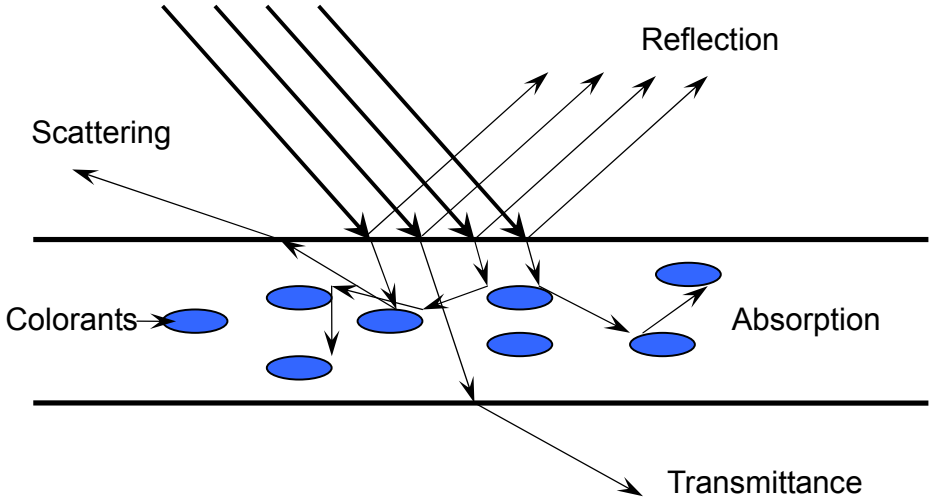

Figure 16. Interactions of light with an object.

3. Color Order Systems and Color Spaces

3.1. Introduction

Color order systems define the location and arrangement of colors according to attributes or gradations using a series of ordered numbers, which represent observable degrees. More than 400 color order systems have been developed since Aristotle designed vaguely three dimensional color space using black, white, and red for describing the states of night and day[29]. Most of these color order systems consist of three attributes, corresponding to a three dimensional color space. Some of the most important color order systems are briefly described in the following sections.

There are two main methods to specify color. One is based on color perception by arrangement of many physical samples. The other is based on color matching which is obtained by matching experiments.

3.2. One-dimensional Color Scales

One-dimensional color scales describe a single attribute of color. For example, the Y tristimulus value represents the lightness of a sample. A high value of Y indicates that the sample is lighter than a sample with a lower Y value. Yellowness scales, whiteness scales, and so on are among the one-dimensional color scales commonly used.

3.3. Two-dimensional Color Order Systems

One of the most common ways to represent the tristimulus values of an object is based on using a two-dimensional color scale known as the chromaticity

diagram. Chromaticity coordinates are defined as shown in Equations 17-19.

$$x = \frac{X}{X + Y + Z} \tag{17}$$

$$y = \frac{Y}{X + Y + Z} \tag{18}$$

$$z = \frac{Z}{X + Y + Z} \tag{19}$$

where,

X, Y, and Z are tristimulus values

From Equations 17-19, Equation 20 can be obtained which shows, if any two of the chromaticity coordinates are known, the third one is fixed and can be calculated.

$$x + y + z = 1 \tag{20}$$

For any given Y, luminance factor, a plot of y against x covers all possible colors. A plot of y against x is known as a chromaticity diagram as shown in Figure 17.

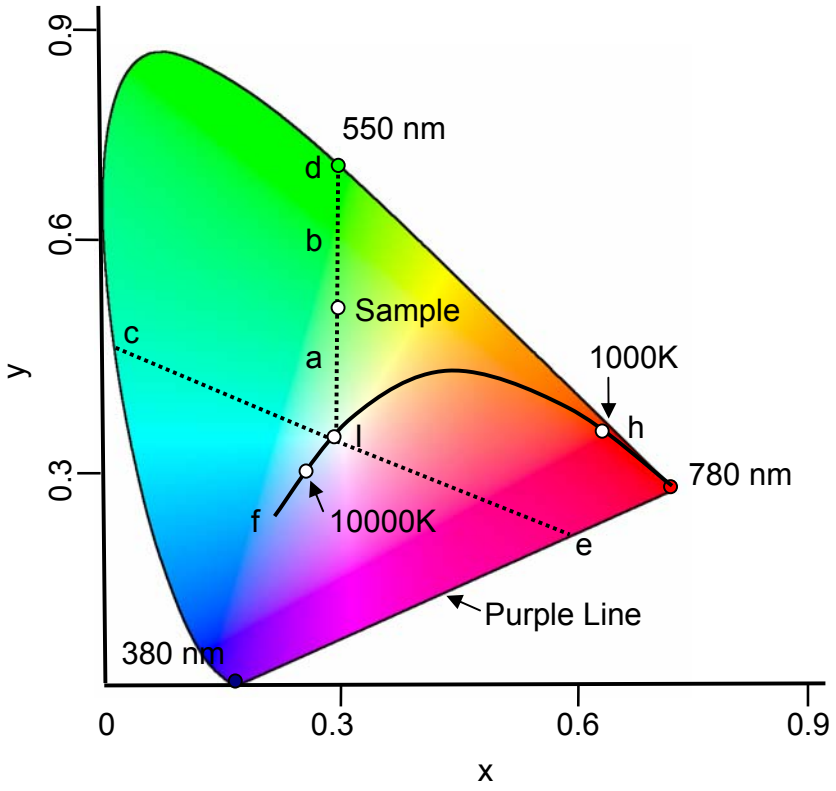

Figure 17. The CIE chromaticity diagram.

The horseshoe shaped line representing the chromaticity of spectral colors, is known as spectrum locus. The curve from *h* to *f* represents the blackbody radiator known as Planckian or blackbody locus. The location of illuminants can be plotted on this line. The point *d* represents the dominant wavelength (λ_d) of a color sample. Dominant wavelength is obtained by extending a straight line between the illuminant *I* and color sample towards the spectrum locus. If the sample lies in the purple region, the line is extended in the opposite direction towards the spectrum locus, to give its complementary dominant wavelength (λ_c). The distance of the sample point to the illuminant (a) is divided by the total distance from the illuminant

to the spectral boundary (a+b) to obtain the excitation purity as shown in Equation 21. Excitation purity gives an indication of the saturation of a color.

$$Pe = \frac{a}{a+b} \tag{21}$$

3.4. Three-dimensional Color Scales

The basic idea of a three-dimensional color space is suggested by three attributes as shown in Figure 18.

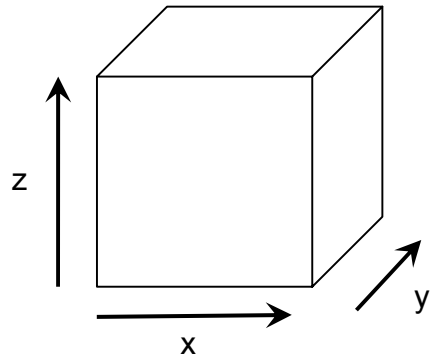

Figure 18. Arrangement of three attributes. x, y, and z are arbitrary components.

For example, hue, lightness, and chroma which are three basic perceptual attributes can be used to describe color on a three-dimensional color space. Modern color space coordinate systems are based on Cartesian coordinates and can be plotted with three axes representing Lightness (L*), the first chromatic component (a*), and the second chromatic component (b*) with hue circle as shown

in Figure 19.

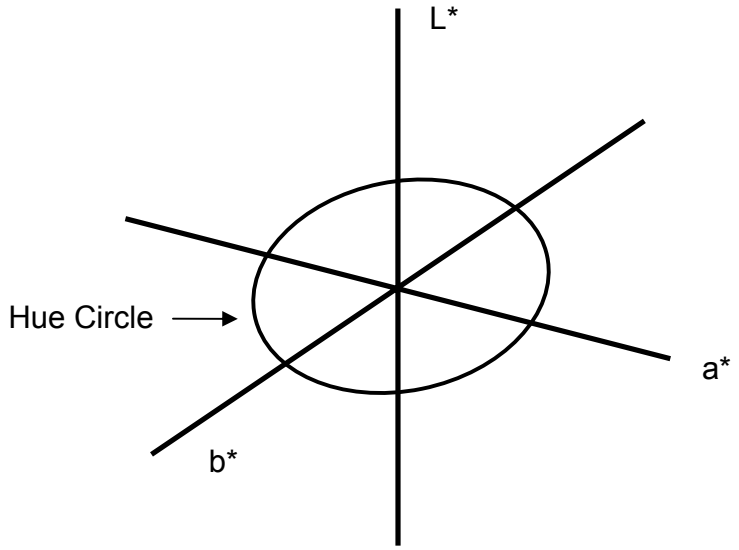

Figure 19. The basic form of a color space based on Cartesian coordinates.

3.4.1. Perceptual Scaling

Perceptual color spaces are based on perceptual scaling as perceived differences. The Munsell System[30], NCS (Natural Color System)[31], and OSA-UCS (Optical Society of America Uniform Color Scales)[32] are based on color perception.

The Munsell system is the most widely used color system and is based on approximately equal visual perception within the three attributes; i.e., hue, chroma, and lightness. The system consists of an irregular cylinder around the lightness axis, arranged so that dark colors are at the bottom of the cylinder and light colors are at the top.

The NCS system is published by the Scandinavian Color Institute (Skandinaviska Färginstitutet AB) of Stockholm, Sweden, and is based on Hering's

color space which is involved in color opponency theory. This system consists of printed reference color chips and is usually used for matching colors.

The Optical Society of America developed a set of approximately perceptually uniformly spaced samples based on a regular rhombohedral lattice space. The merit of this system is that any color is surrounded by 12 nearly perceptually equidistant neighbors, on a Euclidean space.

Perceptual systems are easy to understand and use because physical samples can be used for a particular application. However, the limited number of perceivable colors that can be obtained due to practical limitations associated with colorants as well as cost, deterioration and aging of samples over time, the need to use standardized lighting and background conditions, and difficulties in interconversion between the numerous systems available are amongst the disadvantages of such systems[33].

3.4.2. Color Matching Systems Based on Mathematical Principles

Color matching scaling is based on mathematical color ordering obtained through controlled color matching experiments. The most important space based on this system is the CIELAB color space[18]. CIELAB is based on the CIE XYZ tristimulus values described earlier. CIELAB consists of three attributes of two perpendicular opponent color axes with one vertical line which represents the correlate of lightness, L*. Two perpendicular color axes are represented by a* and b*, where a* is the red-green axis and b* is the yellow-blue axis. In 1976, the CIELAB color space was recommended by the CIE and is defined by Equations 22-25.

$$L^* = 116\left(\frac{Y}{Y_n}\right)^{1/3} - 16 \quad if \ \frac{Y}{Y_n} > 0.008856 \tag{22}$$

$$L^* = 903.3\left(\frac{Y}{Y_n}\right) \quad if \ \frac{Y}{Y_n} \le 0.008856 \tag{23}$$

$$a^* = 500\left[\left(\frac{X}{X_n}\right)^{1/3} - \left(\frac{Y}{Y_n}\right)^{1/3}\right] \tag{24}$$

$$b^* = 200\left[\left(\frac{Y}{Y_n}\right)^{1/3} - \left(\frac{Z}{Z_n}\right)^{1/3}\right] \tag{25}$$

where

X_n, Y_n, and Z_n are tristimulus values of the specified white point "illuminant."

The CIELAB color space is shown in Figure 20.

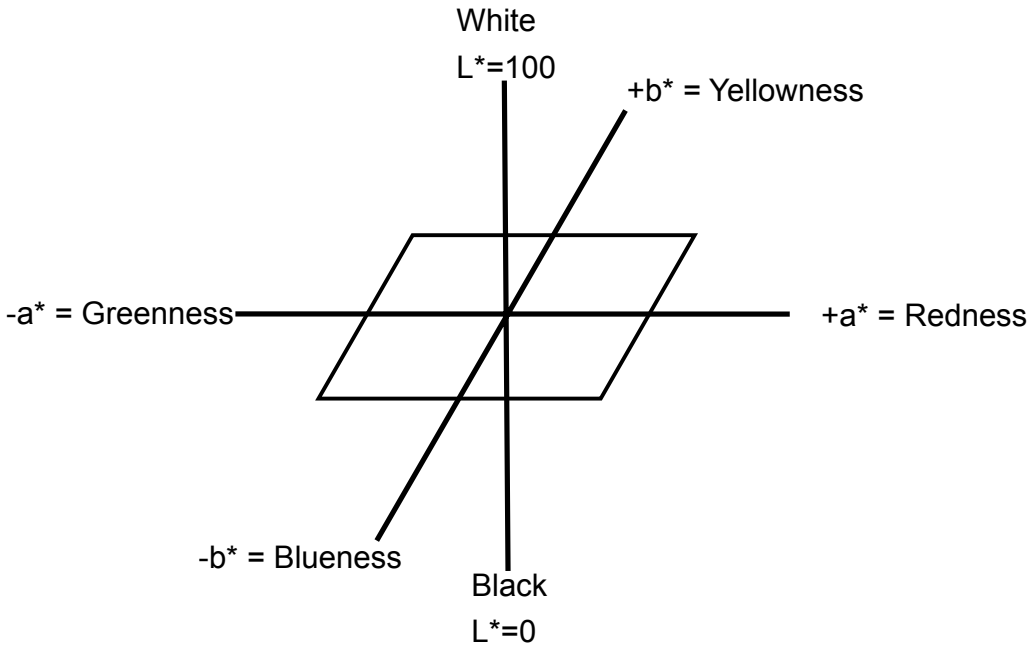

Figure 20. Schematic representation of the CIELAB color space.

The CIELAB color space can also be described by polar coordinates, which is defined as CIELCH (L*C*hº)[18], where C* is chroma, which represents the degree of departure of an object from an achromatic object of equal lightness, and hº is hue angle which varies from 0º-360º. Chroma and hue angle can be calculated according to Equations 26, 27. CIELCH (L*C*hº) color space is shown in Figure 21.

$$C^*_{ab} = \sqrt{a^{*2} + b^{*2}} \tag{26}$$

$$h^\circ_{ab} = \arctan\left(\frac{b^*}{a^*}\right) \tag{27}$$

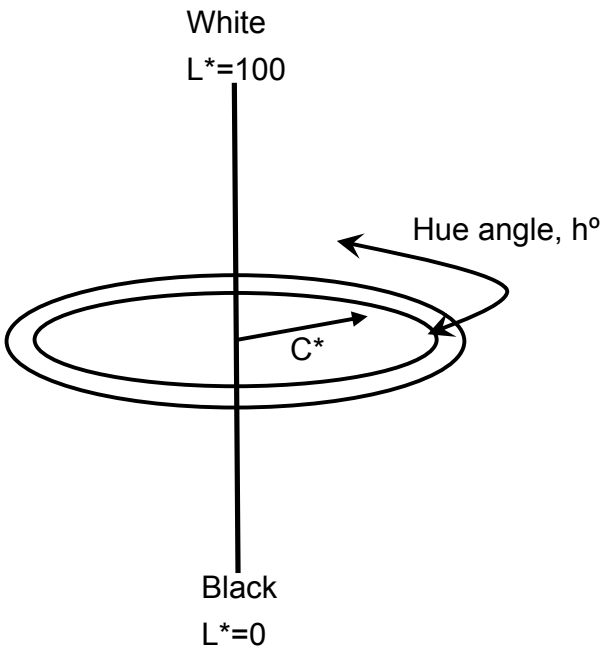

Figure 21. Plot of CIE L*C*hº color space.

4. Evaluation of Color

4.1. Spectrophotometric Measurement

Instrumental color measurement allows for evaluation of color using tristimulus values and is a cost-effective method for objective evaluation of color. The most common instrument for obtaining the colorimetric properties of objects or transparent/translucent objects is a spectrophotometer. Spectrophotometers are commonly used to control color quality using match-prediction methods, calculate the color difference between two objects (e.g. a production standard and batch) under different light sources, detect metamerism and so on. Spectrophotometers record the percentage of light reflected from an object according to Equation 28, and this is then converted to colorimetric data such as XYZ L*a*b* and various color difference metrics. Abridged spectrophotometers usually take readings every 5 or 10 nanometers across the UV and visible region of the electromagnetic spectrum, commonly between 360nm and 760nm.

$$\text{Reflectance} = = \frac{R_{ref}(\lambda)}{R_{inc}(\lambda)} \tag{28}$$

where

$R_{ref}(\lambda)$ is reflected light,

$R_{inc}(\lambda)$ is incident light.

In practice, reflectance is calculated as a fraction of the amount of light reflected from an object compared to that from a standard white tile using Equation 29.

$$\text{Reflectance} = = \frac{R_{ref\,1}(\lambda)}{R_{inc1}(\lambda)} \tag{29}$$

where

$R_{ref\,1}(\lambda)$ is reflected light from object,

$R_{inc1}(\lambda)$ is reflected light from white tile.

4.1.1. Operational Principles of a Spectrophotometer

Principles of operations of a diffuse integrating sphere spectrophotometer are simply shown in Figure 22.

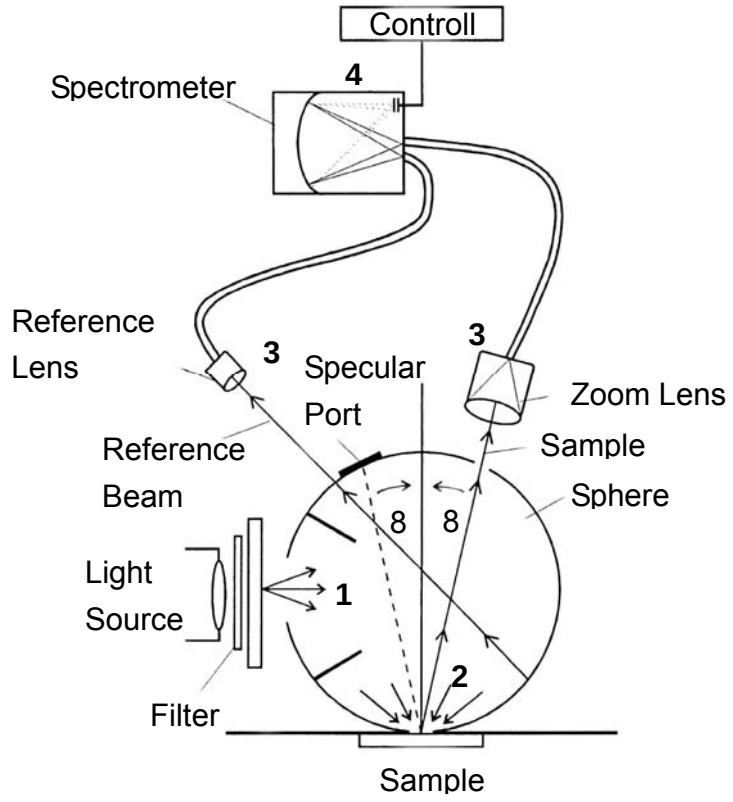

Figure 22. Schematic diagram of an integrating sphere spectrophotometer [34].

Basic principles of the operation are summarized below:

1. The light source shines light within the sphere.

2. The sample absorbs and reflects light.

3. The lenses collect the light. Zoom lens is set for measuring diameters from aperture and the reference lens collects light from the internal surface of the sphere.

4. The spectrophotometer detects the light and converts it into a number (tristimulus values).

4.1.2. Instrumental Geometries

The geometry of measurements is one of the important factors that can significantly affect the assessment of colored objects. The CIE recommended four different instrument geometries, which are briefly described in the following section[35] and are shown in Figure 23.

- 45/Normal (45/0) and Normal/45 (0/45): the sample is illuminated by light beams at an angle of 45±5º or normal (0) from the light source to the surface of the sample and light is detected at normal (0) or at an angle of 45±5º.

- Diffuse/Normal (D/0) and Normal/Diffuse (0/D): in this geometry an integrating sphere is used which is a hollow sphere coated with a highly reflecting material. Light is detected at normal (0) or diffuse according to the geometry used.

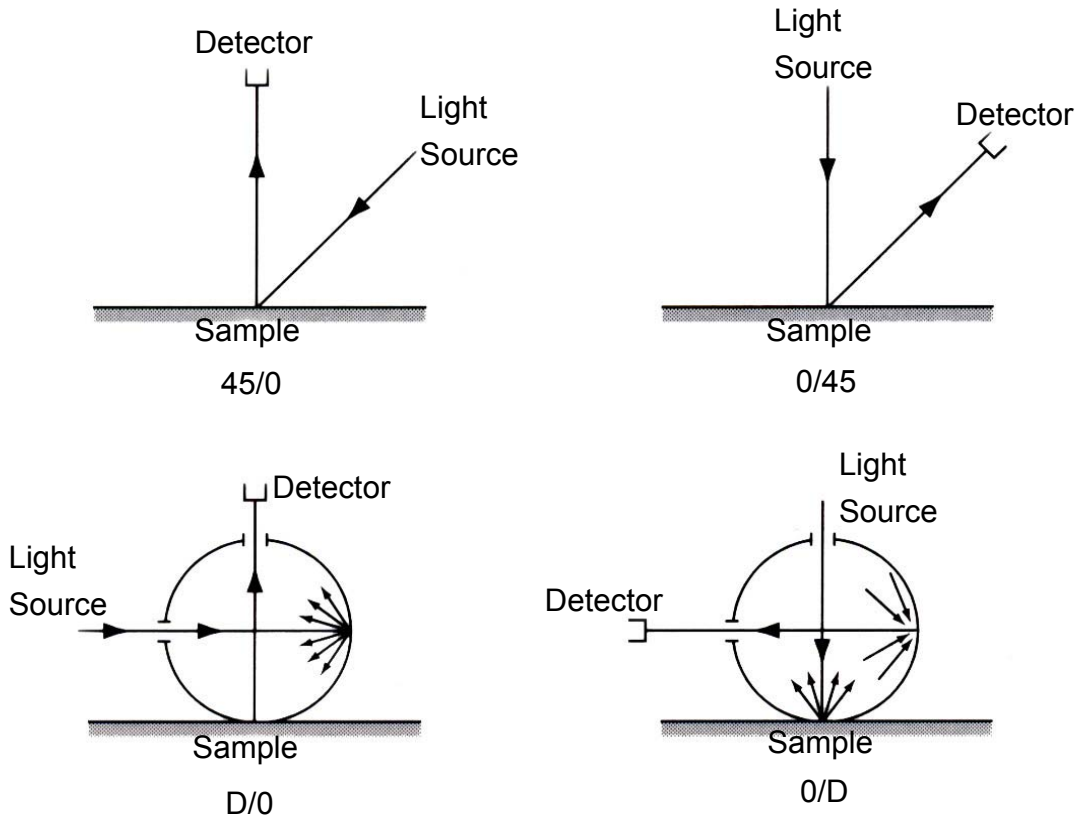

Figure 23. The CIE recommended instrumental geometries[36].

The CIE recommendation on colorimetric measurement allows a gloss port 8º away from the normal in the sphere. The gloss port can collect the specular (gloss) data by controlling whether the port is open or close, as shown in Figure 24. Thus, most of the diffuse integrating sphere instruments operate as d/8 geometries.

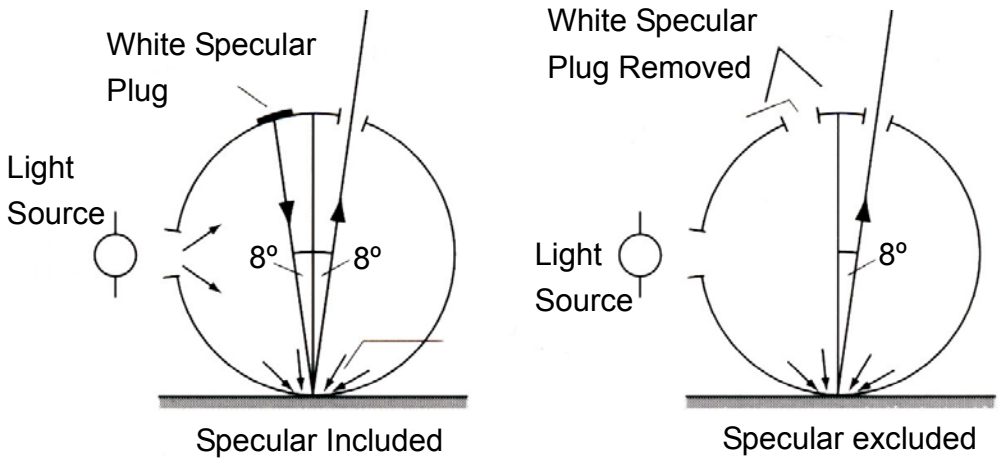

Figure 24. d/8 specular included and excluded mode[36].

4.2. Visual Color Assessment

The American Association of Textile Chemists and Colorists (AATCC) recommends several procedures for visual assessment of color. The general procedure for visual assessment is described in AATCC Evaluation Procedure nine[37]. Some of the important features and conditions for visual assessments are briefly described in the following sections.

4.2.1. Gray Scale for Visual Color Matching

The gray scale is defined by the AATCC Color Measurement and Test Methods Committee, RA 36, as[38]:

“A scale consisting of pairs of standard gray chips, the pairs representing progressive differences in color or contrast corresponding to numerical colorfastness

grades.”

The gray scale can be placed along the edges of the test sample pair which consists of a piece of the standard sample and its corresponding batch or trial sample to compare the perceived visual difference between a standard and a batch sample. Gray scale grades can be transformed to CIELAB color difference values using the colorimetric tolerance data defined for the standards as shown in Table 1[38].

Table 1. Gray scale grades corresponding with CIELAB, CIELAB tolerance, and verbal description.

Gray Scale Grade	Total Color Difference CIELAB Units	Tolerance for Working Standards CIELAB Units	Verbal Description
5	0.0	+ 0.2	Equal
4-5	0.8	± 0.2	
4	1.7	± 0.3	Slight
3-4	2.5	± 0.3	
3	3.4	± 0.4	Noticeable
2-3	4.8	± 0.5	
2	6.8	± 0.6	Considerable
1-2	9.6	± 0.7	
1	13.6	± 1.0	Much

4.2.2. Illumination and Viewing Conditions

Illumination conditions are shown in Table 2[37].

Table 2. Illumination conditions.

Illuminant	Description	Color Temperature
D65	Daylight	6500K ± 200
D75	Daylight	7500K ± 200
A	Incandescent	2856K ± 200
F2	Fluorescent	4230K ± 200

The samples should be placed on a flat, uniform surface, and neutral gray background and surround using Munsell N5/ to N8/. The RA 36 Committee of the AATCC also recommends four possible viewing geometries as shown in Figure 25[37].

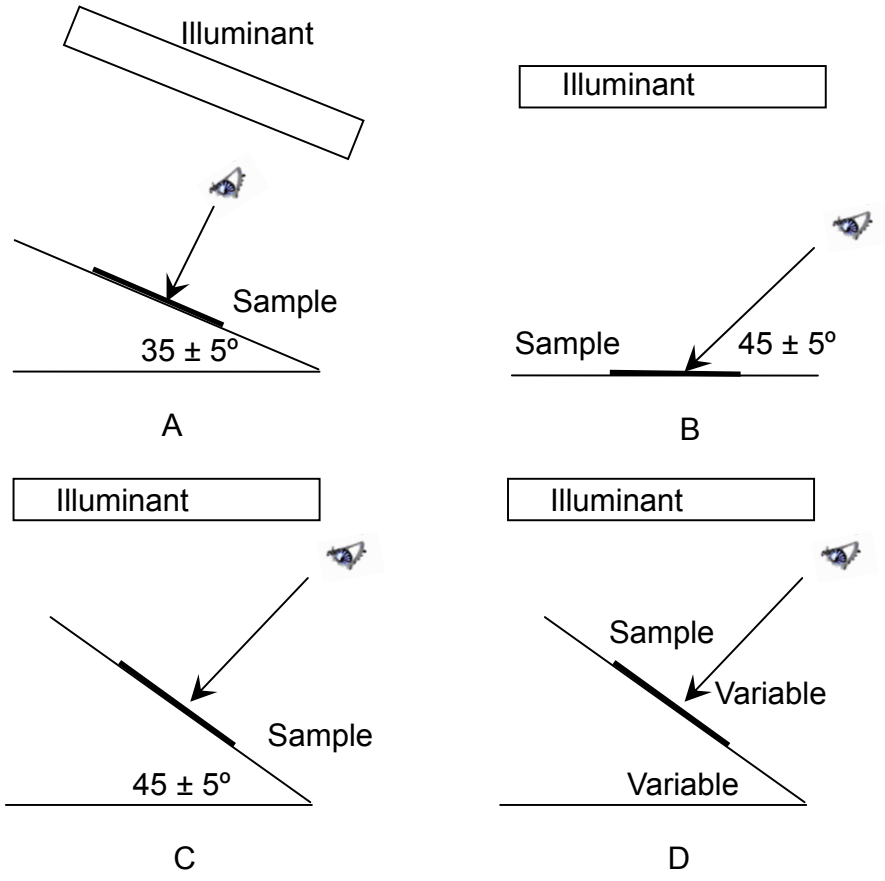

Figure 25. Viewing conditions defined in AATCC Evaluation Procedure nine[37].

Option A shall not be used for evaluations of glossy or non-matte samples. The observer must ensure not to block the incident light form the source. Option B is meant to represent overhead (ceiling) illumination conditions. Option C is used to represent side illumination (window). Option D may be used for special applications.

4.3. Color Difference Formulae

Over the last several decades, more than 40 color difference formulae, based on the XYZ tristimulus values, have been developed[39, 40]. These formulae are based on a single number color difference value (ΔE) representing the overall color difference between two samples, and are generally obtained from visual pass/fail (accept/reject) decisions, or from just noticeable perceptibility experiments. The data are plotted on a Euclidian color space because the color difference values are calculated by Pythagorean sum of differences. This approach does not always correspond with perceived differences as XYZ tristimulus values are based on a highly nonuniform perceptual color system. Significant research is still ongoing to develop formulae that result in better agreement with visual experimental data. Some of the most common color difference formulae are briefly described in the following sections.

4.3.1. CIELAB and CIELUV

In 1976, the CIE defined two color difference formulae as shown in Equations 30 and 31, respectively[18].

$$\Delta E_{uv}^{*} = \sqrt{\left[\left(\Delta L^{*}\right)^{2} + \left(\Delta u^{*}\right)^{2} + \left(\Delta v^{*}\right)^{2}\right]} \qquad (30)$$

where

$$L^{*} = 116\left(\frac{Y}{Y_n}\right)^{1/3} - 16 \quad if \ \frac{Y}{Y_n} > 0.008856$$

$$L^{*} = 903.3\left(\frac{Y}{Y_n}\right) \quad if \ \frac{Y}{Y_n} \le 0.008856$$

$$u^{*} = 13L^{*} + (u' - u'_n)$$

$$v^{*} = 13L^{*} + (v' - v'_n)$$

$$u' = \frac{4X}{X + 15Y + 3Z}$$

$$v' = \frac{9X}{X + 15Y + 3Z}$$

$$u'_n = \frac{4X_n}{X_n + 15Y_n + 3Z_n}$$

$$v'_n = \frac{9X}{X_n + 15Y_n + 3Z_n}$$

$$\Delta E_{ab}^{*} = \sqrt{\left[\left(\Delta L^{*}\right)^{2} + \left(\Delta a^{*}\right)^{2} + \left(\Delta b^{*}\right)^{2}\right]} \qquad (31)$$

where

$$L^{*} = 116\left(\frac{Y}{Y_n}\right)^{1/3} - 16 \quad if \ \frac{Y}{Y_n} > 0.008856$$

$$L^{*} = 903.3\left(\frac{Y}{Y_n}\right) \quad if \ \frac{Y}{Y_n} \le 0.008856$$

$$a^{*} = 500\left[\left(\frac{X}{X_n}\right)^{1/3} - \left(\frac{Y}{Y_n}\right)^{1/3}\right]$$

$$b^{*} = 200\left[\left(\frac{Y}{Y_n}\right)^{1/3} - \left(\frac{Z}{Z_n}\right)^{1/3}\right]$$

$\Delta L^* = L_B^* - L_S^*$,

$\Delta a^* = a_B^* - a_S^*$,

$\Delta b^* = b_B^* - b_S^*$,

and, B = batch and S = standard.

4.3.2. JPC79

In 1979, McDonald introduced a color difference formula based on over 600 polyester color samples around 55 color centers[41]. The formulae are shown in Equation 32.

$$\Delta E_{JPC97} = \sqrt{\left[\left(\frac{\Delta L}{S_L}\right)^2 + \left(\frac{\Delta C}{S_C}\right)^2 + \left(\frac{\Delta H}{S_H}\right)^2\right]} \qquad (32)$$

where,

$$S_L = \frac{0.08195L}{(1 + 0.01765L)},$$

$$S_C = \frac{0.0638C}{(1 + 0.0131C)} + 0.638,$$

$$S_H = S_C T,$$

$T = 1 \; if \; C = 0.638, \; otherwise$

$T = 0.36 + |0.4\cos(h + 35)|, \; unless \; h \; is \; between \; 164° \; and \; 345°, \; then$

$T = 0.56 + |0.2\cos(h + 168)|.$

4.3.3. CMC(l:c)

JPC97 was modified to a new formula by the Color Measurement Committee of the Society of Dyers and Colourists in England to overcome certain errors and

improve the correlation with visual assessment[42]. This formula is recommended by the International Standards Organization (ISO)[43] and AATCC[44], and is shown in Equation 33.

$$\Delta E_{CMC(l:c)} = \sqrt{\left[\left(\frac{\Delta L^*}{lS_L}\right)^2 + \left(\frac{\Delta C^*}{cS_C}\right)^2 + \left(\frac{\Delta H^*}{S_H}\right)^2\right]} \qquad (33)$$

where,

$$S_L = \frac{0.04097L^*}{(1+0.01765L^*)} \; unless \; L^* < 16, then \; S_L = 0.511,$$

$$S_C = \frac{0.0638C^*}{(1+0.0131C^*)} + 0.638,$$

$$S_H = S_C(TF + 1 - F),$$

$$F = \sqrt{\left\{\frac{(C^*)^4}{[(C^*)^4 + 1900]}\right\}}$$

$$T = 1 \; if \; C = 0.638, otherwise$$

$$T = 0.36 + |0.4\cos(h + 35)|, unless \; h \; is \; between \; 164° \; and \; 345°, then$$

$$T = 0.56 + |0.2\cos(h + 168)|.$$

l and c are additional relative weight factors representing lightness and chroma differences. The values l=2 and c=1 are usually used for textile industry.

4.3.4. BFD(l:c)

In 1987, Luo and Rigg introduced BDF(l:c)[45] within the CMC structure as shown in Equation 34.

$$\Delta E_{BFD(l:c)} = \sqrt{\left[\left(\frac{\Delta L^*(BFD)}{l}\right)^2 + \left(\frac{\Delta C^*}{cD_C}\right)^2 + \left(\frac{\Delta H^*}{D_H}\right)^2\right] + R_T\left(\frac{\Delta C^*}{D_C}\right)\left(\frac{\Delta H^*}{D_H}\right)} \quad (34)$$

where

$$D_C = \frac{0.035\overline{C}^*}{(1 + 0.00365\overline{C}^*)} + 0.521,$$

$$D_H = D_C(GT' + 1 - G),$$

$$G = \sqrt{\left\{\frac{(\overline{C}^*)^4}{(\overline{C}^*)^4 + 14000}\right\}},$$

$$T' = 0.627 + 0.055\cos(\overline{h} - 254) - 0.040\cos(2\overline{h} - 136) + 0.070\cos(3\overline{h} - 32) + 0.049\cos(4\overline{h} + 114) - 0.015\cos(5\overline{h} - 103),$$

$$R_T = R_H R_C,$$

$$R_H = -0.260\cos(\overline{h} - 308) - 0.379\cos(2\overline{h} - 160) - 0.636\cos(3\overline{h} + 254) + 0.226\cos(4\overline{h} + 140) - 0.194\cos(5\overline{h} + 280),$$

$$R_C = \sqrt{\left\{\frac{(\overline{C}^*)^6}{(\overline{C})^6 + 7 \times 10^7}\right\}},$$

$$L(BFD) = 54.6\log_{10}(Y + 1.5) - 9.6.$$

$\overline{C}^*$ and $\overline{h}$ are the mean for the standard and sample. Lightness and chroma weights l and c are set to 1.5 and 1, respectively, for predicting acceptability and to 1 for perceptibility of color difference.

4.3.5. CIE94(K_L:K_C:K_H)

Berns and others conducted visual assessments with 156 visual color tolerances around 19 color centers[46]. They proposed a formula with a similar structure to that of CMC(l:c), as shown in Equation 35. The formula was recommended by the CIE in 1994, and became known as CIE94.

$$\Delta E_{94} = \sqrt{\left[\left(\frac{\Delta L^*}{K_L S_L}\right)^2 + \left(\frac{\Delta C^*}{K_C S_C}\right)^2 + \left(\frac{\Delta H^*}{K_H S_H}\right)^2\right]} \qquad (35)$$

where

$S_L = 1,$

$S_C = 1 + 0.045 C_S^*$

$S_H = 1 + 0.015 C_S^*$

C_S^* is the chroma of the standard of a pair of samples. The K_L, K_C, and K_H are the parametric factors. For textile industry, K_L is usually set to 2, and K_C and K_H are set to one[39].

4.3.6. CIEDE2000(K_L:K_C:K_H)

Luo, Cui, and Rigg introduced CIEDE2000(K_L:K_C:K_H) based on analysis of several sets of perceptual color difference data to improve the correlation with visual assessment for blues, dark colors and near neutral colors[47]. The formulae are shown in Equation 36.

$$\Delta E_{00} = \sqrt{\left[\left(\frac{\Delta L'}{K_L S_L}\right)^2 + \left(\frac{\Delta C'}{K_C S_C}\right)^2 + \left(\frac{\Delta H'}{K_H S_H}\right)^2\right] + R_T\left(\frac{\Delta C'}{K_C S_C}\right)\left(\frac{\Delta H'}{K_H S_H}\right)} \qquad (36)$$

where

$$S_L = \frac{0.015(\overline{L'} - 50)^2}{\sqrt{20 + (\overline{L'} - 50)^2}} + 1,$$

$$S_C = 1 + 0.045\overline{C'},$$
$$S_H = 1 + 0.015\overline{C'}T,$$

$$T = 1 - 0.17\cos(\overline{h'} - 30) + 0.24\cos(2\overline{h'}) + 0.32\cos(3\overline{h'} + 6) - 0.20\cos(4\overline{h'} - 63),$$
$$R_T = -\sin(2\Delta\theta)R_C,$$

$$\Delta\theta = 30\exp\left\{-\left[\frac{(\overline{h'} - 275)}{25}\right]^2\right\},$$

$$R_C = 2\sqrt{\frac{\overline{C'}^7}{\overline{C'}^7 + 25^7}},$$

$$L' = L^*,$$
$$a' = (1 + G)a^*,$$
$$b' = b^*,$$
$$C' = \sqrt{a'^2 + b'^2}$$
$$h' = \arctan\left(\frac{b'}{a'}\right)$$
$$G = 0.5\left(1 - \sqrt{\frac{\overline{C'}^7}{\overline{C'}^7 + 25^7}}\right)$$

Five noticeable corrections from CIELAB are included in CIEDE2000(K_L:K_C:K_H)[39], as summarized below:

- Lightness (S_L), a chroma (S_C), and a hue (S_H) adjustment factors.

- An interactive term (R_T) between chroma and hue differences to improve the performance of the model for blue colors.
- A factor (1+G) for rescaling the CIELAB a* scale to improve the performance of the model for gray colors.

This formula is recommended by the CIE for general use. The ISO[43] and AATCC[44] recommend CMC(l:c) formula for use in textiles and the performance of CIEDE2000 is currently being tested by independent researchers.

4.4. Acceptability Tolerance

Color tolerance is the permissible color difference between a sample and a specified color[26]. Color tolerance is determined by pass/fail judgments under standardized lighting and background conditions. Pass/fail decisions are commonly made in comparison to gray scale. For each pair, results can be plotted in a suitable color space and are recorded as % acceptability. This process is repeated for many color standards throughout the color space. In a perceptually uniform Euclidean color space, a tolerance boundary would be a sphere because the same magnitude of perceived color difference for samples when compared to a standard would correlate to the same distance in the space regardless of direction. Using the CIELAB color difference equation to correlate measured results with the experimental pass/fail decisions the best fit results may be placed in an ellipse as shown in Figure 26.

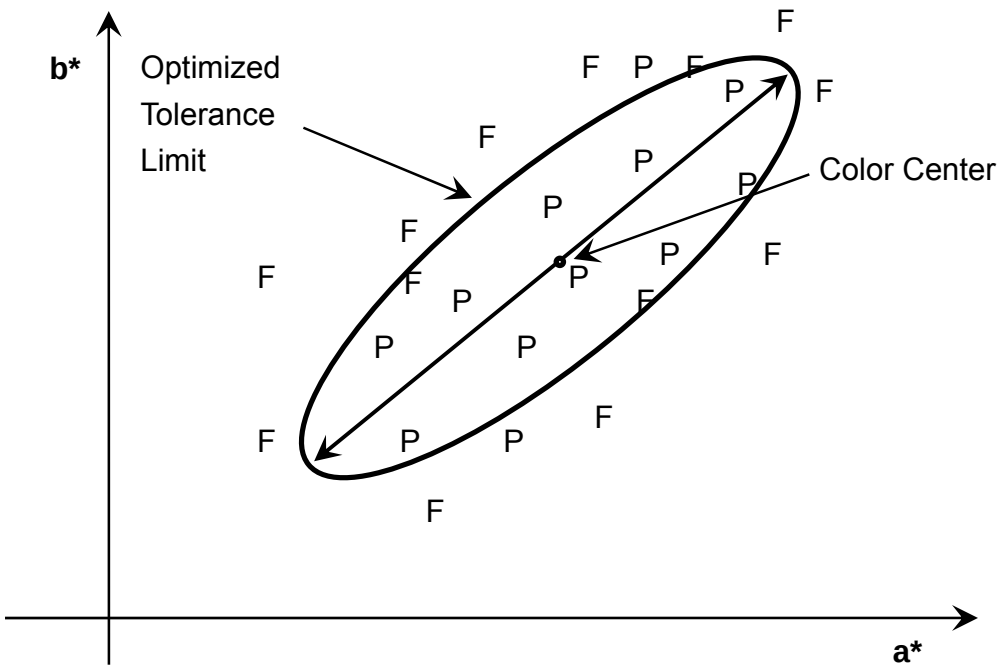

Figure 26. Schematic diagram of an optimized tolerance limit.

In a three-dimensional space, the area covering the acceptability results would take an ellipsoid shape. Ellipsoid shapes have been used to define the experimental tolerance around a given color center. Experimental data show that the shapes and sizes of the tolerance ellipsoids vary through the color space. The cross sections of CMC tolerance ellipsoids on the CIE a*b* plane are shown in Figure 27.

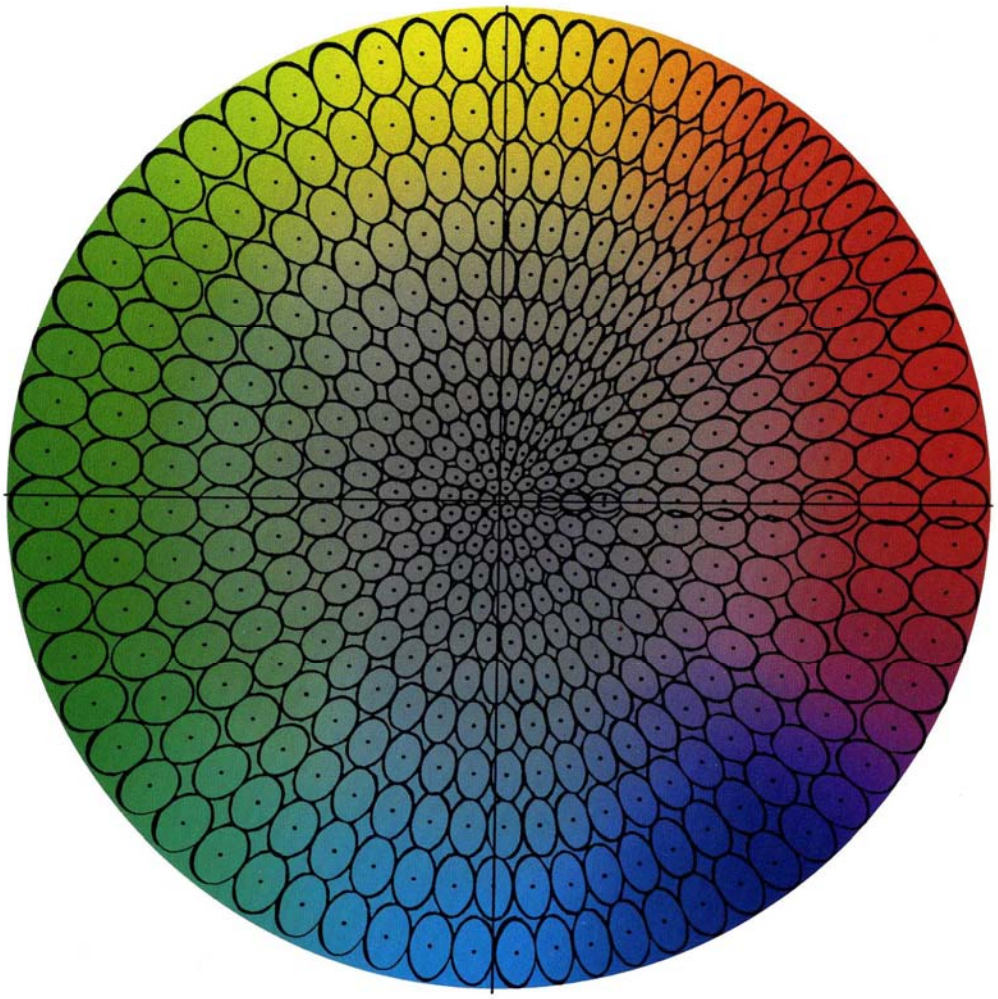

Figure 27. The cross sections of CMC(l:c) tolerance ellipsoids[48].

4.5. Color Difference Evaluations

In a reliable color difference formula increasing ΔE values would correspond with increasing visual color difference values (ΔV). Various measurement methods have been developed to evaluate the performance of a color difference formula against visual datasets. Some of the most important methods for evaluating color difference formulae are briefly discussed in the following sections.

4.5.1. Correlation Coefficient, r

In the earlier studies, the correlation coefficient (r) was widely used to evaluate color difference formulae[49]. The correlation coefficient is obtained using Equation 37

$$r = \frac{N\sum(X_i Y_i) - \sum X_i \sum Y_i}{\sqrt{\left[N\sum {X_i}^2 - \left(\sum X_i\right)^2\right]\left[N\sum {Y_i}^2 - \left(\sum Y_i\right)^2\right]}} \qquad (37)$$

where

X_i is the instrumental value, ΔE, for sample i,

Y_i is the visual value, ΔV, for sample i,

N is the number of pairs of samples.

The correlation coefficient is 1 for a perfect agreement between the visual data and the instrumental data.

4.5.2. Wrong Decision, WD

McLaren introduced the wrong decision method to evaluate the performance of color difference formulae using acceptability data[49]. If the percentage of acceptability for samples is more than 50 it is taken to be visual pass, but if it is less than 50 it is taken to be visual fail. Visual pass/fail decisions corresponding with above/under the ΔE limit are counted as WDs. The color difference formula with a smaller number of WDs is deemed to be performing better.

4.5.3. Performance Factor, PF and PF/3

Luo and Rigg introduced the performance factor (PF), as an evaluation parameter, as shown in Equation 38[45].

$$PF = 100(\gamma + V_{AB} + CV/100 - r) \quad (38)$$

where

$$CV = \frac{\sqrt{\frac{1}{N}\sum (X_i - fY_i)^2}}{\overline{X}} \times 100,$$

$$f = \frac{\sum X_i Y_i}{\sum Y_i^2},$$

$$\log(\gamma) = \sqrt{\frac{1}{N}\sum \left[\log\left(\frac{X_i}{Y_i}\right) - \overline{\log\left(\frac{X_i}{Y_i}\right)} \right]^2},$$

$$V_{AB} = \sqrt{\frac{1}{N}\sum \frac{[X_i - (FY_i)]^2}{X_i F Y_i}},$$

$$F = \sqrt{\frac{\sum \frac{X_i}{Y_i}}{\sum \frac{Y_i}{X_i}}},$$

N is number of pairs,

X_i and Y_i are values of pair.

r indicates the correlation coefficient shown in Equation 37, CV and γ were

introduced by Alder and others[50], and V_{AB} was introduced by Schultz[39]. However, in some cases, the correlation coefficient of PF was stated to be inconsistent with other measures[51] and therefore r was dropped from the model and PF/3 was introduced, as shown in Equation 39.

$$PF/3 = 100\left[(\gamma - 1) + V_{AB} + CV/100)\right]/3 \qquad (39)$$

PF/3 is commonly used as a measurement of fit for deriving or testing color difference formulae. In the case of perfect agreement between visual data and instrumental data, the following values apply; CV = 0, V_{AB} = 0, γ = 1. A PF/3 of 20 indicates a disagreement of about 20%.

5. Dyeing of Polyester

One of the most common synthetic fibers is polyethylene terephthalate (PET) commonly known as polyester. Disperse dyes are usually used to dye polyester. The chemical structure of polyester, some of the major disperse dyes used, and dyeing processes are briefly described in the following sections.

5.1. Chemical Structure of Polyester

PET is made from polymerization of ethylene glycol and terephthalic acid as shown in Figure 28.

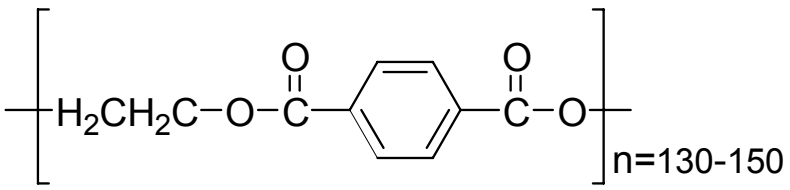

Figure 28. The chemical structure of PET.

5.2. Disperse Dyes

Disperse dyes have very low water solubility and are applied to hydrophobic fibers with the aid of dispersing agents. Disperse dyes have substantivity for hydrophobic fibers. There are two main types of disperse dyes, namely azo and anthraquinone dyes.

5.2.1. Azo Dyes

The azo dyes give mainly light shades such as yellow, orange, and red.

The general structure of azo dyes is shown in Figure 29.

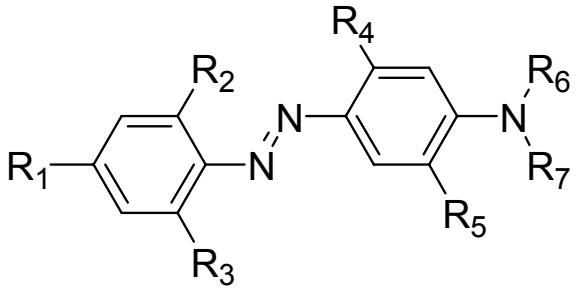

Figure 29. The general structure of azo dyes.

where,

R_1 is electron attracting group, i.e. $–NO_2$, -CN,

R_2, R_3 are H or an electron attracting group,

R_4, R_5 are H or an electron repelling group, i.e. $–CH_3$, $-NH_2$,

R_6, R_7 are H or alkyl or further dye molecule.

5.2.2. Anthraquinone Dyes

The anthraquinone dyes give mainly bright and deep shades such as bluish reds, violets, blues and greens, but the wash fastness obtained is often not very good. The structure of an anthraquinone based disperse dye is shown in Figure 30.

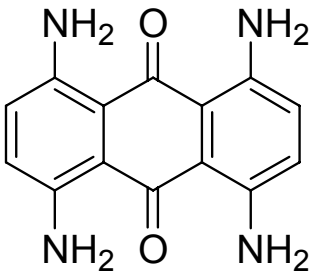

Figure 30. The structure of C.I. Disperse Blue 1.

5.3. Dyeing Process

Polyester fiber can be dyed with three main methods. First of all, polyester can be dyed with dyeing accelerators. Carriers are one of the most common types of dyeing accelerators. Carriers swell fiber and increase dye solubilization. Second, polyester can be dyed at high temperatures. The use of high pressure can elevate temperature up to 130 ºC which allows dyeing without carriers. In addition, DuPont invented a method known as Thermosol® dyeing. Polyester is immersed in a padding solution, the excess liquid is squeezed out, and the fabric is dried at 400-415 ºF for 1-2 minutes. Thermosol® dyeing is a quick process and allows select disperse dyes to move into fiber through sublimation process.

6. Research Proposal

One of the most important aspects of successful industrial colorimetry is the development of an accurate relationship between predicted color difference and visual assessment of the differences between two objects. Many theoretical or empirical models based on mathematical color difference equations have been developed to describe perceptual response to color difference accurately.

Previous researchers have carried out experiments involving samples selected from specific regions of the color space known as color centers. They have determined that a range of correlations exist between visual and predicted measured values and that the performance of the models can be improved.

Kuehni and Marcus carried out an experiment, based on the visual scaling of small color differences involving six color microspaces in the yellow, orange, purple, blue, green, and gray areas of the color space, respectively[52]. The calculation of visual scales was conducted by a ranking experiment, and by subjective estimates. Four color-difference formulas, i.e. CIELAB, CIELUV, FMC-2, and FCM were used to calculate the correlation with the visual scales, and tolerance (or acceptability) ellipsoids were optimized to the visual data. Each of the four color difference formulas produces the highest correlation for at least one of the six sample sets, but each of them is substantially better and substantially worse than the other for some of the other sets.

Witt worked on effects of parameter variations on color difference ellipsoids of sets of painted samples near the five CIE recommended color centers Green, Yellow, Red, Blue, and White[53-55]. The Monte-Carlo method, which was proposed by Alder, was used to determine random colorimetric variations and produce

deviation ellipsoids to describe shells of uncertainty inherent in the data for single observers and for observer groups[56]. The inter-observer and inter-group variability shows random noise, but the variances leave some stability to ellipsoid shapes.

Alman et al. tested the performance of color difference matrices using a color tolerance dataset[57]. 45 color difference vectors varying in five directions at nine color centers under conditions typical of commercial color decisions were used in the dataset. Probit analysis[58] was used to determine the parameters of tolerance distributions for the color difference vectors. A bootstrap technique[57] was used to estimate the variation in uniformity of performance of color difference metrics with sampling of color position and color difference direction. They concluded that there is a significant difference in uniformity of performance of CIE recommended formulae and alternative color difference matrices. Also matrices employing weighted distance based on CIELAB DL*, DC*, DH* color-difference components were shown to be significantly more uniform.

DuPont prepared acrylic painted samples to create multiple color centers around the CIELAB color space[59]. Using a new method of assessing 5 different vectors the authors predicted the tilt of the ellipsoid around the color centers. A response function is found for the observers and a maximum-likelihood model was created (probit analysis). This model works on the basis of rejection probability and tolerances of the rejections. The probit model allows for statistical calculations of the data gathered, which was not possible in the earlier models of the same type. It is found that this new model predicts the tolerances around the color center with a high precision. When plotted against previous color ellipses, the overall agreement was good.

These previous researches indicate that the color difference can be expressed by an ellipsoid shape, because of the nonlinear relationship between visual color-difference perception and values predicted by the particular model. It follows that visual assessment of standard and batch samples that have an equal color difference fall on a xyY plane as an ellipsoid. Ellipsoids are claimed to provide good correlation between the visual assessments and the color difference formulae. However, the CIELAB color difference formula does not predict average color differences with more than 50% accuracy[6]. The ellipsoids corresponding to a visually uniform color space vary greatly in size, eccentricity and orientation.

Especially, the ellipsoids in the blue region have the greatest eccentricity. Luo et al. recently developed a color difference equation based on CIELAB, which was recommended by the CIE as CIEDE2000(K_L:K_C:K_H) [47]. It includes not only lightness, chroma, and hue weighting functions, but also an interactive term between chroma and hue differences for improving the performance of the model in blue region. However, chromaticity discrimination ellipses corresponding to constant DE still have a great eccentricity as shown in Figure 31[39, 60].

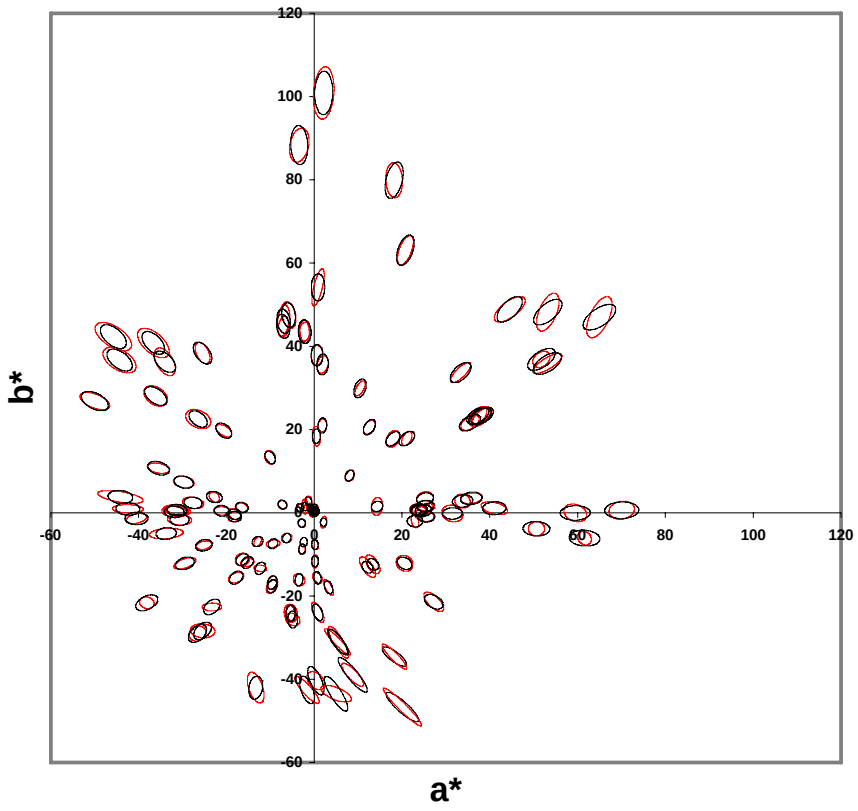

Figure 31. CIEDE2000(K_L:K_C:K_H) predicted ellipses corresponding to BFD and RIT-DuPont experimental datasets[39, 68].

In the present study, 67 blue colored samples around the CIE recommended blue color center (L*=36, a*=5, b*= -31) were produced on plain polyester fabrics dyed with disperse dyes. The color attributes of these samples were measured spectrophotometerically and visual assessments were also obtained. Data were analyzed to assess the performance of several color difference formulae and to obtain the best-fit acceptability model around the blue color center.

II. Experimental

1. Preparation of Blue Samples

A total of 67 blue samples including one of the CIE recommended blue color centers (L*=36, a*=5, b*= -31) were produced. Polyester fabric was dyed with disperse dyes at high temperature conditions (130 ºC). Dye solutions were produced using a Datacolor AutoLab system to precisely control the amount of dye present in each recipe and to minimize variations during the preparation of dyed samples used in visual assessments.

1.1. Fabric Samples

100% knitted polyester fabrics were provided by Color Solutions International, Charlotte, NC. Fabrics were cut into 5 x 5 inch samples for dyeing and dyed samples were cut into 2 x 2 inch dimensions for visual assessment after dyeing. Texture of samples was considered during the preparation of samples to ensure uniformity of all mounted samples.

1.2. Dyes and Auxiliaries

Thirteen Dianix disperse dyes obtained from Dystar® were used to dye samples. The list of dyes is shown in Table 3.

Table 3. List of disperse dyes used in this study.

Dyestuff	Type	Range of pH Stability
Dianix Royal Blue CC	Azo	3.0 - 7.0
Dianix Brilliant Blue R	Unknown	3.0 - 6.5
Dianix Blue CC	Azo	3.0 - 8.0
Dianix Blue S-BG	Anthraquinone	3.0 - 9.0
Dianix Blue XF	Azo	4.0 - 5.0
Dianix Blue UN-SE	Anthraquinone and Azo	4.0 - 7.0
Dianix Navy XF	Azo	4.0 - 5.0
Dianix Red CC	Azo	3.0 - 9.0
Dianix Red CBN-SF	Benzodifuranone	3.0 - 5.5
Dianix Rubine S-2G 150%	Azo	3.0 - 7.0
Dianix Rubine CC	Azo	3.0 - 9.0
Dianix Scarlet CC	Azo	3.0 - 10.0
Dianix Turquoise S-BG	Anthraquinone	3.0 - 9.0

Acetic acid (CH_3COOH) and ammonium sulfate ($(NH_4)_2SO_4$) were used to control pH value around 4.0. Sodium hydroxide (NaOH) and sodium hydrosulfate ($Na_2S_2O_4$) were used in the reduction clearing process to treat dyed samples at a neutral to alkaline pH with an aqueous solution containing a reducing agent, whereby non-bound disperse dyestuff is decomposed such that it does not re-build up on the substrate while the fixed dyestuff remains substantially unaffected.

1.2.1. Laboratory Dyeing Procedures

Dyed samples were distributed around the CIE recommended blue color center (L*=36, a*=5, b*= -31) within 3.00 DE CMC(2:1) or 5.00 DE CIELAB units. Most of the samples, however, were distributed within 2.00 DE CMC(2:1) units from the color center. Samples were prepared such that samples with differences mostly

due to hue alone, chroma alone or lightness alone were obtained. Additional samples with variations due to a combination of hue, chroma and lightness were also obtained. Accurate preparation of dye solutions was needed because the color difference between the standard and batches was very small.

1.2.2. Preparation of Dye Solutions

Precise stock dye solutions were prepared for all dyes used in dyeing recipes. First of all, the blank dyeing was conducted to assess the effects of the dyeing procedure on the color of the substrate. The blank dyeing is a complete dyeing procedure only without any dye present in the dyebath. The blank dyeing procedures include the same auxiliaries, and the same dyeing profiles. Any color change from blank dyeing is considered in an actual dyeing procedure. Second, eight to twelve concentrations of dyes which covered the range used during the dyeing process were selected to characterize the build-up behavior of each dye.

A total of 67 recipes were produced using Datacolor MATCH$_{TM}$ TEXTILE program which is a recipe prediction software based on Dianix disperse dyes dataset. The dataset were provided by Datacolor International. Automatic solution making procedures were applied to obtain precisely controlled dye-stock solutions using Datacolor Solution Maker AutoLab SM and Laboratory Dispenser AutoLab Modulo GT 108/100 as shown in Figures 32 and 33, respectively.

Figure 32. Solution Maker AutoLab SM.

Figure 33. Laboratory Dispenser AutoLab Modulo GT 108/100.

A Solution Maker Autolab SM was used to produce dye-stock solutions automatically, and a Laboratory Dispenser AutoLab Modulo GT 108/100 was used to produce dye solutions based on recipes.

1.2.3. Dyeing Procedures

Dyeing procedures were carried out in the Datacolor Ahiba Spectradye Plus which is an IR heated dyeing machine, as shown in Figure 34.

Figure 34. Ahiba Spectradye Plus.

The dyeing procedures were carried out at high temperature (130 ºC). 1 g/L of Acetic acid (CH_3COOH) and 1 g/L of ammonium sulfate ($(NH_4)_2SO_4$) were used to control the pH around 4.0. pH values were measured using Accumet® pH meter 50 (Fisher Scientific) for each dyeing procedure. A liquor-to-goods ratio was set at 30:1. Temperature was increased to 80 ºC from 50 ºC at a rate of 2 ºC /min, and to 130 ºC from 80 ºC at a rate of 1 ºC /min, respectively. Dyeing time was 45 minutes

at 130 ºC, then the temperature was reduced to 80 ºC. The profile of the dyeing procedure is shown in Figure 35.

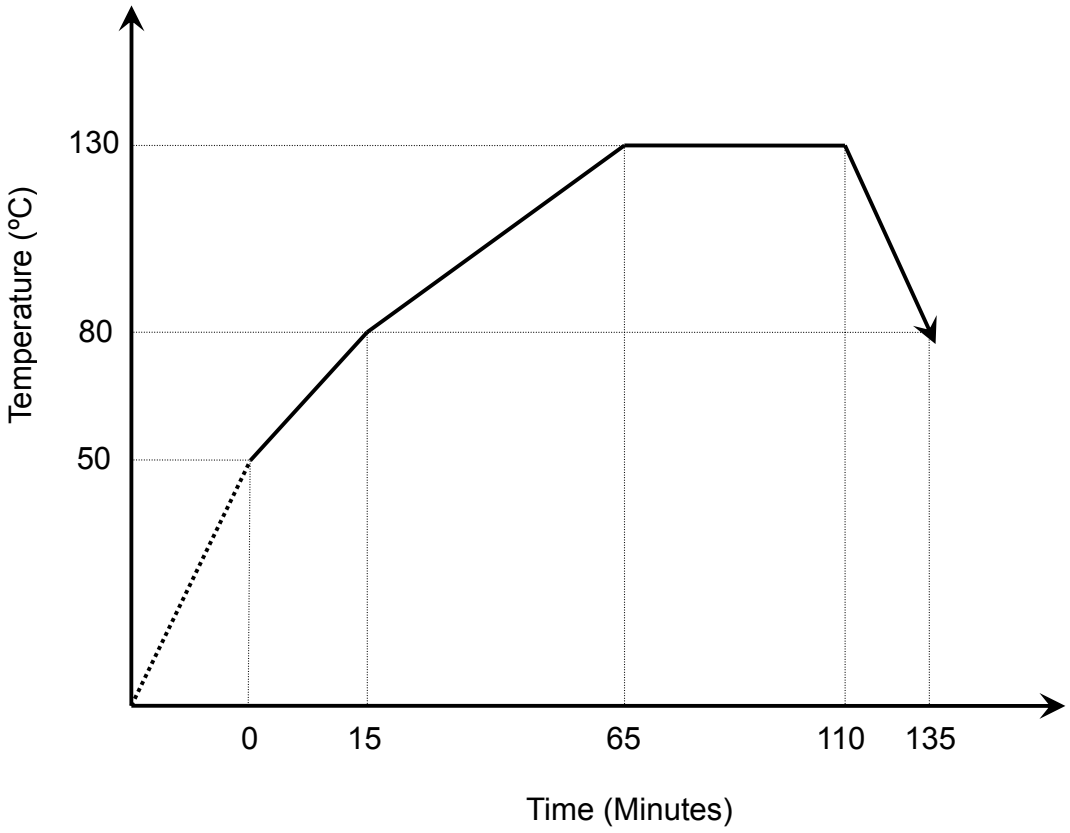

Figure 35. Profile of the dyeing procedure.

Reduction clearing was carried out in an aqueous solution containing sodium hydroxide (2 g/L) and sodium hydrosulfate (2 g/L) at 80 ºC for 15 minutes and a liquor ratio of 50:1. Finally, dyed polyester fabrics were rinsed in aqueous solution with AATCC standard detergent without optical brightener at 80 ºC for 5 minutes and then were dried.

2. Instrumental Measurement Procedures

The color attributes of fabrics were measured by Datacolor Spectraflash SF600X spectrophotometer depicted in Figure 36.

Figure 36. Spectraflash SF600X.

CIE illuminant D65 and CIE 10° supplemental standard observer were used for all colorimetric calculations. Large Area View (LAV) aperture was used, UV light was excluded and specular light was included. Each sample was folded into 4 layers to ensure opacity and was measured a total of 8 times and averaged. Samples were rotated 90° and repositioned after each reading to reduce measurement variability due to fabric construction, directionality of yarns, and unleveled dyeing.

3. Visual Assessment Procedures

Visual assessments were conducted using 26 observers. A total of three repetitions were conducted. Samples consisted of a standard CIE recommended blue color center (L*=36, a*=5, b*= -31) and 66 batch samples. Thus, each repeat consisted of 66 sample pairs and was divided into 2 groups with 33 random sample pairs each to avoid observer fatigue during assessments. The interval between repeat sessions for each observer was at least one week. A total of 5148 visual assessments were conducted.

3.1. Preparation of Samples for Visual Assessment

The samples were mounted on PVC backing. Each PVC was precisely cut into 1 x 9 and 2 x 9 inch sections for each sample. These backings were then glued together using PVC cement and allowed to dry. The 2 x 9” PVC was then painted with a gray paint that corresponded to the Munsell value of 7.25 (N7.25). The 2 x 2” blue dyed sample was then mounted onto the PVC using a double-sided adhesive film and a thin, but stiff plastic. The picture of front and reverse sides of a sample mount is shown in Figures 37 and 38, respectively.

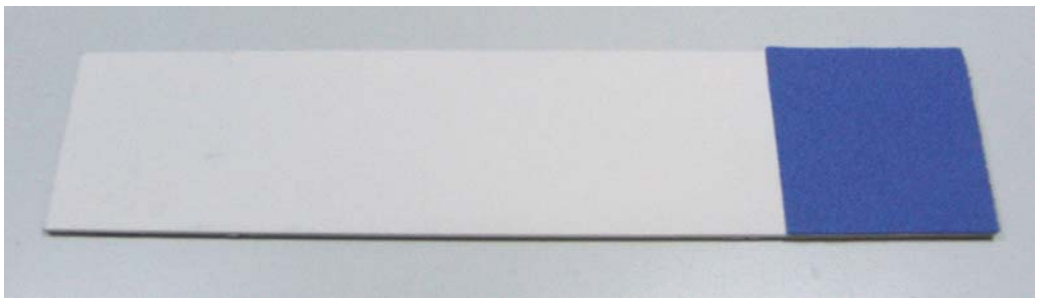

Figure 37. Front side of a sample mount including dyed sample.

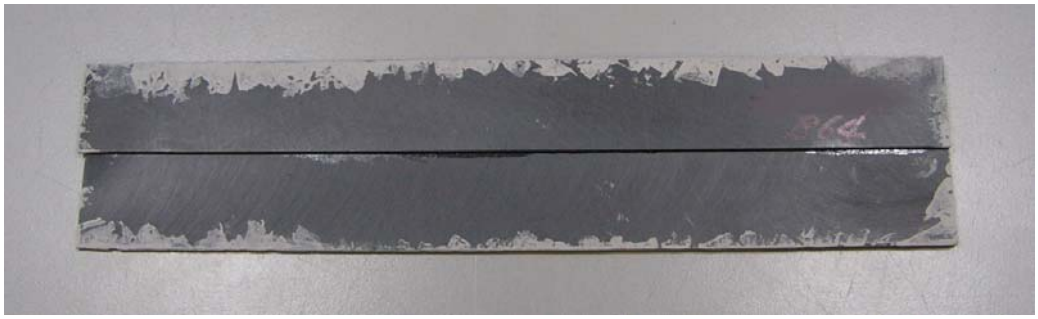

Figure 38. Reverse side of a sample mount.

A total of 67 dyed samples were prepared, in the manner described above, for visual assessments as shown in Figure 39.

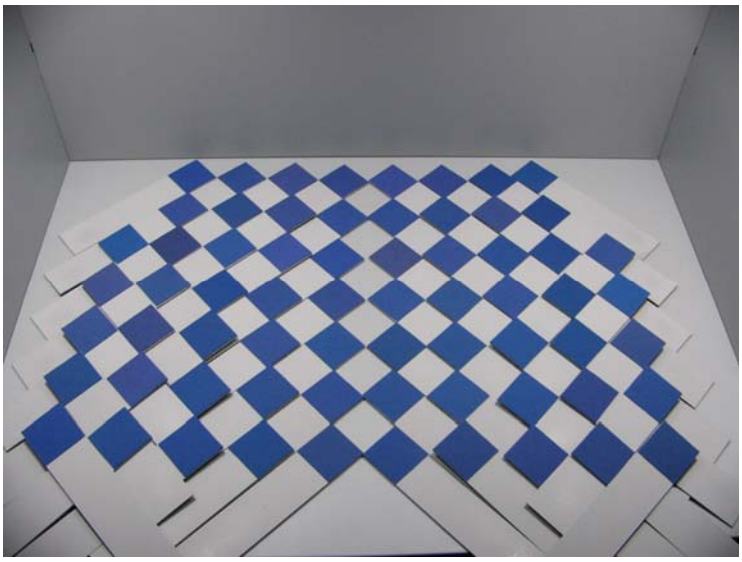

Figure 39. Mounted dyed samples used in visual assessments.

3.2. Preparations of Gray Scale

Although standard gray scale papers, supplied by X-rite, were used in this

study, a special set of gray scale were produced in-house for visual assessments. Standard gray papers were cut into 2 x 2 inch dimensions corresponding to the size of fabric samples used in the study to reduce variability due to size with sample pairs. The standard AATCC gray scale and gray scale produced at NCSU are shown in Figure 40.

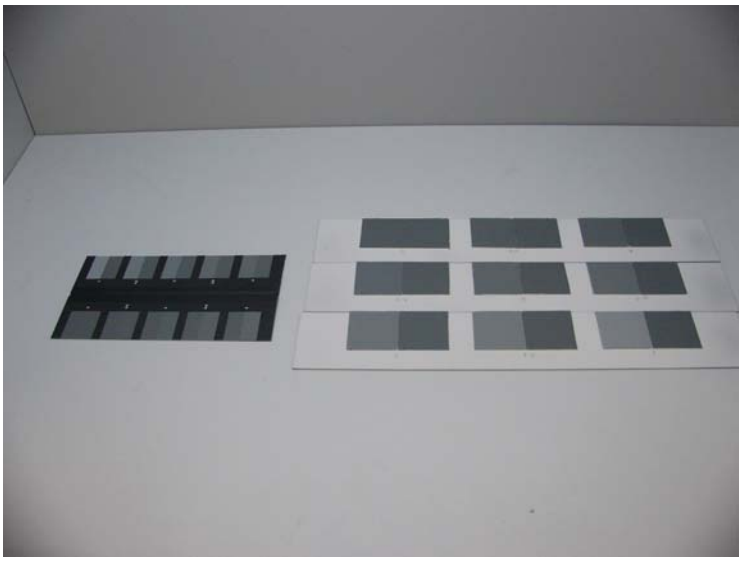

Figure 40. AATCC standard gray scale (left) and gray scale used in this study (right).

The gray scale grades range from 1 to 5 by 0.5 intervals (i.e. 1, 1.5, 2, 2.5, 3, 3.5, 4, 4.5, and 5). Each grade is consisted of a pair of two gray samples. Higher grades represent smaller color difference between a pair of samples. A grade of 5 represents no color difference between the samples within the pair. The pairs of gray scale were also mounted on PVC. Each PVC piece was cut into 3 x 18 inch dimensions. The PVC was then painted with a gray paint corresponding to the Munsell value of 7.25 (N7.25). Two sets of gray scale were prepared. In one of

the sets the location of the darker sample within pairs was reversed to facilitate observer rating during visual assessment without the need to rotate gray scale as shown in Figures 41 and 42, respectively.

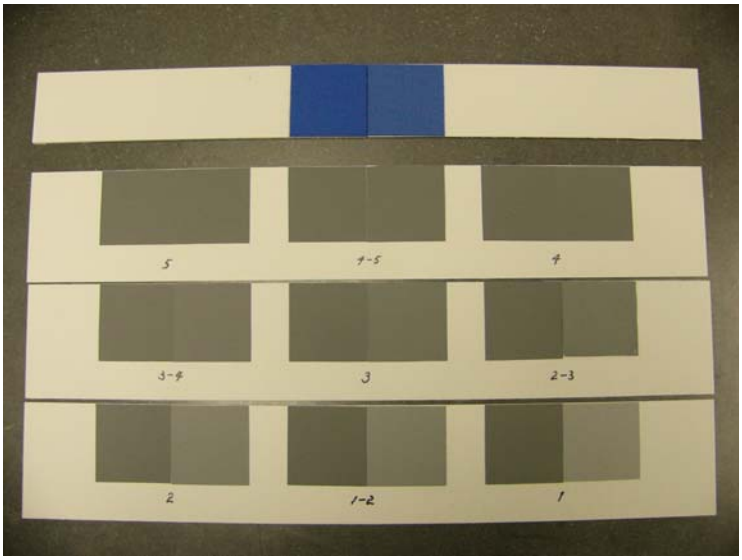

Figure 41. Gray scale with the darker samples on the left.

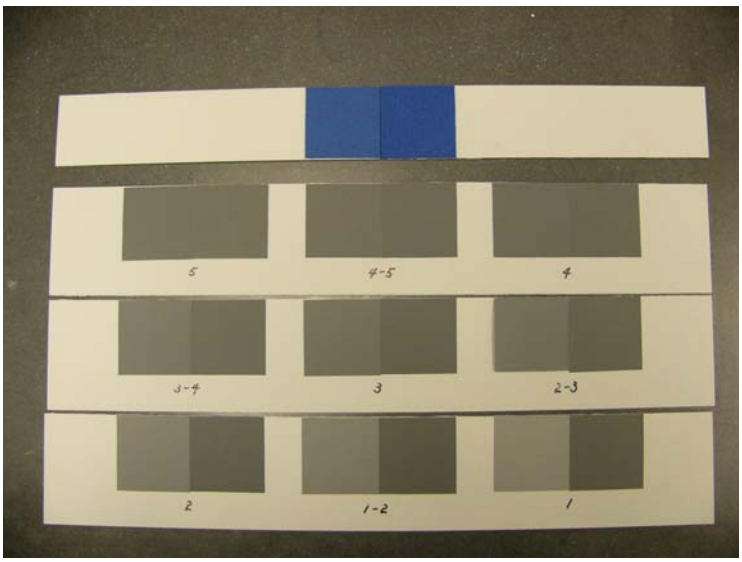

Figure 42. Gray scale with the darker samples on the right.

3.3. Observers

A total of 26 observers participated in visual assessments. All observers were tested for normal color vision using the Isihara confusion plates[61]. 16 observers were male, and 10 observers were female. Observers ranged between 21-36 years of age. Half of the observer population comprised of Korean students and the rest were from diverse cultural backgrounds. Most of the observers were students and would be considered naïve for the purpose of visual assessment.

3.4. Visual Assessments

Spectralight® III (X-rite) was used as a viewing booth and a filtered incandescent daylight simulating lamp was used as light source. All other extraneous light sources were excluded during the assessment. The light booth is shown in Figure 43.

Figure 43. Light booth with D65 illuminant.

The viewing conditions for the visual assessment included 45/0 illumination viewing geometry. The observers viewed sample pairs at a 90º angle relative to the specimen. This is schematically shown in Figure 44.

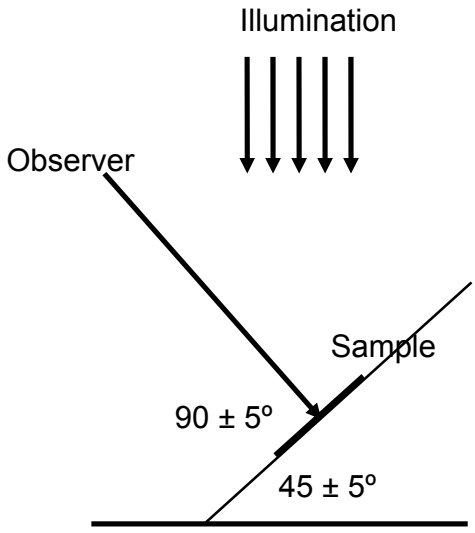

Figure 44. Viewing conditions used in visual assessments.

The samples were placed on railings on a custom made panel together with the gray scale as shown in Figures 45 and 46.

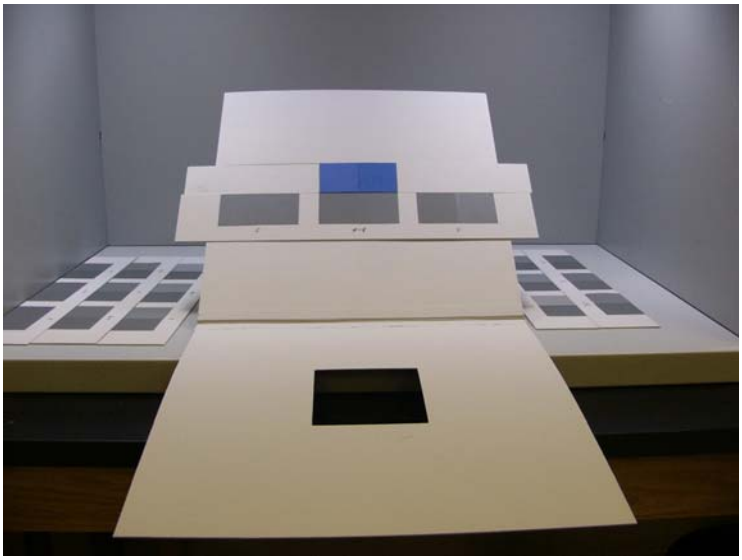

Figure 45. Sample stand with front panel open showing dyed samples as well as gray scale.

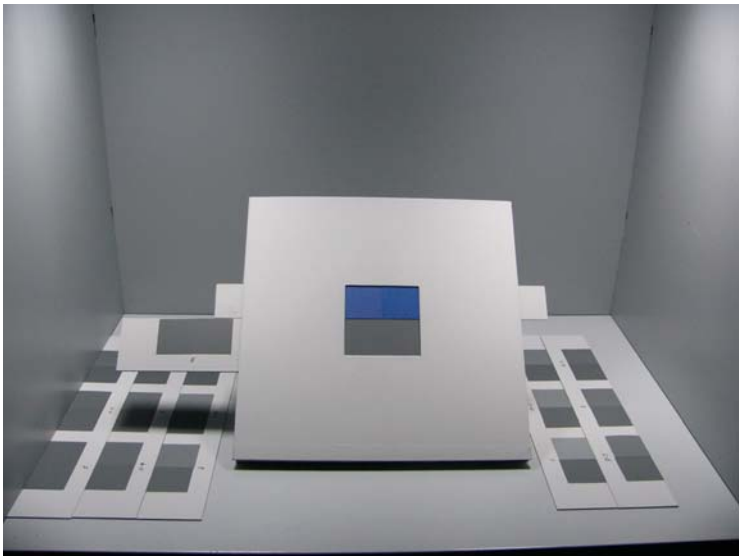

Figure 46. Sample stand as viewed by observers.

A custom made sample stand painted in neutral gray (Munsell N7.25) was used that housed two samples (standard and a batch) as well as a pair of gray scale

underneath dyed samples. The stand included a front panel to provide a viewing window of dyed samples on top and gray scale samples below dyed samples. The viewing window was cut at a 45 degree angle to avoid casting shadow on samples during illumination. Gray scale pairs mounted on PVC could slide inside railings to facilitate comparison of a suitable set against the dyed sample pair inside the viewing window. All samples were cut with sharp edges and there was no distance between samples. Samples were placed on the stand by the assessor who wore a gray lab coat and gray gloves. Observers were also asked to wear a gray lab coat and gloves. They were adapted to light for at least 2 minutes during which the following instructions were read:

“Thank you for agreeing to be an observer in this visual assessment. I am going to let you adapt to the light for two minutes. In the meantime I will explain to you what we are going to do. The purpose of this study is to understand the perception of color. There is no right or wrong answer.
This is the first of four sessions in which you will be assessing for me. I will be presenting to you a colored pair and two sets of gray scale. I would like you to tell me which gray scale difference is closest in agreement with the perceived color difference of the displayed colored pair. The result can be between two steps, such as 3-4. In such case, please be specific and try to give me a decimal point. The two gray scale are identical. The one to your right has the darkest samples on the right and the one to your left has the darkest samples on the left. So you don’t have to rotate the gray scale when comparing with the colored pair. The gray scale can move along the bar on which it rests to aid the evaluation. The gray scale is very delicate, so please be careful when handling it. It scratches easily.
Do you understand the instructions? Are you ready to begin?”

Observers were asked to rate the color difference of the pair of dyed samples presented to them compared to the gray scale, as shown in Figure 47.

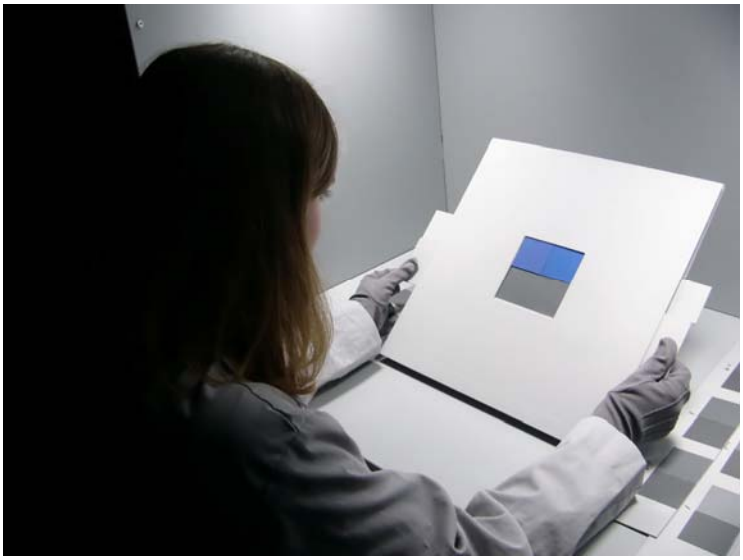

Figure 47. Visual assessment with one of the observers.

The observers gave responses of the perceived color difference between the standard and the batch in reference to the gray scale for 66 pairs of dyed samples. The pairs were presented in two sessions (33 pairs in session 1 and 33 pairs in session 2) to prevent observer fatigue due to a large number of color observations in a single session. A random number set generator was used to create a pair presentation order for each observer. A total of 3 repetitions were conducted to assess inter, intra-group variability, and individual observer repeatability.

III. Results and Discussion

1. Instrumental Measurements

A total of 67 blue samples around one CIE recommended color center were measured using a Datacolor SF600X spectrophotometer. The color attributes of the blue color center are given in L*, a*, and b*, respectively. All color attributes of samples and color differences calculated based on CIELAB, CMC, CIE94, and CIEDE2000 are shown in Appendix A.

The plots of these color attributes in CIE L*a*b* planes are shown in Figures 48-51. The image on the right broadly shows the location of the color center; while the image on the left illustrates the distribution of samples around the standard.

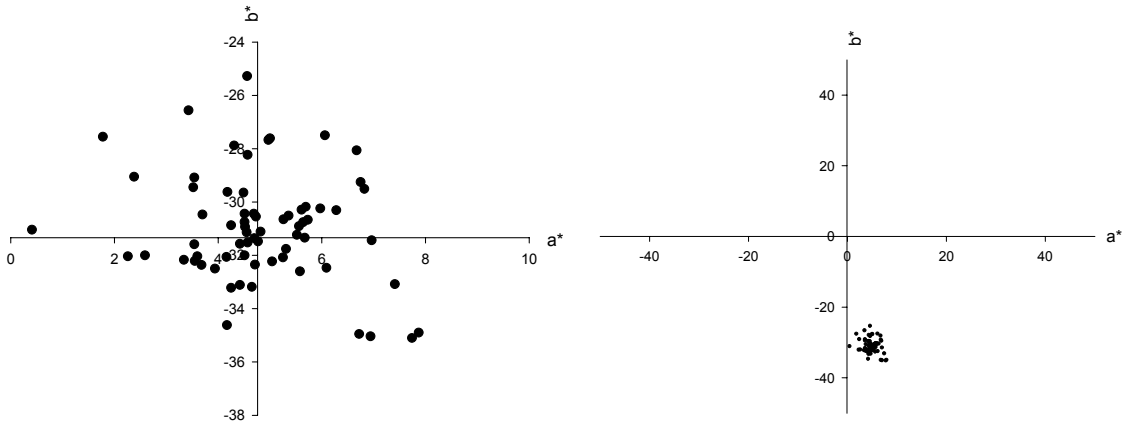

Figure 48. Position of samples on a CIE a*b* plane.

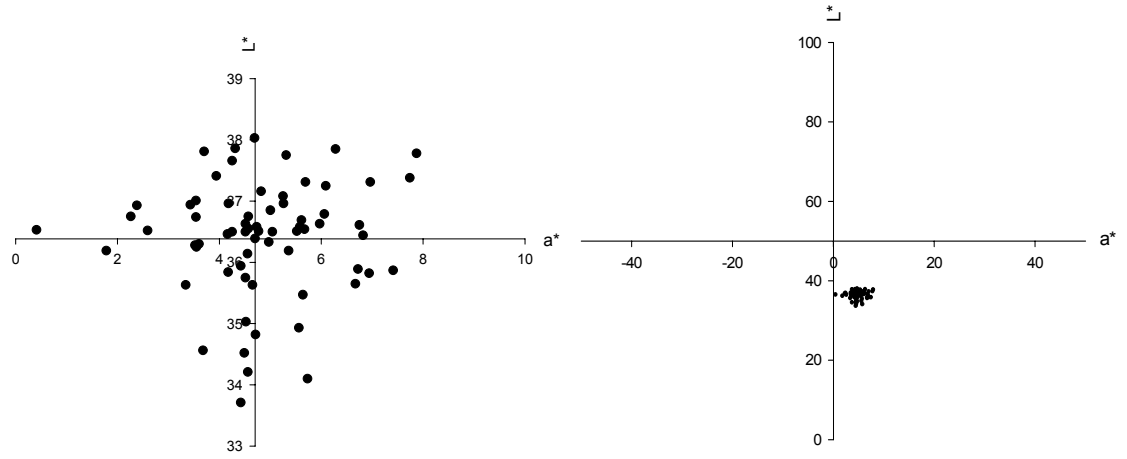

Figure 49. Position of samples on a CIE L*a* plane.

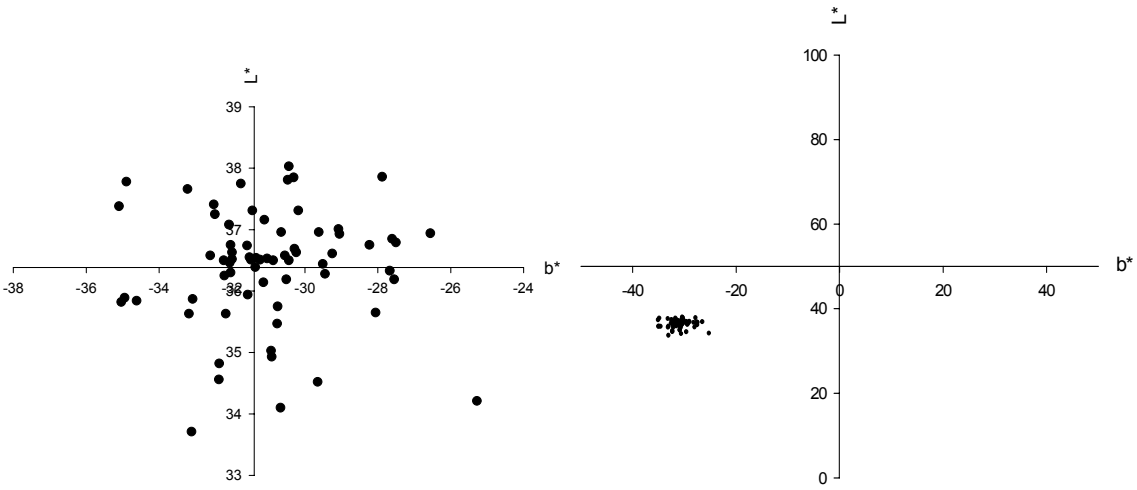

Figure 50. Position of samples on a CIE L*b* plane.

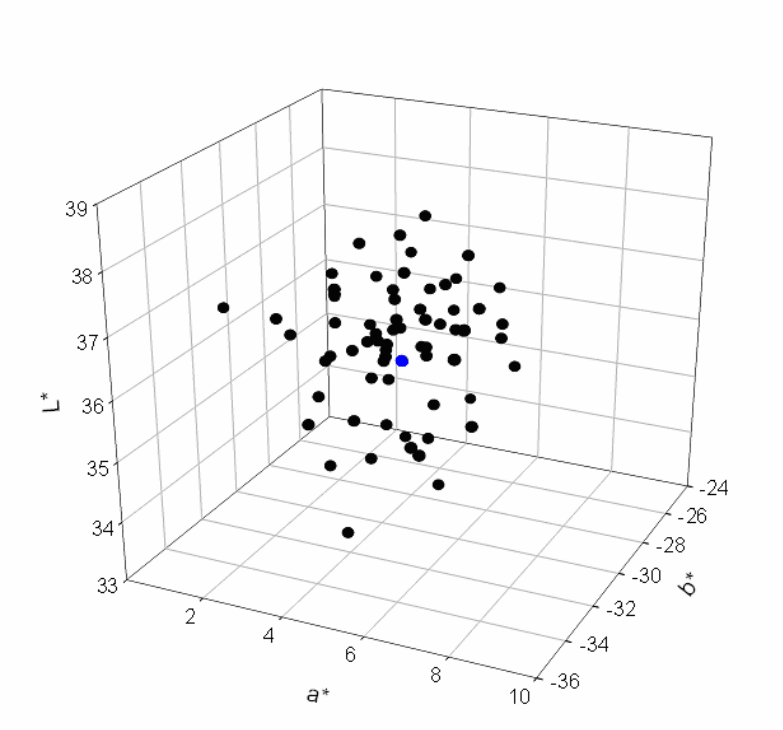

Figure 51. Location of all samples on a CIE L*a*b* color space (the blue dot shows the location of the standard).

2. Conversion of Gray Scale to Visual Color Differences

Visual assessments were conducted using the gray scale described in section 4.2.1. Gray scale ratings and associated color differences using CIELAB, CIE94(1:1:1), CMC(1:1), and CIEDE2000(1:1:1) are shown in Table 4. Raw data is given in Appendix F. Apart from size the gray scale used in this study was identical to that used and recommended by the AATCC[38].

Table 4. Gray scale ratings corresponding to CIELAB, CIE94(1:1:1), CMC(1:1), and CIEDE2000(1:1:1) color differences.

Gray Scale Rating	Measured				Calculated DE			
	L*	a*	b*	ΔL*	CIELAB	CIE94 (1:1:1)	CMC (1:1)	CIEDE2000 (1:1:1)
5	42.14	-0.93	-1.04	0.00	0.00	0.00	0.00	0.00
4.5	42.97	-0.84	-0.98	0.83	0.84	0.84	0.85	0.77
4	43.73	-1.19	-1.22	1.59	1.62	1.62	1.66	1.51
3.5	44.62	-0.97	-1.43	2.48	2.51	2.51	2.56	2.32
3	45.46	-1.41	-1.11	3.32	3.36	3.35	3.42	3.16
2.5	46.84	-1.15	-1.28	4.70	4.71	4.71	4.77	4.43
2	49.03	-1.28	-1.29	6.89	6.90	6.90	6.98	6.61
1.5	51.28	-1.40	-1.44	9.14	9.16	9.16	9.27	8.91
1	55.76	-1.14	-1.52	13.62	13.63	13.63	13.77	13.58

Gray scale ratings can be converted to visual color difference values using a polynomial fitting. A forth-degree and a third-degree polynomial equation were initially tested. Equations were examined using a statistical analysis program (SAS) to prevent over-fitting of data to equations. It was found that the difference between third and fourth-degree polynomial coefficients, obtained for all color difference equations at 95% confidence levels, was statistically insignificant. The results of a

third-degree polynomial fitting were, however, statistically significant when tested against other fitting functions. The use of fourth-degree polynomial equation to convert gray scale ratings to visual data results in over-fitting. Therefore, a third-degree polynomial equation was used for data analysis. Full SAS results are shown in Appendix B. Figures 51-54 show best fit curves for CIELAB, CIE94(1:1:1), CMC(1:1) and CIEDE2000(1:1:1) against gray scale ratings using third-degree polynomial Equations 40-43, respectively.

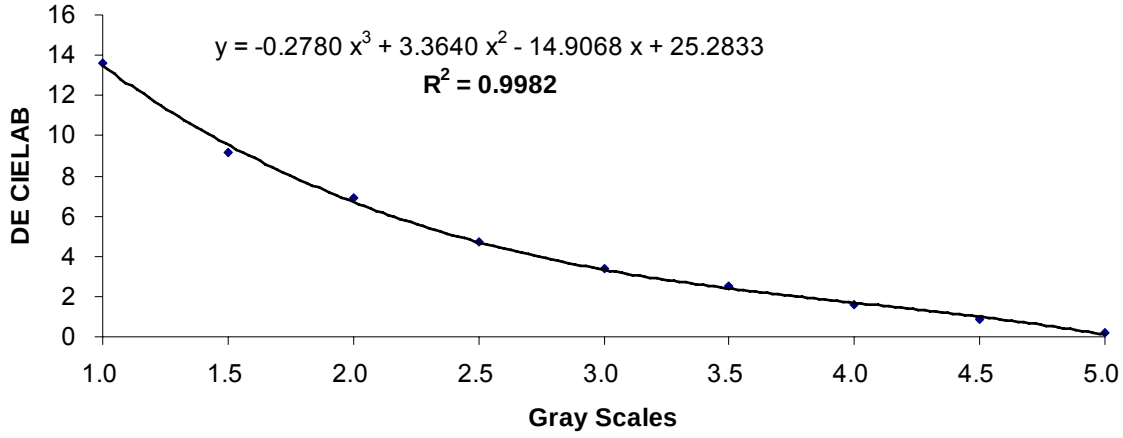

Figure 51. Third-degree polynomial best fit curve for CIELAB.

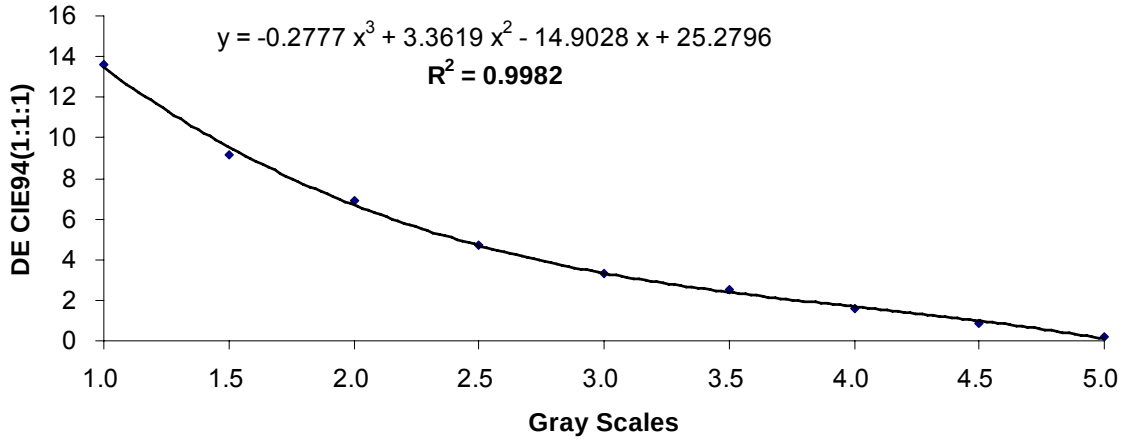

Figure 52. Third-degree polynomial best fit curve for CIE94(1:1:1).

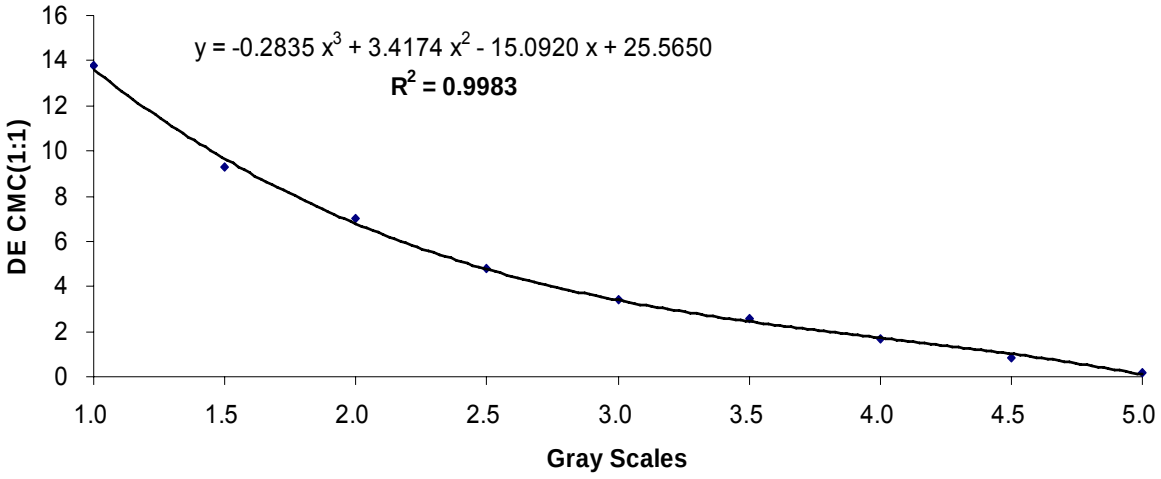

Figure 53. Third-degree polynomial best fit curve for CMC(1:1).

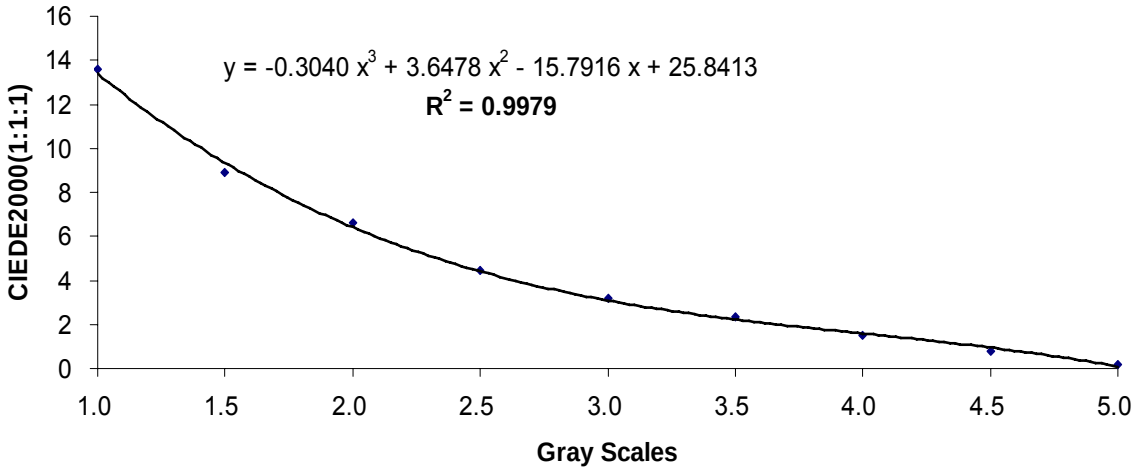

Figure 54. Third-degree polynomial best fit curve for CIEDE2000(1:1:1).

All equations demonstrate high coefficient of determination (R^2) which is the proportion of variability in response variables. The third-degree polynomial equations for transforming gray scale ratings given for each pair *i* (G) to visual color

differences, DV, are shown in Equations 40-43 below:

$$DV_{i(CIELAB)} = 25.2833 - 14.9068G_i + 3.3640G_i^2 - 0.2780G_i^3 \quad (40)$$

$$DV_{i(CIE94(1:1:1))} = 25.2796 - 14.9028G_i + 3.3619G_i^2 - 0.2777G_i^3 \quad (41)$$

$$DV_{i(CMC(1:1))} = 25.5650 - 15.0920G_i + 3.4174G_i^2 - 0.2835G_i^3 \quad (42)$$

$$DV_{i(CIEDE2000(1:1:1))} = 25.8413 - 15.7916G_i + 3.6478G_i^2 - 0.3040G_i^3 \quad (43)$$

Each observer's gray scale ratings were transformed to color differences using above Equations. Correlation between the results of transformed visual color differences (DV) and respective calculated color difference equations (DE) are shown in Figure 55.

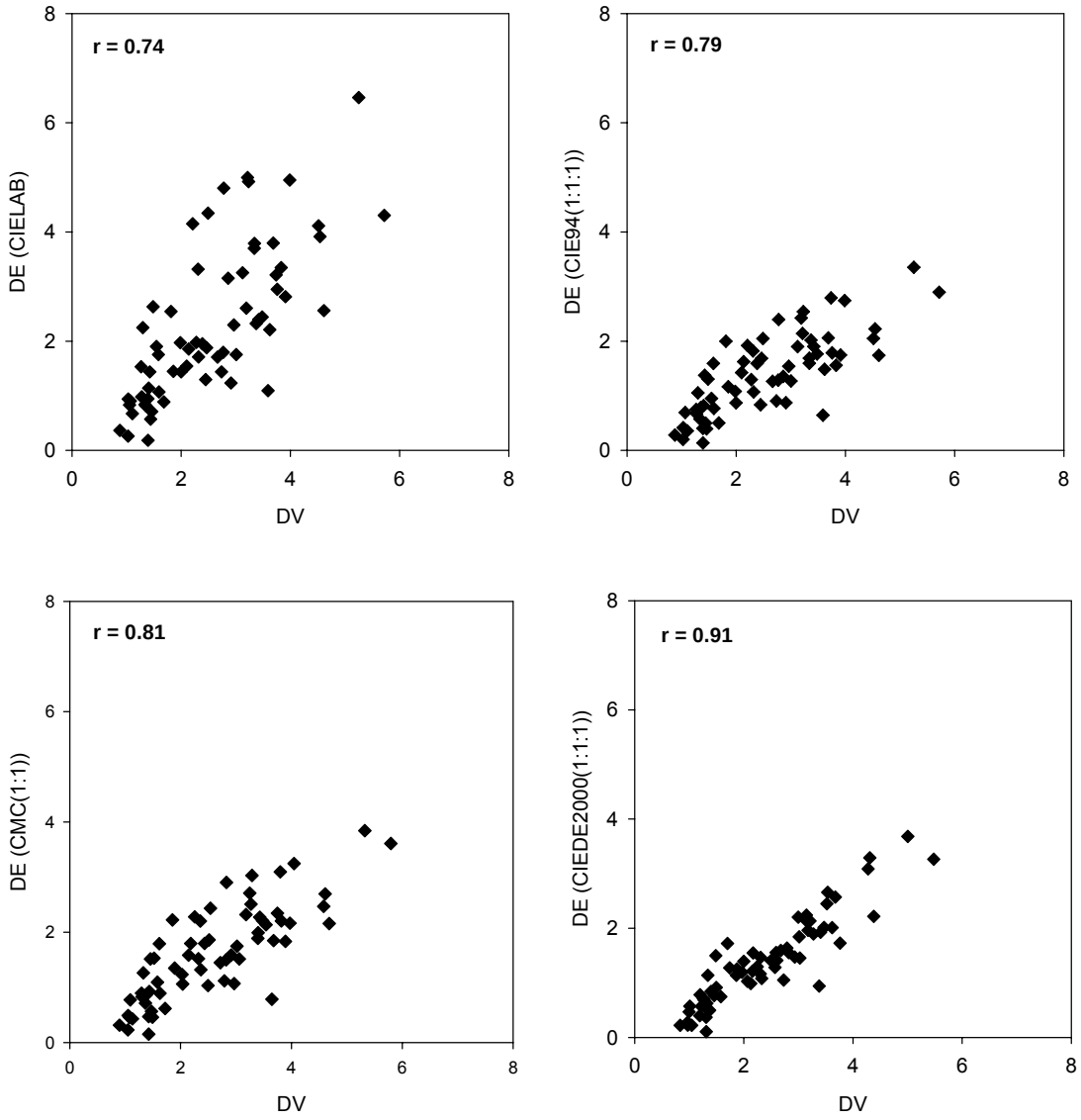

Figure 55. Correlation between the results of transformed visual color differences (DV) and calculated color difference (DE) equations.

As can be seen the correlation between converted gray scale ratings and calculated color difference values improves from CIELAB to CIE94(1:1:1) to CMC(1:1) and finally the CIEDE2000(1:1:1) which shows the best performance compared to other equations. The CIELAB equation shows the lowest correlation

with visual data (r = 0.74), however, CIEDE2000(1:1:1) shows the best results, (r = 0.91) among the color difference formulae examined.

A close examination of equations 40-43 reveals that coefficients obtained from four different polynomial equations are very similar to each other. When using gray scale, the lightness difference is the main factor affecting the results of color difference during the conversion process. Thus, lightness factor (i.e. lightness adjustment factor) in each color difference formula can significantly affect the correlations obtained with various formulae. The polynomial equations obtained for CIELAB and CIE94 (1:1) are almost identical since no lightness adjustment factor exists for CIELAB and the lightness adjustment factor (S_L) is fixed at 1 for CIE94(1:1) as shown in Equations 31 and 35, respectively. CMC(1:1) and CIEDE2000(1:1:1) equations use different lightness adjustment factor as shown in Equations 33 and 36, respectively, but the results from lightness difference from gray scale pairs are not far away from where lightness adjustment factor (S_L) differs significantly from 1. Thus, there is little or no difference between each of the polynomial equations. It was decided therefore to use the CIELAB based polynomial function, shown in Equation 40, to transform gray scale grades to DV values. The correlations between the results of transformed visual color differences (DV) and color difference (DE) equations using the CIELAB based polynomial function are shown in Figure 56. A comparison of Figures 55 and 56 shows that the correlation between visual assessments and calculated values is not changed when a single fit function is used for all formulae. The performance of the CMC(1:1) and CIEDE2000(1:1:1) equations according to PF/3 assessments is also not significantly affected when the CIELAB based polynomial function is used for conversions as shown in Table 5.

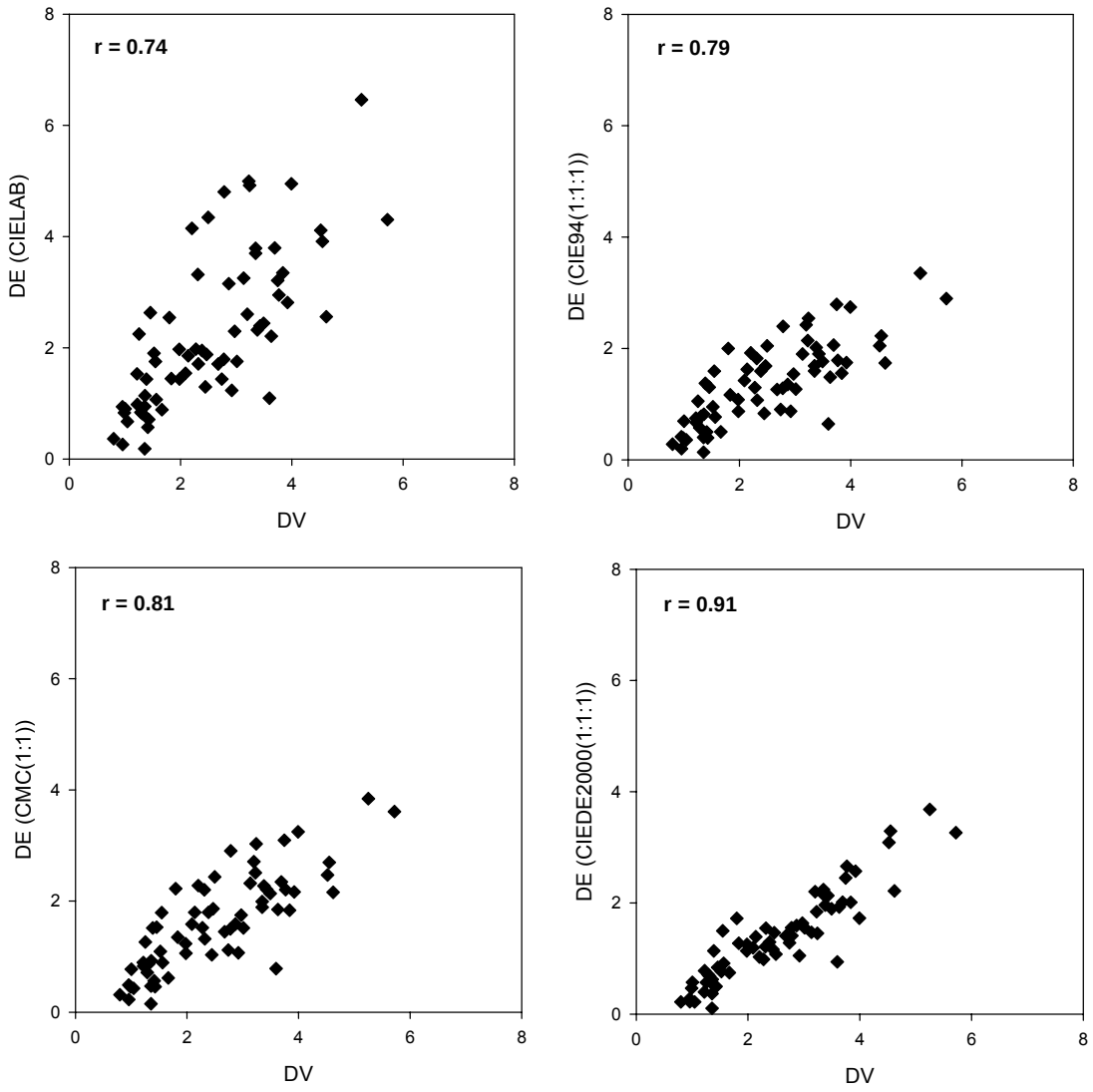

Figure 56. Correlation between the results of transformed visual color differences (DV) and calculated color difference values (DE) using CIELAB based polynomial function.

Table 5. PF/3 of color difference formulae based on the use of individual polynomial functions and based on using CIELAB based polynomial function.

	CIELAB	CIE94 (1:1:1)	CMC (1:1)	CIEDE2000 (1:1:1)
PF/3 when CIELAB based polynomial function is used	50.01	43.13	41.93	37.96
PF/3 when individual polynomial functions are used	50.01	43.12	41.95	37.97

The change in the performance of the color difference equations is insignificant when a single function is used. Therefore, it is reasonable to use a single best-fit function to compare converted gray scale ratings (DV) to various color difference equations.

3. Group (Inter-observer), Individual (Intra-group) Variability and Observer Repeatability

A total of 3 repetitions (Trial 1, 2, and 3) were conducted with 26 observers. *Group (Inter-observer) variability* means the variability between groups of observers for each repetition or repeatability of trial responses for the whole group. The significance of differences between repetitions was tested by comparing group responses from each trial against group mean visual results obtained from each pair. *Intra-group variability* is the variability between responses of an individual observer compared to group mean responses for each trial. The significance of differences between responses obtained from an individual observer for each trial was tested using individual observer's mean visual results calculated for each pair. *Individual observer repeatability* was tested by comparing the variability between responses given for each trial by an individual observer. In other words, it indicates the repeatability of assessments by an observer. Two statistical methods, i.e. paired t-test and PF/3, were used to assess inter and intra-group variability. Results are shown in the following sections.

3.1. Paired t-test

The paired t-test determines whether two sets of data differ from each other in a significant way under the assumption that the paired differences are independent. The paired t-test is generally used when measurements are taken from the same population with one or more variable changes. The formula is shown in Equation 44.

$$t = \frac{\bar{d}}{\sqrt{s^2/n}} \qquad (44)$$

where

$\bar{d}$ is the mean difference, s^2 is the sample variance ,and n is the sample size.

Since the existing AATCC recommended gray scale is perceptually non-linear, the gray scale ratings were converted to linear visual responses. Gray scale ratings were transformed to CIELAB color differences using a third-degree polynomial equation. Group variability based on paired t-tests for the CIELAB is shown in Table 6.

The hypotheses are:

Null hypothesis (H_0): mean of the paired difference between trial A and trial B is 0, i.e.: (H_0: $\mu_A - \mu_B = 0$)

Alternative hypothesis (H_a): mean of the paired difference between trial A and trial B is not 0, i.e.: (H_a : $\mu_A - \mu_B \neq 0$)

Confidence interval was set at 95%. If null hypothesis is proved there would be no significant difference between two sets of data. Confidence level determined the range of p-value.

Table 6. Group (Inter-observer) variability using paired t-test.

Difference	DF	T-Statistic	P-value	Adoption
Trial 1- Trail 2	65	-2.73	0.0080	H_a
Trial 2- Trail 3	65	-0.91	0.3677	H_0
Trial 1- Trail 3	65	-2.61	0.0112	H_a

At 95% confidence level, if p-value is greater then 0.05 there is no significant difference between the results. The difference between trials 1&2 and 1&3 is significant as the p-value is smaller than 0.05. This may be due to a training effect, for instance, most observers may feel more comfortable in providing responses to visual assessments after familiarization with the procedure. The summary of the variability between each trial for individual repeatability is shown in Table 7. The full table of the variability between each trial for an individual observer is given in Appendix C.

Table 7. The summary of the variability between each trial for individual observers (individual repeatability).

Difference	No. of H_0 (N=26)	% Adoption of H_0
Trial 1- Trail 2	17 / 26	65.38
Trial 2- Trail 3	17 / 26	65.38
Trial 1- Trail 3	14 / 26	53.85
Total	48 / 78	61.54

The *No. of null hypothesis, H_0,* refers to the number of observers that provide statistically repeatable results between assessments in two trials. The percentage adoption refers to total out of 100 of observers that do provide statistically repeatable assessments between trials. In other words a large adoption of *alternative* hypothesis would indicate poor repeatability of individual observer assessments between trials. Results indicate that percentage adoption of null hypothesis, for differences between trial 1 and trial 3 are slightly decreased compared to other sets. This may be due to observer training effect during repeat assessments. The

variability between each trial for an individual observer (individual repeatability) was also tested according to gender. The results are shown in Table 8.

Table 8. The summary of the variability between each trial for an individual observer (individual repeatability) by gender.

	Gender			
	Male (N=16)		Female (N=10)	
Difference	No. of H_0	% Adoption of H_0	No. of H_0	% Adoption of H_0
Trial 1- Trial 2	10 / 16	62.50	7 / 10	70.00
Trial 2- Trial 3	11 / 16	68.75	6 / 10	60.00
Trial 1- Trial 3	11 / 16	68.75	3 / 10	40.00
Total	32 / 48	66.67	16 / 30	53.33

According to % adoption of H_0, the repeatability between trial 2 and trial 3 as well as for trial 1 and trial 3 for males is more significant than that for females. Also, perhaps because the number of male observers is larger than that of females, male observers on average provided more repeatable assessments. The variability between each trial for an individual repeatability was also conducted by nationality of the observers as 13 out of 26 observers (9 males, 4 females) were from South Korea. The results are shown in Table 9. Nine observers in total provided repeatable assessments between trials, 7 were male (3 Korean, 4 international) and 2 were female (0 Korean, 2 international).

Table 9. The summary of the variability between each trial for an individual observer (individual repeatability) by nationality.

	Nationality			
	Korean (N=13)		International (N=13)	
Difference	No. of H_0	% Adoption of H_0	No. of H_0	% Adoption of H_0
Trial 1- Trail 2	7 / 13	53.85	10 / 13	76.92
Trial 2- Trail 3	7 / 13	53.85	10 / 13	76.92
Trial 1- Trail 3	6 / 13	46.15	8 / 13	61.54
Total	20 / 39	51.28	28 / 39	71.79

According to % adoption of H_0, the repeatability in responses between trials is higher for international observers. None of the Korean female observers gave statistically repeatable assessments between trials, whereas three out of 9 Korean male observers were found to give statistically repeatable responses. However, the number of observers may not be large enough to enable assessing the repeatability of subsets of data, such as those related to gender or nationality of observers, and therefore such analyses should be treated with caution.

Paired t-test was also conducted to assess the intra-group variability between responses given by an individual observer and mean group responses for each trial. The summary of results is shown in Table 10 and full results for intra-group variability are given in Appendix D.

Table 10. The summary of intra-group variability.

Difference	No. of H_0 (N=26)	% Adoption of H_0
Observer- Group Mean - Trial 1	6 / 26	23.08
Observer- Group Mean - Trial 2	5 / 26	19.23
Observer- Group Mean - Trial 3	3 / 26	11.54
Group Mean – Trial Mean for each observer	1 / 26	3.85

Results indicate that the variability between individual observer responses compared to mean group response for each trial is significant. It further indicates that most observers give significantly different responses compared to the mean group response.

3.2. PF/3

The definition of PF/3 is given in section 4.5.3. PF/3 can be used to verify intra-group variability as well as observer repeatability. In order to obtain intra-group variability, PF/3 is calculated with individual observer's DV results for each trial and the mean group visual DV results for each trial (i.e. DV for observer 1 in trial 1 versus group mean DV for trial 1). To assess observer repeatability, PF/3 is calculated by taking into account individual observer response between the trials (i.e. DV for observer 1 in trial 1 versus DV for observer 1 in trial 2, etc.). In these cases, PF/3 scaling factors f and F were set to 1. This means that all the visual results from an experiment are already in the same scale. For example, in the visual assessment using the gray scale, all observers carry out the assessment against the same gray scale. The observer repeatability is shown in Table 11 and Figure 57.

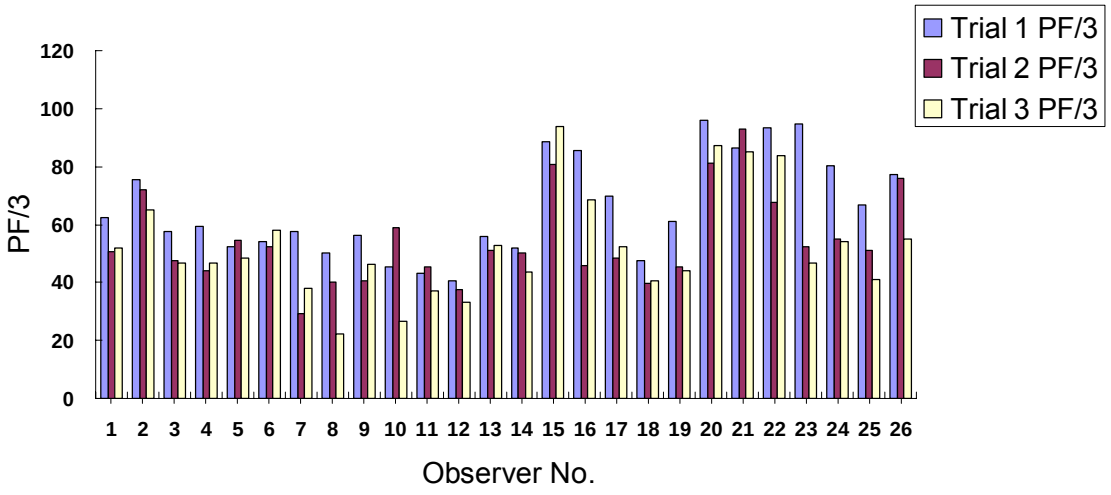

Figure 57. The plot of intra-group variability using PF/3.

Table 11. Intra-group variability using PF/3.

Observer No	Trial 1 PF/3	Trial 2 PF/3	Trial 3 PF/3	Average PF/3
1	62.60	50.69	52.03	55.11
2	75.32	71.89	65.04	70.75
3	57.77	47.44	46.79	50.66
4	59.44	44.11	46.70	50.08
5	52.34	54.58	48.37	51.77
6	54.12	52.48	58.06	54.89
7	57.62	29.27	38.01	41.63
8	49.99	40.12	22.29	37.47
9	56.20	40.60	46.35	47.72
10	45.51	58.71	26.79	43.67
11	43.37	45.38	37.15	41.97
12	40.59	37.48	33.18	37.08
13	55.73	51.09	53.01	53.27
14	51.75	50.04	43.82	48.54
15	88.70	80.88	93.81	87.80

Table 11 (continued).

Observer No	Trial 1 PF/3	Trial 2 PF/3	Trial 3 PF/3	Average PF/3
16	85.69	45.76	68.32	66.59
17	69.67	48.36	52.15	56.73
18	47.63	39.67	40.75	42.68
19	61.28	45.52	44.16	50.32
20	96.15	81.01	87.44	88.20
21	86.42	92.83	85.12	88.12
22	93.44	67.58	83.72	81.58
23	94.76	52.30	46.56	64.54
24	80.36	55.07	54.08	63.17
25	66.65	51.05	41.22	52.97
26	77.18	76.00	55.18	69.45
AVE	65.78	54.23	52.70	57.57
MAX	96.15	92.83	93.81	88.20
MIN	40.59	29.27	22.29	37.08
STD DEV	17.16	15.32	18.30	15.49

The repeatability of observers is shown in Table 12 and Figure 58.

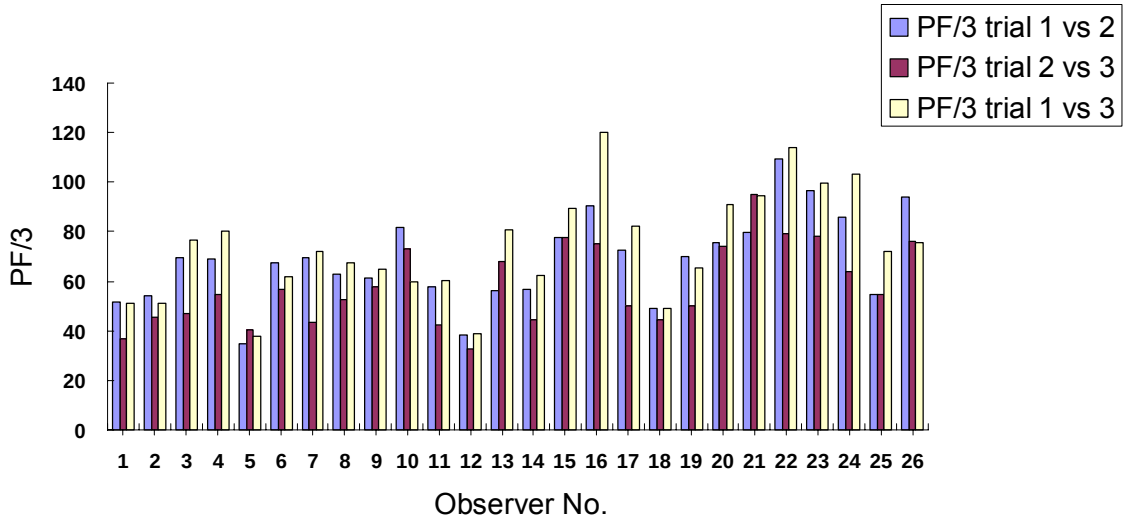

Figure 58. The plot of repeatability of observers using PF/3.

Table 12. The repeatability of observers using PF/3.

Observer No	PF/3 Trial 1 vs 2	PF/3 Trial 2 vs 3	PF/3 Trial 1 vs 3	Average
1	51.73	37.01	51.01	46.58
2	53.93	45.25	50.89	50.02
3	69.52	47.10	76.53	64.38
4	69.08	54.77	80.35	68.07
5	34.63	40.56	37.78	37.66
6	67.22	56.51	61.62	61.78
7	69.59	43.37	72.11	61.69
8	62.81	52.42	67.68	60.97
9	61.38	57.78	65.06	61.41
10	81.79	72.85	59.68	71.44
11	57.76	42.29	60.24	53.43
12	38.43	32.88	38.66	36.66
13	55.96	67.81	80.62	68.13
14	56.88	44.33	62.49	54.56
15	77.74	77.82	89.60	81.72
16	90.61	75.31	119.96	95.29
17	72.60	50.22	82.33	68.39
18	49.16	44.63	49.22	47.67
19	70.06	50.12	65.35	61.84
20	75.55	73.89	90.75	80.07
21	79.80	94.88	94.46	89.71
22	109.47	79.14	113.70	100.77
23	96.40	78.10	99.69	91.40
24	85.97	63.67	103.39	84.34
25	54.62	54.81	72.09	60.51
26	93.77	76.00	75.59	81.78
AVE	68.71	58.21	73.88	66.93
MAX	109.47	94.88	119.96	100.77
MIN	34.63	32.88	37.78	36.66
STD DEV	17.84	16.11	21.39	17.18

The PF/3 of intra-group variability follows a decreasing trend according to the data shown in Table 11. This may be due to a training effect during the visual assessments. In other words, it indicates that observers perform more repeatable assessments over time and with increased experience.

In most cases, PF/3 of trial 2 versus trial 3 is the lowest, while PF/3 of trial 1 versus trial 3 is the highest. This could further indicate that a training effect may be present. This tendency is also observed in observer repeatability responses. An examination of observer data for intra-group variability and individual observer repeatability indicates that one observer (No. 12) provided repeatable assessments with good agreement compared to group mean. However, another observer (No. 21) did the opposite.

4. Performance of Color Difference Formulae

An important method for evaluating different a color-difference formula is based on examining the differences between DE obtained from color difference formulae and DV from visual assessments.

4.1. Correlation Coefficient, r

The correlation coefficient (r) can be used to indicate the strength and direction of a linear relationship between two independent variables. The correlation coefficient is obtained using Equation 37.

The correlation coefficient of 1 indicates a perfect agreement between visual DV and the calculated color difference, DE, values. Values obtained from CIELAB, CIE94(1:1:1), CMC(1:1), BFD(1:1), CIEDE2000(1:1:1), CIE94(2:1:1), CMC(2:1), BFD(2:1), and CIEDE2000(2:1:1) equations are represented as scatter plots against DV as shown in Figures 56, and 59-62 and the summary of results of correlations is shown in Table 13, respectively.

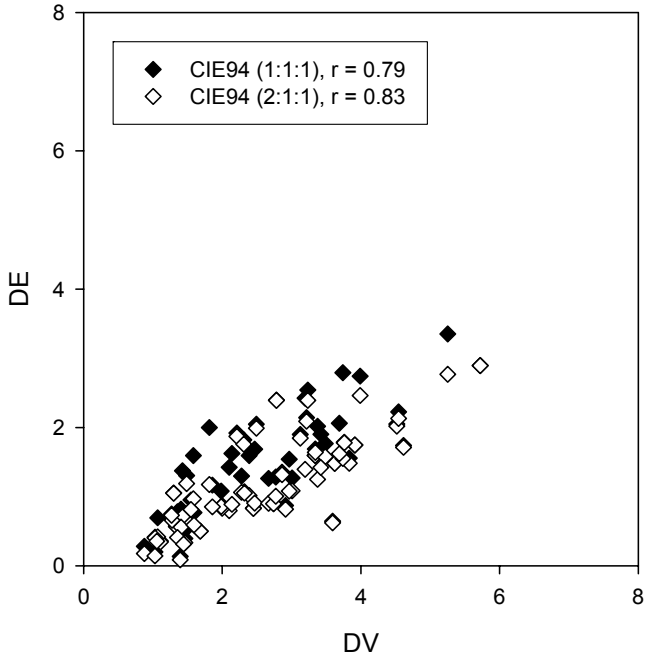

Figure 59. Correlations between DE CIE94(1:1:1) & CIE94(2:1:1) and DV.

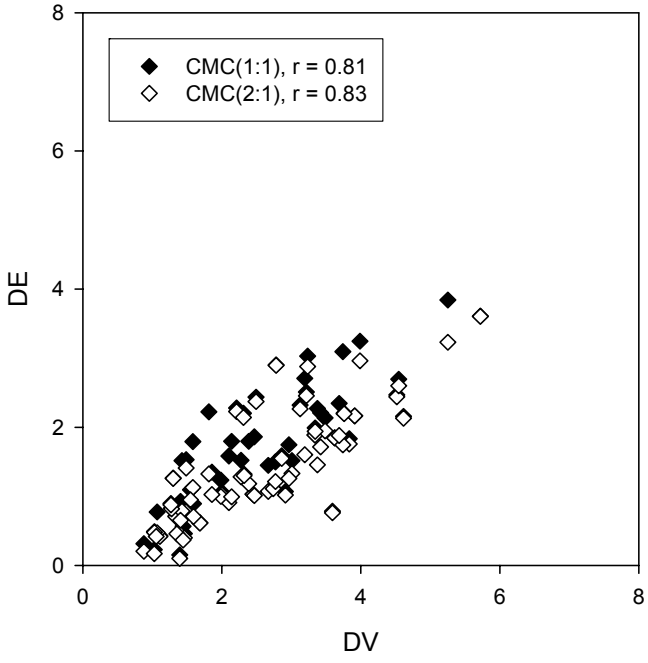

Figure 60. Correlations between DE CMC(1:1) & CMC(2:1) and DV.

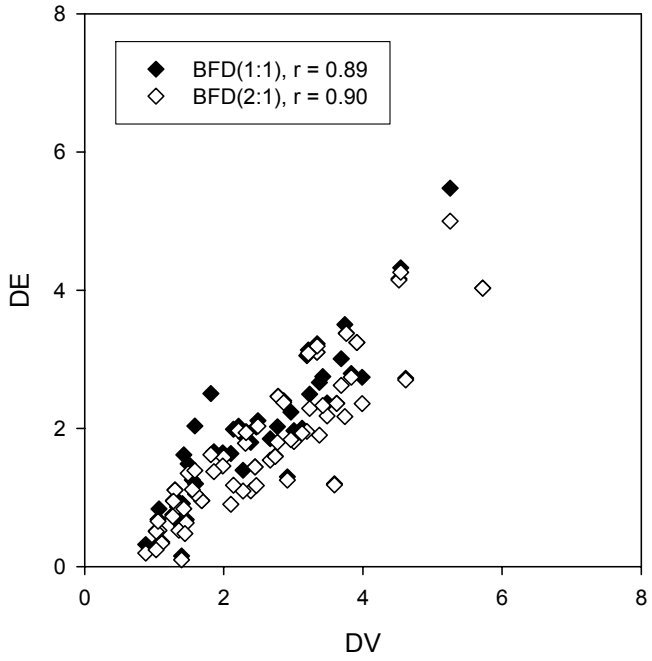

Figure 61. Correlations between DE BFD(1:1) & BFD(2:1) and DV.

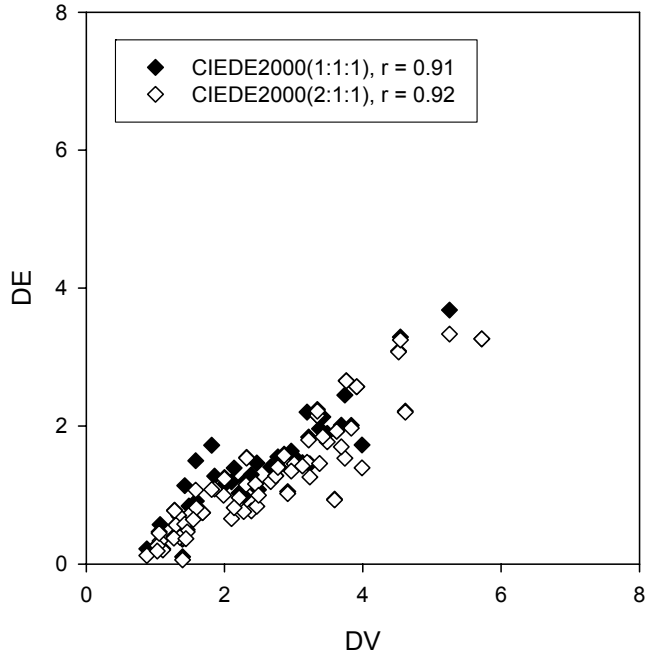

Figure 62. Correlations between CIEDE2000(1:1:1) & CIEDE2000(2:1:1) and DV.

Table 13. The summary of the results of correlation between DE using various color difference formulae and DV.

	CIELAB	CIE94	CMC	BFD	CIEDE2000
Correlation at (K_L or l = 1)	0.74	0.79	0.81	0.89	**0.91**
Correlation at (K_L or l = 2)	N/A	0.83	0.83	0.90	**0.92**

According to the results, CIEDE2000 correlated best with DV, followed closely by BFD, then CMC, CIE94 and finally CIELAB which correlated worst with DV. In every case, the correlations are increased by setting K_L or *l* to 2 and the correlation order remains the same, i.e.: CIELAB < CIE94 < CMC < BFD < CIEDE2000.

4.2. PF/3

In the gray scale visual assessment method, one of the main methods for evaluating color difference formulae is based on PF/3 assessments. Guan and Luo[51] developed Equation 45 as a measure to compare visual assessments against various color difference formulae. In order to assess the performance of color difference formulae, PF/3 was calculated between the mean visual and the calculated assessments. The PF/3 results obtained in this study for various color difference equations based on different lightness weights (K_L or l) are shown in Table 14.

Table 14. The results of PF/3 using various color difference formulae.

	CIELAB	CIE94	CMC	BFD	CIEDE2000
PF/3 at (K_L or l = 1)	50.01	43.13	41.93	**37.46**	37.96
PF/3 at (K_L or l = 2)	N/A	43.67	44.13	**42.46**	44.44

According to PF/3 results at K_L or l = 1, the BFD equation provides the best performance, and CIELAB gives the worst. The BFD equation also gives the best performance at K_L or l = 2, but CIEDE2000 gives the worst, although the differences with other equations are not large. In the textile industry, K_L or l values are usually set to 2 for evaluation purposes and to account for texture. All equations examined in this study seem to give similar results at K_L or l = 2.

4.3. Optimization of K_L

The optimization of K_L values was also investigated for CIE94(K_L:K_C:K_H), CMC(l:c), BFD(l:c), and CIEDE2000(K_L:K_C:K_H) color difference formulae. This was achieved by using a range of K_L values between 0.2-3.0 with an interval of 0.1 initially to determine the range and then 0.01 to obtain the lowest PF/3 values for each formula. Figure 63 shows that the shape of graphs obtained for various formulae is similar. The lowest value of PF/3 for the dataset developed in this study was found to be around K_L = 1, as shown in Table 15, and the PF/3 values slightly increase beyond this point. The region inside the dashed lines highlights the optimal K_L range for various formulae.

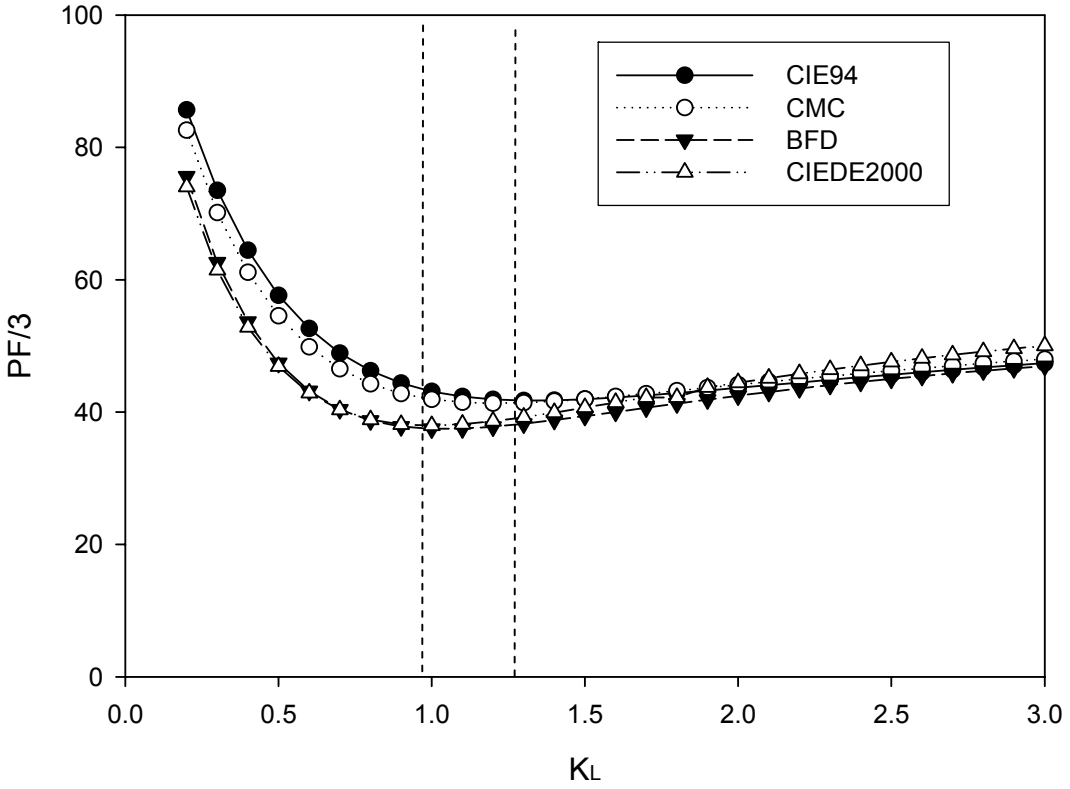

Figure 63. The relationship between K_L and corresponding PF/3 for various color difference formulae.

Table 15. The results of optimal K_L and corresponding PF/3.

	CIE94	CMC	BFD	CIEDE2000
Optimal K_L	1.33	1.21	1.04	0.99
PF/3 at Optimal K_L	41.75	41.34	**37.44**	37.96

4.4. Comparison with Previous Datasets

The dataset produced during this study was compared with four previous datasets (RIT-DuPont[59], Witt[55], Leeds[62], and BFD-P[63]) using the PF/3 method. Such comparisons, however, should be treated with caution because each dataset employed a different experimental set up as shown in Table 16. However, the comparison provided useful information in terms of the general performance of various color difference formulae. Luo[39] and Cui *et al.*[64] used PF/3 to test various color difference formulae based on these four datasets: RIT-DuPont, Witt, Leeds, and BFD-P. The comparison with the dataset developed in this study is shown in Table 17.

Table 16. Experimental conditions for five datasets.

Dataset	Observers	Background Conditions		Sample Type	Pairs	Method[(d)]
	No.	Background	Panel		No.	
RIT-DuPont	50	L^*=39.4	L^*=38	Glossy Painted	156	PC
Witt	22-24	Light Booth (Gray)	Y_{10}=20 (L^*=51.8)	Glossy Painted	418	PC
BFD-P	20	Light Booth (Gray)	Y_{10}=14.2 (L^*=44.5)	Textiles (Wool)	2776	GS
Leeds	12-15	L^*=30,49,95[(a)]		Glossy Painted	307[(b)]	PC & GS
Lee-Shamey	26	Light Booth (Gray)	L^*=74	Textiles (Polyester)	66[(c)]	GS

(a) using different background conditions

(b) 104 pairs for pair comparison method, 203 pairs for gray scale method

(c) all pairs are blue samples

(d) PC indicates pair comparison method; GS denotes gray scale method

Table 17. Performance of color difference formulae using PF/3.

Dataset	CIELAB	CIE94 (1:1:1)	CMC (1:1)	BFD (1:1)	CIEDE2000 (1:1:1)
RIT-DuPont	22.1	19.4	28.1	24.6	**19.0**
Witt	70.3	41.6	46.3	44.3	**38.4**
Leeds	46.7	34.0	28.1	28.0	**23.1**
BFD-P	56.2	42.7	39.7	**34.4**	37.2
Lee-Shamey	50.0	43.1	42.0	**37.5**	38.0

Results indicate that CIEDE2000 performs best for three of the five datasets namely RIT-DuPont, Witt, and Leeds dataset, while BFD performs best for two datasets, namely BFD-P and the Lee-Shamey blue dataset. The results are also shown in Figure 64.

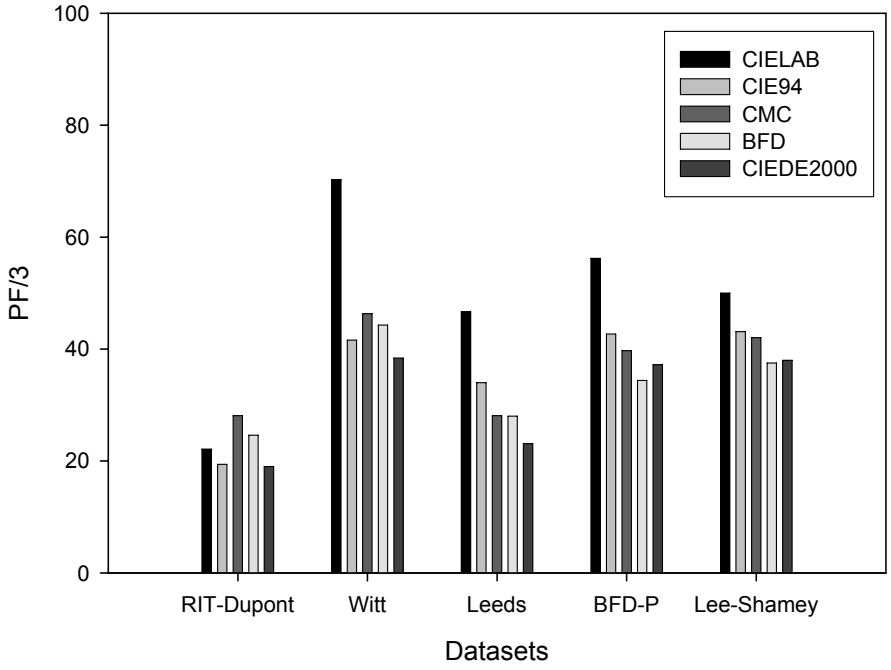

Figure 64. PF/3 results of dataset based on various color difference formulae.

5. Calculating Best-fit Tolerance Ellipsoids (and Ellipses)

In order to calculate the best-fit shape for a visual dataset around a given color center several methods can be used. One of these methods is based on minimizing the difference between visual and measured color difference responses as shown in Equation 45.

$$\Delta E^2 = b_{11}(\Delta a^*)^2 + b_{22}(\Delta b^*)^2 + b_{33}(\Delta L^*)^2 + 2b_{12}(\Delta a^*)(\Delta b^*) + 2b_{13}(\Delta a^*)(\Delta L^*) + 2b_{23}(\Delta b^*)(\Delta L^*) \quad (45)$$

A constant ΔE represents the surface of an ellipsoid. The chromaticity-discrimination ellipse can be obtained when $\Delta L^* = 0$ which gives the cross section of the ellipsoid on that plane. Similarly the coordinates of the lightness discrimination ellipse can be calculated.

5.1. Ellipsoid Coefficients

The first task to obtain a best fit ellipsoid is based on characterization of the six metric coefficients (b_{11}, b_{22}, b_{33}, b_{12}, b_{13}, and b_{23}) for each ellipsoid by minimizing the S^2 function[65] shown in Equation 46.

$$S^2 = \sum \left(\Delta V^2 - \Delta E^2\right)^2 \quad (46)$$

where

ΔV is the visual color difference.

Combining Equations 45 and 46 gives Equation 47:

$$S^2 = \sum \left(\begin{array}{l} \Delta V^2 - (b_{11}(\Delta a^*)^2 + b_{22}(\Delta b^*)^2 + b_{33}(\Delta L^*)^2 + \\ 2b_{12}(\Delta a^*)(\Delta b^*) + 2b_{13}(\Delta a^*)(\Delta L^*) + 2b_{23}(\Delta b^*)(\Delta L^*)) \end{array} \right)^2 \quad (47)$$

Let $\Delta a^* = x, \Delta b^* = y, \Delta L^* = z$ as shown in Equation 48.

$$S^2 = \sum (\Delta V^2 - (b_{11}x^2 + b_{22}y^2 + b_{33}z^2 + 2b_{12}xy + 2b_{13}xz + 2b_{23}yz))^2 \quad (48)$$

Setting partial derivative of S^2 with respect to the six metric coefficients equals to zero results in Equations 49-54.

$$\frac{\delta S}{\delta b_{11}} = 2\sum (\Delta V^2 x^2 - \begin{bmatrix} x^4 & x^2y^2 & x^2z^2 & 2x^3y & 2x^3z & 2x^2yz \end{bmatrix} \begin{bmatrix} b_{11} \\ b_{22} \\ b_{33} \\ b_{12} \\ b_{13} \\ b_{23} \end{bmatrix}) = 0 \quad (49)$$

$$\frac{\delta S}{\delta b_{22}} = 2\sum (\Delta V^2 y^2 - \begin{bmatrix} x^2y^2 & y^4 & y^2z^2 & 2xy^3 & 2xy^2z & 2y^3z \end{bmatrix} \begin{bmatrix} b_{11} \\ b_{22} \\ b_{33} \\ b_{12} \\ b_{13} \\ b_{23} \end{bmatrix}) = 0 \quad (50)$$

$$\frac{\delta S}{\delta b_{33}} = 2\sum (\Delta V^2 z^2 - \begin{bmatrix} x^2z^2 & y^2z^2 & z^4 & 2xyz^2 & 2xz^3 & 2yz^3 \end{bmatrix} \begin{bmatrix} b_{11} \\ b_{22} \\ b_{33} \\ b_{12} \\ b_{13} \\ b_{23} \end{bmatrix}) = 0 \quad (51)$$

$$\frac{\delta S}{\delta b_{12}} = 2\sum(\Delta V^2 xy - \begin{bmatrix} x^3y & xy^3 & xyz^2 & 2x^2y^2 & 2x^2yz & 2xy^2z \end{bmatrix} \begin{bmatrix} b_{11} \\ b_{22} \\ b_{33} \\ b_{12} \\ b_{13} \\ b_{23} \end{bmatrix}) = 0 \qquad (52)$$

$$\frac{\delta S}{\delta b_{13}} = 2\sum(\Delta V^2 xz - \begin{bmatrix} x^3z & xy^2z & xz^3 & 2x^2yz & 2x^2z^2 & 2xyz^2 \end{bmatrix} \begin{bmatrix} b_{11} \\ b_{22} \\ b_{33} \\ b_{12} \\ b_{13} \\ b_{23} \end{bmatrix}) = 0 \qquad (53)$$

$$\frac{\delta S}{\delta b_{23}} = 2\sum(\Delta V^2 yz - \begin{bmatrix} x^2yz & y^3z & yz^3 & 2xy^2z & 2xyz^2 & 2y^2z^2 \end{bmatrix} \begin{bmatrix} b_{11} \\ b_{22} \\ b_{33} \\ b_{12} \\ b_{13} \\ b_{23} \end{bmatrix}) = 0 \qquad (54)$$

Equations 49-54 can be represented in a matrix form as shown in Equation 55.

$$\begin{bmatrix} \sum \Delta V^2 x^2 \\ \sum \Delta V^2 y^2 \\ \sum \Delta V^2 z^2 \\ \sum \Delta V^2 xy \\ \sum \Delta V^2 xz \\ \sum \Delta V^2 yz \end{bmatrix} = \begin{bmatrix} \sum x^4 & \sum x^2y^2 & \sum x^2z^2 & \sum 2x^3y & \sum 2x^3z & \sum 2x^2yz \\ \sum x^2y^2 & \sum y^4 & \sum y^2z^2 & \sum 2xy^3 & \sum 2xy^2z & \sum 2y^3z \\ \sum x^2z^2 & \sum y^2z^2 & \sum z^4 & \sum 2xyz^2 & \sum 2xz^3 & \sum 2yz^3 \\ \sum x^3y & \sum xy^3 & \sum xyz^2 & \sum 2x^2y^2 & \sum 2x^2yz & \sum 2xy^2z \\ \sum x^3z & \sum xy^2z & \sum xz^3 & \sum 2x^2yz & \sum 2x^2z^2 & \sum 2xyz^2 \\ \sum x^2yz & \sum y^3z & \sum yz^3 & \sum 2xy^2z & \sum 2xyz^2 & \sum 2y^2z^2 \end{bmatrix} \begin{bmatrix} b_{11} \\ b_{22} \\ b_{33} \\ b_{12} \\ b_{13} \\ b_{23} \end{bmatrix} \qquad (55)$$

Equation 55 can be transformed to Equation 56 to calculate the six metric coefficients as shown:

$$\begin{bmatrix} b_{11} \\ b_{22} \\ b_{33} \\ b_{12} \\ b_{13} \\ b_{23} \end{bmatrix} = \begin{bmatrix} \sum x^4 & \sum x^2y^2 & \sum x^2z^2 & \sum 2x^3y & \sum 2x^3z & \sum 2x^2yz \\ \sum x^2y^2 & \sum y^4 & \sum y^2z^2 & \sum 2xy^3 & \sum 2xy^2z & \sum 2y^3z \\ \sum x^2z^2 & \sum y^2z^2 & \sum z^4 & \sum 2xyz^2 & \sum 2xz^3 & \sum 2yz^3 \\ \sum x^3y & \sum xy^3 & \sum xyz^2 & \sum 2x^2y^2 & \sum 2x^2yz & \sum 2xy^2z \\ \sum x^3z & \sum xy^2z & \sum xz^3 & \sum 2x^2yz & \sum 2x^2z^2 & \sum 2xyz^2 \\ \sum x^2yz & \sum y^3z & \sum yz^3 & \sum 2xy^2z & \sum 2xyz^2 & \sum 2y^2z^2 \end{bmatrix}^{-1} \begin{bmatrix} \sum \Delta V^2 x^2 \\ \sum \Delta V^2 y^2 \\ \sum \Delta V^2 z^2 \\ \sum \Delta V^2 xy \\ \sum \Delta V^2 xz \\ \sum \Delta V^2 yz \end{bmatrix} \quad (56)$$

For sample pair *i*, Equation 56 is shown as Equation 57.

$$\begin{bmatrix} b_{11} \\ b_{22} \\ b_{33} \\ b_{12} \\ b_{13} \\ b_{23} \end{bmatrix} = \begin{bmatrix} \sum x_i^4 & \sum x_i^2y_i^2 & \sum x_i^2z_i^2 & \sum 2x_i^3y_i & \sum 2x_i^3z_i & \sum 2x_i^2y_iz_i \\ \sum x_i^2y_i^2 & \sum y_i^4 & \sum y_i^2z_i^2 & \sum 2x_iy_i^3 & \sum 2x_iy_i^2z_i & \sum 2y_i^3z_i \\ \sum x_i^2z_i^2 & \sum y_i^2z_i^2 & \sum z_i^4 & \sum 2x_iy_iz_i^2 & \sum 2x_iz_i^3 & \sum 2y_iz_i^3 \\ \sum x_i^3y_i & \sum x_iy_i^3 & \sum x_iy_iz_i^2 & \sum 2x_i^2y_i^2 & \sum 2x_i^2y_iz_i & \sum 2x_iy_i^2z_i \\ \sum x_i^3z_i & \sum x_iy_i^2z_i & \sum x_iz_i^3 & \sum 2x_i^2y_iz_i & \sum 2x_i^2z_i^2 & \sum 2x_iy_iz_i^2 \\ \sum x_i^2y_iz_i & \sum y_i^3z_i & \sum y_iz_i^3 & \sum 2x_iy_i^2z_i & \sum 2x_iy_iz_i^2 & \sum 2y_i^2z_i^2 \end{bmatrix}^{-1} \begin{bmatrix} \sum \Delta V_i^2 x_i^2 \\ \sum \Delta V_i^2 y_i^2 \\ \sum \Delta V_i^2 z_i^2 \\ \sum \Delta V_i^2 x_iy_i \\ \sum \Delta V_i^2 x_iz_i \\ \sum \Delta V_i^2 y_iz_i \end{bmatrix}$$

(57)

The ellipsoid coefficients corresponding to ΔE = 1 were calculated from the b values in the usual manner. The six metric coefficients obtained thus are shown in Equation 58.

$$\begin{bmatrix} b_{11} \\ b_{22} \\ b_{33} \\ b_{12} \\ b_{13} \\ b_{23} \end{bmatrix} = \begin{bmatrix} 1.9566679849 \\ 0.6596106104 \\ 1.5712975175 \\ 0.7580572226 \\ 0.1724320994 \\ 0.1410070849 \end{bmatrix} \tag{58}$$

Therefore, the ellipsoid equation in the CIELAB color space (at ΔE=1) based on Lee-Shamey Blue dataset is shown in Equation 59.

$$\begin{aligned} \Delta E^2 = {} & 1.9567(\Delta a^*)^2 + 0.6596(\Delta b^*)^2 + 1.5713(\Delta L^*)^2 + \\ & 2(0.7581)(\Delta a^*)(\Delta b^*) + 2(0.1724)(\Delta a^*)(\Delta L^*) + 2(0.1410)(\Delta b^*)(\Delta L^*) = 1 \end{aligned} \tag{59}$$

5.2. Plotting Ellipsoid in CIELAB Color Space

The ellipsoid based on the blue dataset developed in this study was plotted in the CIELAB color space, as shown in Figure 65.

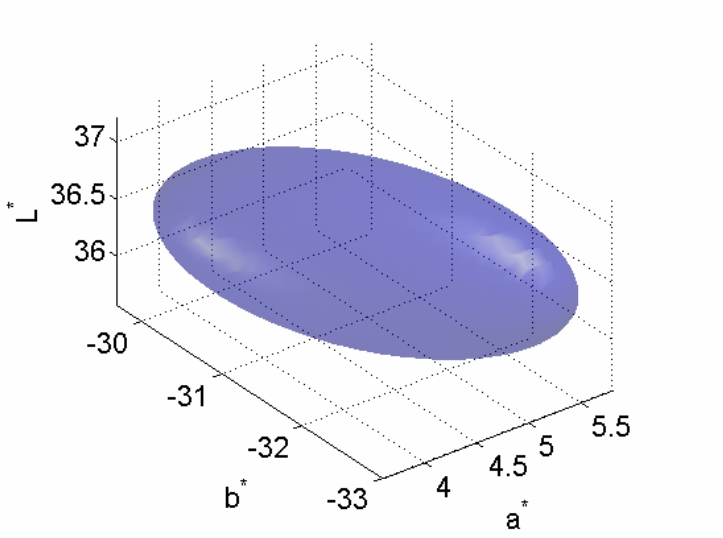

Figure 65. Ellipsoid based on Lee-Shamey Blue dataset in CIELAB color space. (center: a*=4.70, b*=-31.36, L*=36.39)

This ellipsoid was decomposed into the a*b*, a*L*, and b*L* planes and plotted together with ellipsoids based on RIT-DuPont dataset. Melgosa *et al.* [66] published the coefficients and parameters of ellipsoids based on RIT-DuPont dataset which were converted from CIExyY color space to CIELAB color space. These ellipses and their properties are shown in Figures 66-67 and Tables 18-19, respectively.

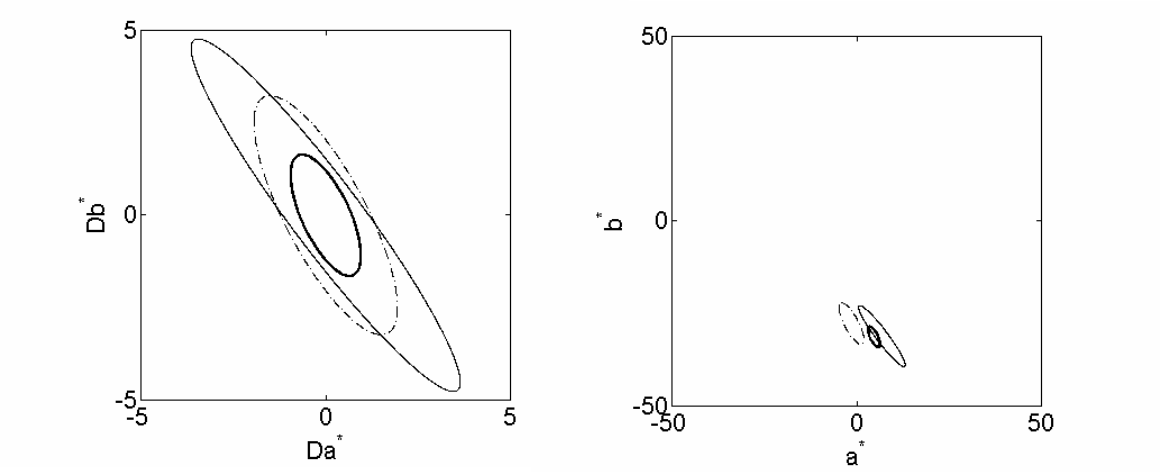

Figure 66. Chromaticity-discrimination ellipses in the CIE a*b* plane at the blue center, from RIT-DuPont (Moderate Blue, -·-), RIT-DuPont (Dark Blue, -), and Lee-Shamey (CIE Blue, **-**) datasets. Each ellipse shown in the left-side graph was enlarged threefold.

Ratio of axes (A/B) indicates the shape of the ellipse. For a small ratio of axes, the shape of the ellipse gets closer to a circle, and at a ratio of 1 becomes a circle. The ellipse based on the blue dataset developed in this study has the smallest ratio of axes as shown in Table 18.

Table 18. Comparison of chromaticity-discrimination ellipses at threshold on CIE a*b* plane.

	Color Center			Cross Section for ΔY*=0				
Dataset	A*	b*	L*	A[(a)]	B[(b)]	A/B	Θ (deg)[(c)]	Area[(d)]
RIT-DuPont (Moderate Blue)	-1.40	-27.81	35.34	3.6179	1.1022	3.28	117.10	3.13
RIT-DuPont (Dark Blue)	6.83	-31.15	30.19	5.9423	0.9424	6.31	126.98	4.40
Lee-Shamey (CIE Blue)	4.70	-31.36	36.39	1.7946	0.6585	**2.73**	**114.42**	**0.93**

(a) major axis length

(b) minor axis length

(c) angle between major axis and a*-axis

(d) area = 1/4(ABπ)

This means the shape of the ellipse based on Lee-Shamey Blue dataset is closer to a sphere than those based on RIT-DuPont sets. The area of the ellipse based on Lee-Shamey Blue dataset is also the smallest among the sets studied. This indicates that the tolerance based on the blue dataset developed in this study is small. Also, the angle of the ellipse based on this dataset is small, and that of the major axis faces more towards the origin.

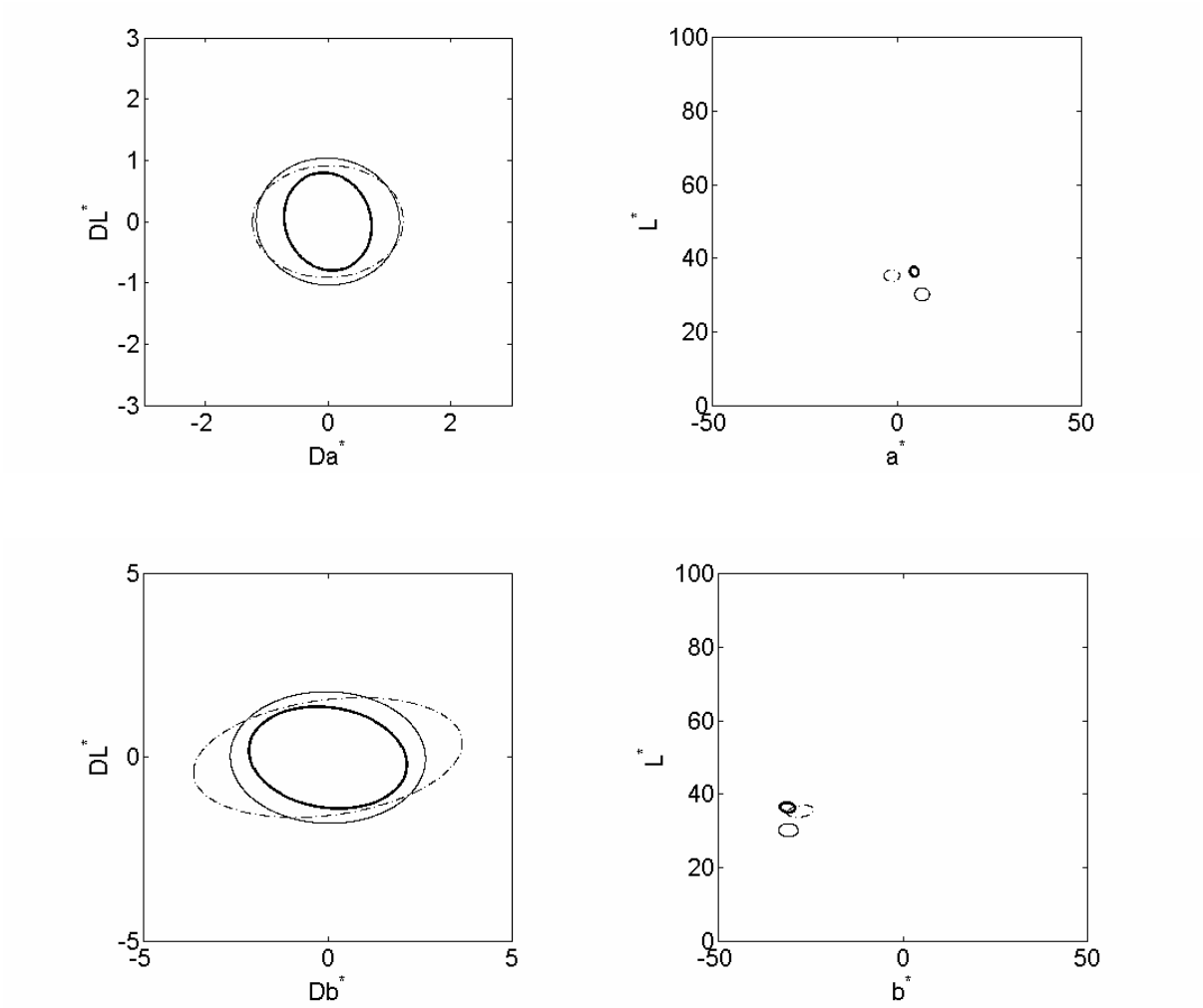

Figure 67. Ellipses in CIE L*a* and CIE L*b* plane at the blue center, from RIT-DuPont (Moderate Blue, -·-), RIT-DuPont (Dark Blue, -), and Lee-Shamey (CIE Blue, -) datasets. Each ellipse in the left-side graphs was enlarged threefold.

In both planes, the ellipse based on RIT-DuPont dataset of dark blue has the smallest ratio of axes. However, the ellipsoid based on the dataset from this study has a much smaller ratio of axes compared to ellipsoids based on RIT-DuPont datasets which have a similar L* value. The area of the ellipse based on Lee-Shamey is also smallest on the L*a* and L*b* planes.

Table 19. Comparison of ellipses at threshold on CIE a*L* and CIE b*L* planes.

	Cross Section for Δb*=0				Cross Section for Δa*=0			
Dataset	A[(a)]	B[(b)]	A/B	Area[(d)]	A[(a)]	B[(b)]	A/B	Area[(d)]
RIT-DuPont (Moderate Blue)	1.2301	0.9085	1.35	0.88	2.1272	1.1022	2.34	1.52
RIT-DuPont (Dark Blue)	1.1713	1.0363	**1.13**	0.95	1.5335	1.0362	**1.48**	1.25
Lee-Shamey (CIE Blue)	0.8150	0.7032	1.16	**0.45**	1.2517	0.7924	1.58	**0.78**

(a) major axis length

(b) minor axis length

(c) angle between major axis and a*-axis

(d) area = 1/4(ABπ)

The three-dimensional plots of the ellipsoid based on the above ellipses are shown in Figures 68-73.

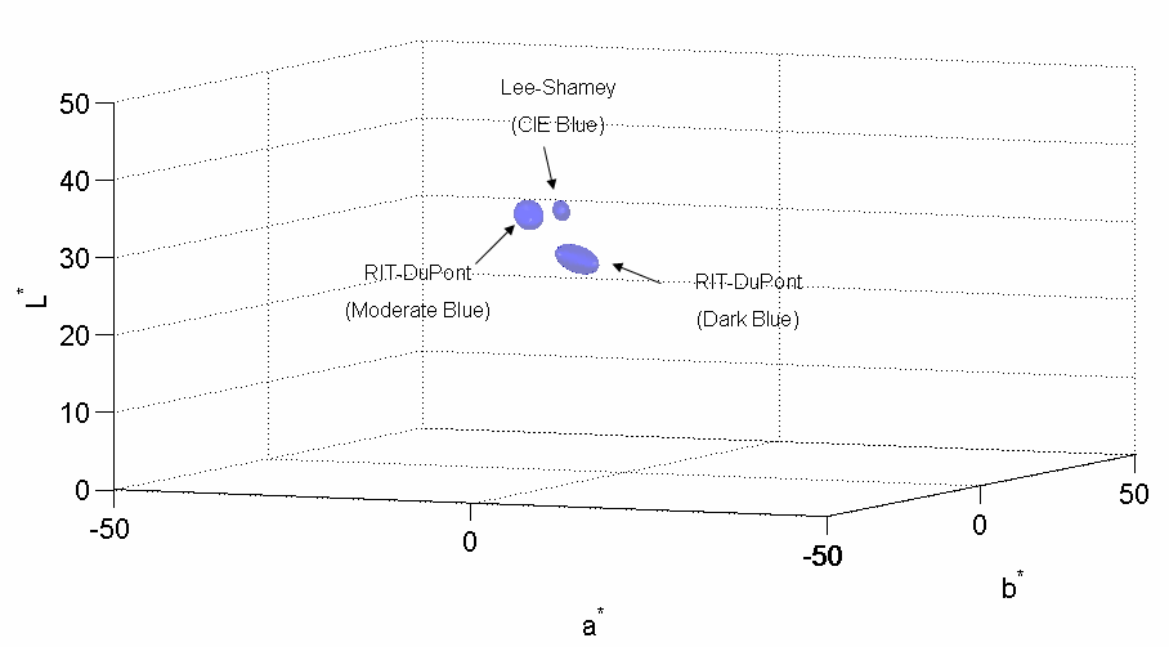

Figure 68. Ellipsoids in CIELAB color space (view point from a*L* plane). Each ellipsoid was enlarged threefold.

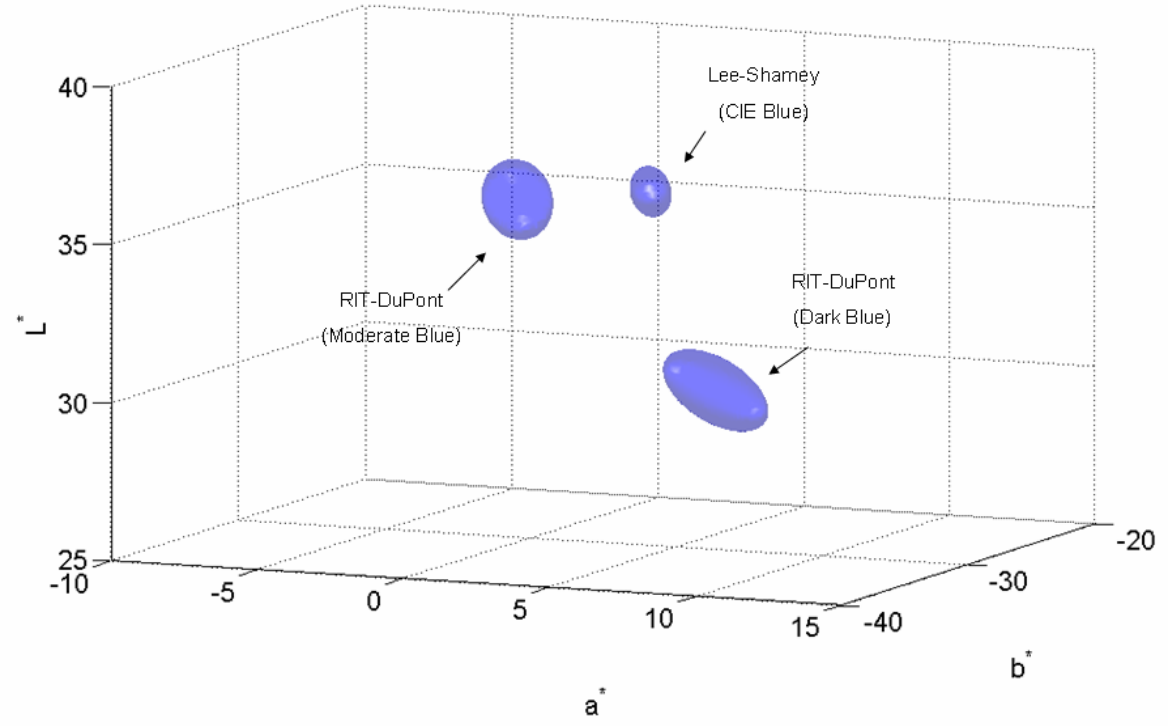

Figure 69. Ellipsoids in CIELAB color space (zoom in view point from a*L* plane).

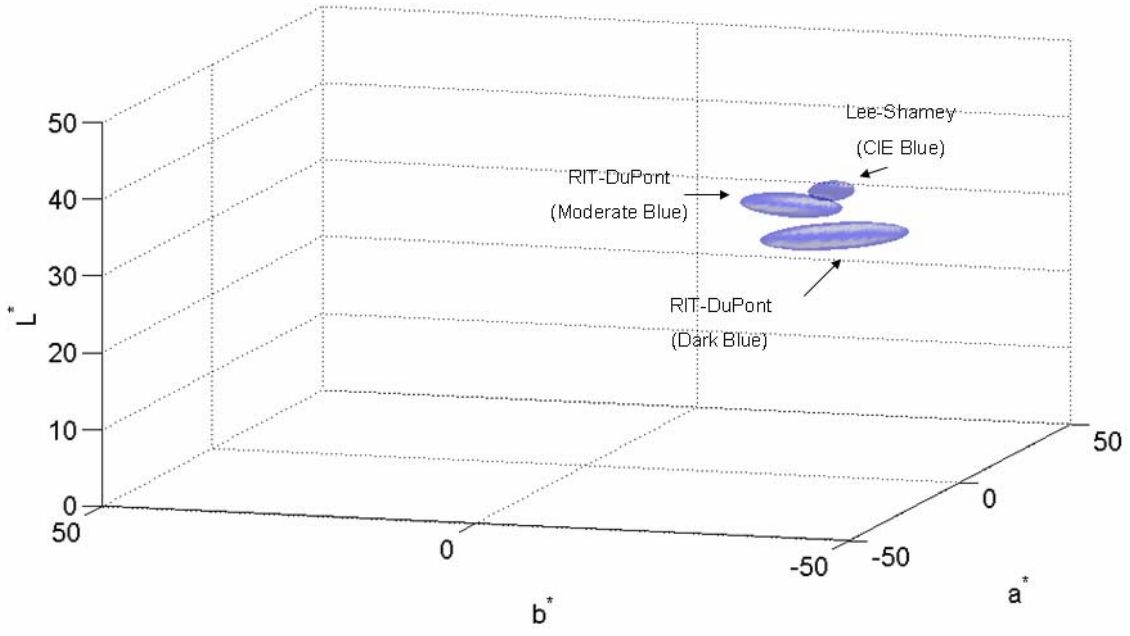

Figure 70. Ellipsoids in CIELAB color space (view point from b*L* plane). Each ellipsoid was enlarged threefold.

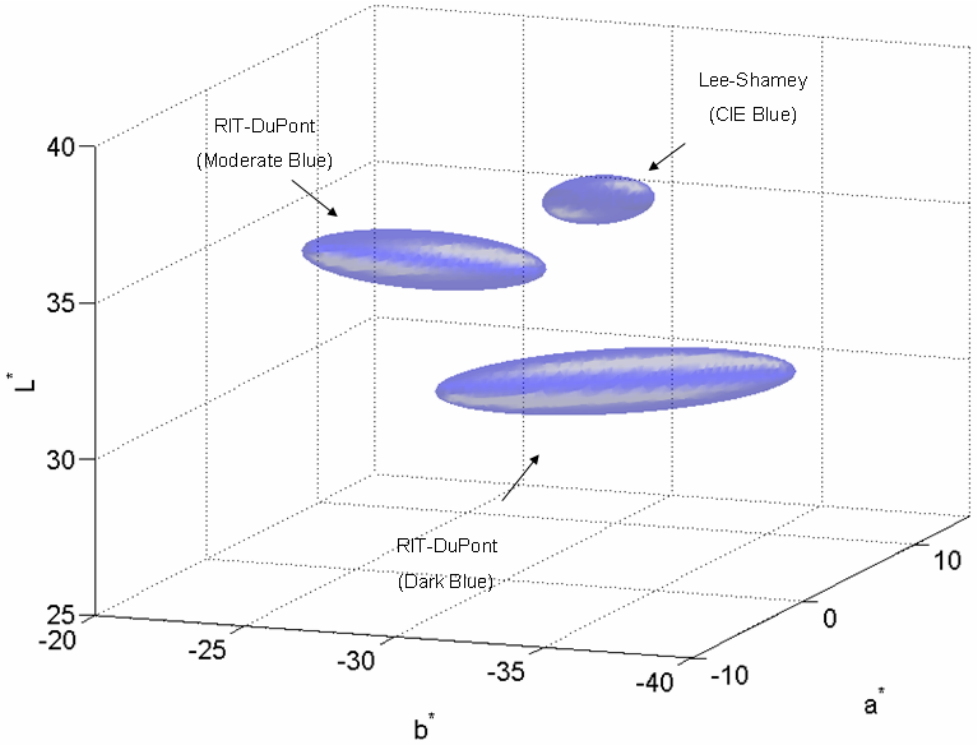

Figure 71. Ellipsoids in CIELAB color space (zoom in view point from b*L* plane).

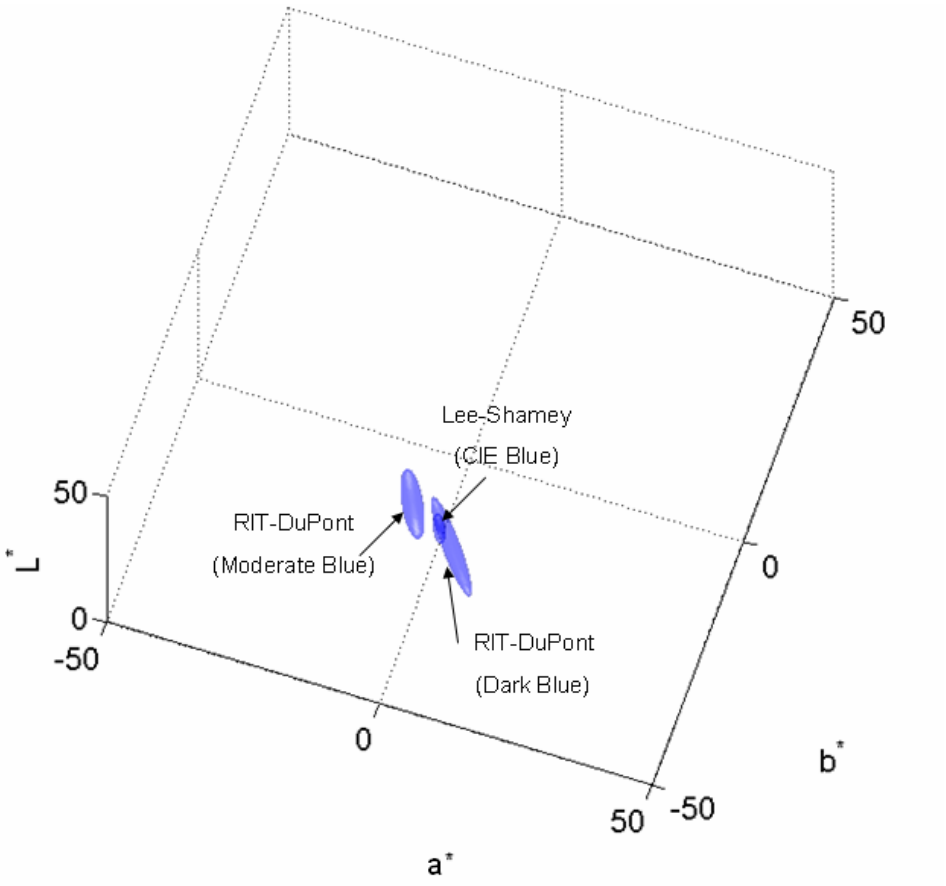

Figure 72. Ellipsoids in CIELAB color space (view point from a*b* plane). Each ellipsoid was enlarged threefold.

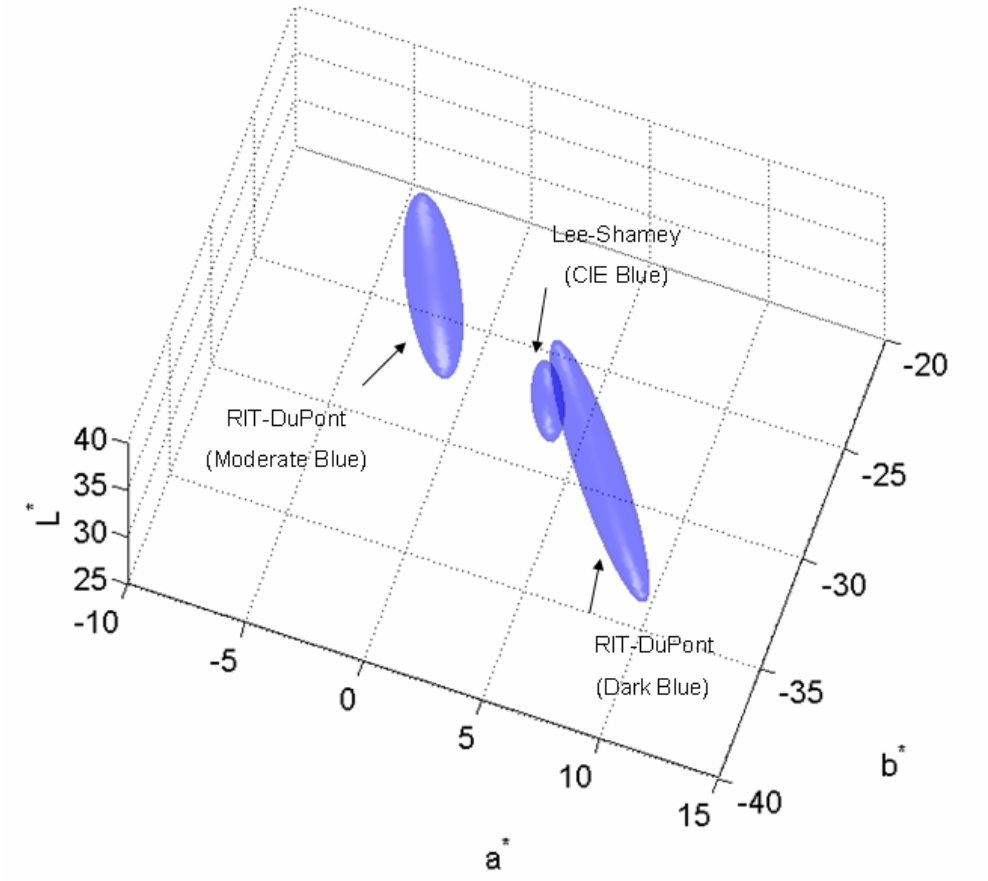

Figure 73. Ellipsoids in CIELAB color space (zoom in view point from a*b* plane).

5.3. Comparison with Chromaticity-Discrimination Ellipses in CIExy Plane

The results of previous color difference studies were generally given by chromaticity ellipses based on the CIExy plane. Thus, Lee-Shamey Blue dataset was converted to CIExyY for comparison[65] purposes. The ellipsoid equation for CIExyY color plane (at ΔE=1) based on Lee-Shamey Blue dataset is obtained according to the same procedure used for CIELAB color plane. The ellipsoid equation for CIExyY plane (at ΔE=1) is shown in Equation 60.

$$\Delta E^2 = 281043(\Delta x)^2 + 155971(\Delta y)^2 + 6.1131(\Delta Y)^2 + 2(-185587)(\Delta x)(\Delta y) + 2(-52.0189)(\Delta x)(\Delta Y) + 2(-41.1702)(\Delta y)(\Delta Y) = 1 \quad (60)$$

The chromaticity-discrimination ellipse equation can be obtained by setting ΔY=0. Chromaticity-discrimination and properties of ellipses from RIT-DuPont, Witt, BFD, and Lee-Shamey are shown in Figure 74 and Table 20, respectively. The CIE recommended blue color center[66] was published in 1978 in xyY coordinates and was used in the RIT-DuPont[67], Witt[54] and BFD[68] datasets. The Lee-Shamey dataset, however, is based on the more recent CIE recommended blue color center[69] defined in L*a*b* coordinates in 1995.

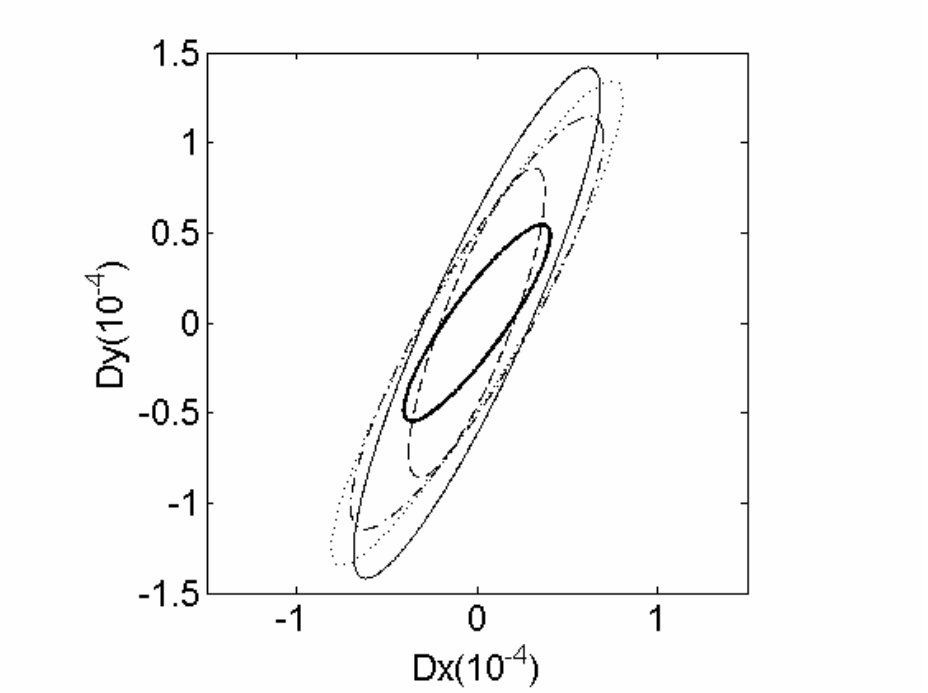

Figure 74. Chromaticity-discrimination ellipses in xy plane at the blue center, from several experimental datasets: RIT-DuPont[67] (Moderate Blue, -·-), RIT-DuPont[67] (Dark Blue, -), Witt[54] (CIE Blue, --), BFD[68] (CIE Blue, ···), and Lee-Shamey (CIE Blue, -)

The ratio of axes as well as the area of ellipse based on Lee-Shamey Blue dataset is the smallest. This smaller tolerance may be due to the highly controlled experimental method used. In other words, strictly controlled illumination, sample presentation and assessment conditions may have resulted in observers becoming more discriminating in regard to variations in lightness, chroma and hue directions compared to practical less stringent conditions.

Table 20. Comparison of chromaticity-discrimination ellipses at threshold on CIE xy plane.

	Color Center			Cross Section for ΔY=0				
Dataset	x	y	Y	A[(a)]	B[(b)]	A/B	Θ (deg)[(c)]	Area[(d)]
RIT-DuPont (Moderate Blue)	0.213	0.229	8.67	1.3147	0.2746	4.79	59.66	0.28
RIT-DuPont (Dark Blue)	0.212	0.203	6.31	1.5511	0.2729	5.68	65.19	0.33
Witt (CIE Blue)	0.219	0.216	8.80	0.9192	0.1905	4.83	65.14	0.14
BFD (CIE Blue)	0.219	0.216	8.80	1.5472	0.2699	5.95	58.54	0.33
Lee-Shamey (CIE Blue)	0.218	0.216	9.21	0.6642	0.1554	**4.27**	54.79	**0.08**

(a) major axis length

(b) minor axis length

(c) angle between major axis and a*-axis

(d) area = 1/4(ABπ)

IV. Conclusions

1. Conversion of gray scale to visual color differences

The gray scale rating method is an important method to carry out visual assessments. The current AATCC recommended gray scale is based on geometrically spaced steps, i.e. the distance between adjacent gray samples, which is due to lightness differences only, is perceptually non-linear. Gray scale ratings are therefore converted to a linear scale using a polynomial fitting. A forth-degree and a third-degree polynomial equation were initially tested. The use of a fourth-degree polynomial fitting resulted in over-fitting of data. It was found the third-degree polynomial equation produced statistically satisfactory correlation results at a 95% confidence level.

Third-degree polynomial equations were obtained from converting gray scale ratings to CIELAB, CIE94(1:1:1), CMC(1:1), and CIEDE2000(1:1:1) equation, respectively. Polynomial equations thus obtained were found to be very similar to each other because gray scale pairs are mainly different in terms of lightness attribute and at the ratios selected this does not influence the conversion process greatly. The polynomial equations obtained for CIELAB and CIE94(1:1) equations are very similar since there is no lightness adjustment factor in the CIELAB formula and the lightness adjustment factor (S_L) is fixed at 1 for CIE94(1:1). In the case of CMC(1:1) and CIEDE2000(1:1:1), different lightness adjustment factors are used, but the converted results were very close to the lightness adjustment factor, $S_L = 1$. Thus, there is little or no difference between each of the polynomial equations, and

therefore a single fit function was used for all formulae

2. Group (inter-observer), individual (intra-group) variability, and individual observer repeatability

Paired t-test and PF/3 assessments were carried out and the following results were obtained.

• Paired t-test assessment of inter-observer variability: The difference between trials 1&2 and 1&3 was found to be significant at the 95% confidence level. Trials 2&3 were not statistically significantly different at the 95% confidence level. This may be due to a training effect; for instance, observers may feel more comfortable in providing responses to visual datasets after familiarization with the procedure.

• Paired t-test for individual observer repeatability: Approximately 61.5% of observers provided statistically repeatable assessments between trials.

• Paired t-test for intra-group variability: Responses obtained from an observer were compared to the mean group responses for each trial. Approximately 23% of observers in trial one, 19% in trial two, and 11% in trial three provided statistically same responses compared to the mean group response.

• Paired t-test for individual observer repeatability by gender and nationality: Approximately 67% of male and 53% of female observers provided statistically repeatable assessments between trials. As a subset of overall observer population,

approximately 51% of Korean and 72% of international observers provided statistically repeatable responses. However, the size of the observer population may not be sufficiently large to allow statistically conclusive assessment of subsets of observer responses due to gender or nationality.

• PF/3 assessment of intra-group variability: Individual observer's DV results for each trial were compared to the mean group visual DV results for each trial. An average PF/3 of 57.57 was obtained which indicates significant variability within the group. In most cases, PF/3 of trial 2 versus trial 3 was the lowest.

• PF/3 assessment of individual observer repeatability: Individual observer responses between the trials were compared. An approximately PF/3 value of 67 was obtained. In most cases, PF/3 of trial 2 versus trial 3 was the lowest. This could further indicate that a training effect may be present.

3. Performance of color difference formulae

Correlation coefficient (r) and PF/3 assessments were used to assess the performance of different formulae and the following results were obtained.

• Assessments based on correlation coefficient (r): When K_L or l is set at 1, CIEDE2000(1:1:1) formula correlated best with DV, followed closely by BFD(1:1), then CMC(1:1), CIE94(1:1:1) and finally CIELAB which correlated worst with DV. The same results were obtained when K_L or l is set at 2.

• Assessments based on PF/3: When K_L or l =1, the BFD(1:1) equation provides the best performance, and CIELAB gives the worst. When K_L or l is set at 2, for the evaluation of textile samples, the BFD equation provides the best performance. All equations, however, gave PF/3 responses in a close range according to the rank shown below; values inside brackets show PF/3 responses:

BFD(42.46) > CIE94(43.67) > CMC(44.13) > CIEDE2000(44.44)

• Optimization of K_L: Optimal K_L values were obtained for various color difference formulae using PF/3 values as a metric. The lowest PF/3 value would therefore correspond to the optimal K_L. Results obtained in this study show that in the K_L range of 0.99 to 1.33 different equations show optimal performance with values for optimal K_L shown next to each formula:

CIEDE2000 (0.99), BFD (1.04), CMC (1.21), and CIE94 (1.33)

According to the results obtained from these assessments CIEDE2000 and BFD provide the best performance at around K_L or l of 1. Published results obtained from other studies comparing various datasets (RIT-DuPont, Witt, Leeds, and BFD-P) also indicate that CIEDE2000 and BFD provide the best performance at K_L or l = 1. As can be seen CMC and CIE94 perform best at slightly higher values of 1.2 and 1.3, respectively. However, such comparisons must be treated with caution as each study employed a different experimental set up. The PF/3 results obtained for the blue textile samples when K_L or l is set at 2 do not match well with those obtained from the correlation coefficient.

4. Calculating best fit tolerance ellipsoids (ellipses)

The equation describing the best fit ellipsoid in the CIELAB color space for the dataset developed in this study, Lee-Shamey Blue dataset, is shown below:

$$\Delta E^2 = 1.9567(\Delta a^*)^2 + 0.6596(\Delta b^*)^2 + 1.5713(\Delta L^*)^2 + 2(0.7581)(\Delta a^*)(\Delta b^*) + 2(0.1724)(\Delta a^*)(\Delta L^*) + 2(0.1410)(\Delta b^*)(\Delta L^*) = 1$$

This ellipsoid was compared with Dark Blue and Moderate Blue ellipsoids based on RIT-DuPont dataset. On the CIE a*b* plane the ellipse based on Lee-Shamey blue dataset has the smallest ratio of axes (2.73) and area (0.93) when compared to other datasets. Results shown on the CIE a*L* and b*L* planes also follow a similar pattern. The ellipses based on RIT-DuPont Dark Blue dataset have a ratio of axes of 1.13 and 1.48, respectively and those based on Moderate Blue have a ratio of 1.35 and 2.34, respectively. The ellipsoid based on Lee-Shamey dataset, however, has a ratio of axes on these planes with values of 1.16 and 1.58, respectively. The area of the ellipses based on Lee-Shamey is also the smallest on the CIE L*a* and L*b* planes with values of 0.45 and 0.78, respectively. These differences are possibly due to a different experimental setup used in this study, which results in tighter observer tolerances around each of the axes.

• Different background and panel conditions: RIT-DuPont database was developed based on a background with L* =39.4 and panel L*=38. The background used in this study had a L* of 74 with a similar value for the panel. In addition to being ISO and AATCC recommended conditions, this minimizes crispening issues since all

sample pairs had a much lower L* value.

• Different sample conditions: RIT-DuPont samples were glossy painted samples whereas textile samples were used in this study.

• Different number of pairs for blue center: Only 9 and 7 pairs were used in the RIT-DuPont dataset for moderate blue and dark blue color center, respectively whereas 66 pairs were used in this study.

• Different visual assessment method: Pair Comparison (Anchor Pair) method was used for RIT-DuPont samples, but gray scale method was used in this study.

The Lee-Shamey Blue dataset was also converted to CIExyY coordinates for comparison purposes as some of the previously published studies are generally given by chromaticity ellipses based on the CIExy plane. The chromaticity-discrimination ellipse based on Lee-Shamey Blue dataset has the smallest ratio of axes (4.27) and area (0.08) among the ellipses obtained from RIT-DuPont, Witt, and BFD datasets.

V. Future Work

The following are suggested topics for additional research:

• The assessment of viewing conditions in all datasets may be needed to analyze observer variability. All experimental datasets may have to be examined to obtain an accurate assessment of color difference formulae.

• A significant amount of work has been carried out to obtain experimental data and evaluate existing color difference formulae in many countries and by several research groups. However, there are many complexities in obtaining the experimental data from previously published data. Some of the work is based on laboratory trials and others based on industrial assessments. Various conditions, and often different media are typically employed. Often it is very difficult to obtain the exact methodology employed. It is therefore envisaged that a suitably maintained world wide web domain could be established to store such data and allow all interested parties to share, and access the contents. This would be a significant addition to the public knowledge domain in the color science arena.

• A linear gray scale could be developed to assess the variation between samples. If a linear gray scale is used to evaluate samples, the need to use a polynomial fitting procedure to data would be eliminated.

• Visual assessment methods based on pair comparison could be used to get acceptability responses for textile samples. The results should be compared with those obtained from visual assessments based on gray scale.

• The analysis of data from another color center in the blue region (High chroma blue, L* = 34, a* = 7, b* = -44) was initiated in this study but due to the limited period of time available was not completed. The dyeing of samples to produce a set with a large number of samples around the center needs to be completed and the results should be examined in detail. These could be used to compare data against other established datasets and to further verify the findings of this work.

• Ultimately, more color centers, well distributed throughout the color space, could be developed to assess the viability of alternative color difference formulae.

The large number of sample pairs around the blue center used in this work means that an effective look-up table for color difference is likely feasible. The performance of color difference prediction using an optimized look-up table could be compared to the performance of all existing color difference formulae to provide evidence for whether such an approach could provide an advancement in quantifying color difference of textile, and perhaps other materials.

VI. References

1. Gove, P. B. Color. In *Webster's Third New International Dictionary*; 3rd Ed. The Merriam-Webster editorial staff. Ed. Merriam-Webster INC: Springfield, MA, 1986.
2. Berns, R. S. *Principles of Color Technology;* John Wiley & Sons. INC: New York, NY, 2000; pp 13-20.
3. National Eye Institute. Macular Hole Resource Guide. http://www.nei.nih.gov/health/macularhole/index.asp (retrieved Dec/06).
4. Cajal, S. R. Retina. http://en.wikipedia.org/wiki/Image:Fig_retine.png (retrieved 11/06/03).
5. Bowmaker, J. K.; Dartnall, H. J. A. Visual Pigments of Rods and Cones in a Human Retina. *J. Physiol.* 1980, *298*, 501.
6. Hinks, D.; Shamey, R.; Aspland, R.; Jasper, W.; Kuehni, R.; Cassill, N. Annual Reports. In *Optimizing color control throughout the textile supply chain*. National Textile Center: Spring House, PA, 2006.
7. Cardenas, L.; Lee, S. G.; Hinks, D.; Shamey, R.; Jasper, W.; Cassill, N.; Aspland, R. Annual Forum. In *Optimizing color control throughout the textile supply chain*. National Textile Center: Hilton Head, SC, 2007.
8. Newton, I.; Cohen, I. B.; Einstein, A.; Whittaker, E. *Opticks: Or a Treatise of the Reflections, Refractions, Inflections & Colours of Light-Based on the Fourth Edition London, 1730;* Dover Publications: New York, NY, 1952.
9. Wyszecki, G.; Stiles, W. S. *Color Science: Concepts and Methods, Quantitative Data and Formulae;* John Wiley & Sons, INC: New York, NY,

2000; pp 117-130.

10. Krantz, D. H. Color Measurement and Color Theory: I. Representation Theorem for Grassmann Structures*. J. Math. Psychol.* 1975, *12*, 283.
11. Patterson, D. The Development of Colour Science. *Rev. Prog. Coloration.* 1976, 7, 46.
12. American Society for Testing and Materials. *Standard Practice for Computing the Colors of Objects by Using the CIE System*; ASTM E 308-01; ASTM: PA, 2006.
13. Commission Internationale de l'Eclairage. *2° Spectral luminous efficiency function for photopic vision*; CIE Publication No. 86; CIE: Vienna, Austria, 1990.
14. Commission Internationale de l'Eclairage. *Brightness-Luminance Relations: Classified Bibliography;* CIE Publication No. 78; CIE: Vienna, Austria, 1988.
15. Guild, J. The Colorimetric Properties of the Spectrum. *Philos. T. Roy. Soc. A.* 1931, *230*, 149.
16. Wright, W. D. A Re-determination of the Trichromatic Coefficients of the Spectral Colours. *Transactions of the Optical Society*. 1928, *30*, 141.
17. Berns, R. S. *Principles of Color Technology;* John Wiley & Sons. INC: New York, NY, 2000; pp 50.
18. Commission Internationale de l'Eclairage. *Colorimetry, 2nd edition;* CIE Publication No. 15.2; CIE: Vienna, Austria, 1986.
19. Stiles, W. S.; Burch, N. P. N.P.L. Colour-matching Investigation: Fianl report, *Opt. Acta*. 1959, *6*, 1.
20. Trezona, L. T.; Parkins, R. P. Derivation of the 1964 Colorimetric Standards,

Color Res. Appl. 1998, *23*, 221.

21. Commission Internationale de l'Eclairage. *Special Metamerism Index: Change in Observer;* CIE Publication No. 80; CIE: Vienna, Austria, 1989.
22. Nayatani, Y.; Takahama, K.; Sobagaki, H. A Proposal of New Standard Deviate Observers, *Color Res. Appl*. 1983, *8*, 47.
23. Ohta, N. Formulation of a Standard Deviate Observer by a Nonlinear Optimization Technique, *Color Res. Appl.* 1985, *10*, 156.
24. Alfvin, R. L.; Fairchild, M. D. Observer Variability in Metameric Color Matches using Color Reproduction Media, *Color Res. Appl.* 1997, *22*, 174.
25. Wyszecki, G.; Stiles, W. S. *Color Science: Concepts and Methods, Quantitative Data and Formulae;* John Wiley & Sons, INC: New York, NY, 2000; pp 11-19.
26. American Society for Testing and Materials. *Standard Terminology of Appearance*; ASTM E 284-06b; ASTM: PA, 2006.
27. Borbely, A.; Samson, A.; Schanda, J. The Concept of Correlated Colour Temperature Revisited, *Color Res. Appl.* 2001, *26*, 450.
28. Berns, R. S. *Principles of Color Technology;* John Wiley & Sons. INC: New York, NY, 2000; pp 6-7.
29. *Colour Physics for Industry*, 2nd ed.; Mcdonald, R.; Society of Dyer and Colourists: Bradford, England, 1997; pp 121-123.
30. Newhall, S.M.; Nickerson, D.; Judd,D. B. Final Report of the OSA Subcommittee on the Spacing of the Munsell Colors. *J. Opt. Soc. Am*. 1943, *33*, 385.
31. Scandinavian Colour Institute. The NCS System.

http://83.168.206.163/webbizz/mainPage/main.asp (retrieved 2005).

32. Macadam, D. L. Uniform Color Scales. *J. Opt. Soc. Am*. 1974, *64*, 1691.
33. Choudhury, A. K. R. Colour Order Systems. *Rev. Prog. Coloration.* 1996, *26,* 54.
34. Datacolor Inc. *Spectraflash 600 Plus Operators Manual*; Part No. 4230-0323; Datacolor Inc: NC, 1997.
35. Hunt, R. W. G. Colour Measurement. *Rev. Prog. Coloration.* 1971, *2*, 11.
36. *Colour Physics for Industry*, 2nd ed.; Mcdonald, R.; Society of Dyer and Colourists: Bradford, England, 1997; pp 65-68.
37. American Association of Textile Chemists and Colorists. *Visual Assessment of Color Difference of Textiles*; AATCC RA 36 Evaluation Procedure 9; AATCC: NC, 2002.
38. American Association of Textile Chemists and Colorists. *Gray Scale for Color Change*; AATCC RA 36 Evaluation Procedure 1; AATCC: NC, 2002.
39. Luo, M. R. Development of colour-difference formulae. *Rev. Prog. Coloration.* 2002, *32*, 28.
40. *Color Space and Its Division: Color Order from Antiquity to the Present*.; Kuehni, R. G.; John Wiley & Sons. INC: New York, NY, 2003; pp 204-270.
41. McDonald, R. Industrial pass/fail color matching. Part III- Development of a pass/fail formula for use with instrumental measurement of color difference. *J. Soc. Dyers Col*. 1980, *96*, 286.
42. Clarke, F. J. J.; McDonald, R.; Rigg, B. Modification to JPC79 colour-difference formula. *J. Soc. Dyers Col*. 1984, *100*, 128.
43. International Organization for Standardization. *Textiles - Tests for colour*

fastness - Part J03: Calculation of colour differences; ISO 105-J03; ISO: 1995.

44. American Association of Textile Chemists and Colorists. *CMC: Calculation of Small Color Differences for Acceptability*; AATCC Test Method 173-1989; AATCC: NC, 1992.
45. Luo, M. R.; Rigg, B. BFD (l:c) colour difference formula, Part I-Development of the formula. *J. Soc. Dyers Col.* 1987, *103*, 86.
46. Commission Internationale de l'Eclairage. *Colorimetry, Industrial Colour-Difference Evaluation;* CIE Publication No. 116; CIE: Vienna, Austria, 1995.
47. Luo, M. R.; Cui, G.; Rigg, B. The Development of CIE 2000 Color-Difference Formula: CIEDE2000. *Color Res. Appl*. 2001, *26*, 348.
48. X-Rite. *A Guide to Understanding Color Tolerancing*; X-Rite: MI, 1994.
49. McLaren, K. Colour Passing – Visual or Instrumental? *J. Soc. Dyers Col.* 1970, *86*, 389.
50. Alder, C.; Chaing, K. P.; Chong, T. F.; Coates, E.; Khalili, A. A.; Rigg, B. Uniform Chromaticity Scales – New Experimental Data. *J. Soc. Dyers Col.* 1982, *98*, 14.
51. Guan, S. S.; Luo, M. R. A Colour-difference Formula for Assessing Large Color Differences. *Color Res. Appl.* 1999, *24*, 344.
52. Kuehni, R. G.; Marcus, R. T. An Experiment in Visual Scaling of Small Color Differences. *Color Res. Appl*. 1979, *4*, 83.
53. Witt, K.; Doring, G. Parametric Variations in a Threshold Color-Difference Ellipsoid for Green Painted Samples, *Color Res. Appl*. 1983, *8*, 153.
54. Witt, K. Three-Dimensional Threshold of Color-Difference probability in

Painted Samples: Variability of Observers in Four CIE Color Regions, *Color Res. Appl*. 1987, *12*, 128.

55. Witt, K. Geometric Relations between Scales of Small Colour Differences, *Color Res. Appl*. 1999, *24*, 78.
56. Alder, C. A Monte Carlo Method for the Validation of Discrimination Ellipse Data, *J. Soc. Dyers Col.* 1981, *97*, 514.
57. Alman, D. H.; Berns, R. S.; Snyder, G. D.; Larsen, W. A. Performance Testing of Color Difference Matrices Using a Color Tolerance Dataset, *Color Res. Appl*. 1989, *14*, 139.
58. Finney, D. J. *Probit Analysis,* 3rd ed., Cambridge U. Press: Cambridge, 1971.
59. Berns, R. S.; Alman, D. H.; Reniff, L.; Snyder, G. D.; Balonon-Rosen, M. R. Visual Determination of Supra Threshold Color-Difference Tolerances Using Probit Analysis, *Color Res. Appl*. 1991, *16*, 297.
60. Hinks, D.; Shamey, R.; Cardenas, L.; Lee, S. G.; Kuehni R.; Jasper, W. ISCC 2007 Annual Meeting. *Variability in Visual Small Color Difference Assessment: What it means for Color Difference Formula Performance*. Inter-Society Color Council (ISCC): Kansas City, Missouri, 29-30 April, 2007, 35.
61. American Optical Company, *Pseudo-isochromatic Plates for Testing Color Perception*, Beck Engraving Company, Inc.: New York, PA.
62. Kim, D. H., The Influence of Parametric Effects on the Appearance of Small Colour Differences. Ph.D. Dissertation, The University of Leeds, U.K., 1997.
63. Luo, M. R.; Rigg, B. Chromaticity-discrimination ellipses for surface colours, *Color Res. Appl*. 1986, *11*, 25.
64. Cui, G.; Luo, M. R.; Rigg, R.; Roesler, G.; Witt, K. Uniform Colour Spaces

Based on the DIN99 Colour-Difference Formula, *Color Res. Appl*. 2002, *27*, 282.

65. EasyRGB. Math: Color Conversion Formulas. http://www.easyrgb.com/math.html (accessed March 3, 2007)
66. Robertson, A. R. CIE Guidelines for Coordinated Research on Colour-Difference Evaluation. *Color Res. Appl*. 1978, *3*, 149.
67. Melgosa, M.; Hita, E.; Poza, A. J.; Alman, D. H.; Berns, R. S. Suprathreshold Color-Difference Ellipsoids for Surface Colors, *Color Res. Appl*. 1997, *22*, 148.
68. Cheung, M.; Rigg, B. Colour-Difference Ellipsoids for Five CIE Colour Centres, *Color Res. Appl*. 1986, *11*, 185.
69. Witt, K. CIE Guidelines for Coordinated Future Work on Industrial Colour-Difference Evaluation. *Color Res. Appl*. 1995, *20*, 399.

VII. Appendices

Appendix A. The color attributes and color differences of blue samples.

Samples	L*	DL*	a*	Da*	b*	Db*	CIELAB	CMC (1:1)	CIE94 (1:1:1)	CIEDE 2000 (1:1:1)
Standard	36.39	0.00	4.70	0.00	-31.36	0.00	0.00	2.90	0.00	0.00
1	36.19	-0.20	1.78	-2.92	-27.55	3.81	4.80	1.58	2.40	1.41
2	37.75	1.36	5.31	0.61	-31.76	-0.40	1.54	2.28	1.42	1.19
3	35.89	-0.50	6.72	2.02	-34.95	-3.59	4.15	0.79	1.92	1.03
4	36.19	-0.20	5.36	0.66	-30.51	0.85	1.09	2.47	0.65	0.94
5	36.79	0.40	6.06	1.36	-27.50	3.86	4.11	0.43	2.05	3.09
6	36.50	0.11	4.25	-0.45	-30.87	0.49	0.67	1.83	0.36	0.22
7	35.84	-0.55	4.17	-0.53	-34.62	-3.26	3.35	1.07	1.56	2.01
8	36.74	0.35	3.54	-1.16	-31.59	-0.23	1.23	0.47	0.87	1.05
9	36.50	0.11	4.51	-0.19	-30.44	0.92	0.95	1.53	0.40	0.37
10	37.01	0.62	3.54	-1.16	-29.08	2.28	2.63	1.89	1.30	0.84
11	36.33	-0.06	4.97	0.27	-27.67	3.69	3.70	1.85	1.59	2.15
12	36.52	0.13	2.59	-2.11	-32.00	-0.64	2.21	3.84	1.48	1.93
13	34.21	-2.18	4.56	-0.14	-25.28	6.08	6.46	2.20	3.35	3.68
14	36.93	0.54	2.38	-2.32	-29.05	2.31	3.32	2.69	1.82	1.21
15	35.65	-0.74	6.67	1.97	-28.06	3.30	3.91	2.14	2.22	3.29
16	37.31	0.92	6.96	2.26	-31.44	-0.08	2.44	0.71	1.77	1.90
17	36.51	0.12	5.52	0.82	-31.23	0.13	0.84	2.16	0.58	0.71
18	36.44	0.05	6.82	2.12	-29.51	1.85	2.81	1.06	1.75	2.57
19	36.69	0.30	5.61	0.91	-30.29	1.07	1.44	2.21	0.87	1.25
20	36.61	0.22	6.75	2.05	-29.25	2.11	2.95	1.03	1.79	2.66
21	36.30	-0.09	3.60	-1.10	-32.04	-0.68	1.30	1.26	0.83	1.16
22	36.28	-0.11	3.52	-1.18	-29.45	1.91	2.25	0.77	1.05	0.57
23	35.75	-0.64	4.51	-0.19	-30.75	0.61	0.90	1.23	0.69	0.57
24	35.63	-0.76	4.65	-0.05	-33.18	-1.82	1.97	1.52	1.08	1.14
25	35.63	-0.76	3.34	-1.36	-32.17	-0.81	1.76	1.35	1.27	1.55
26	35.47	-0.92	5.64	0.94	-30.76	0.60	1.45	3.09	1.17	1.27
27	33.71	-2.68	4.42	-0.28	-33.11	-1.75	3.21	2.71	2.79	2.45
28	34.10	-2.29	5.73	1.03	-30.67	0.69	2.60	1.52	2.42	2.20
29	35.03	-1.36	4.52	-0.18	-30.93	0.43	1.44	2.22	1.37	1.14

Appendix A (continued).

Samples	L*	DL*	a*	Da*	b*	Db*	CIELAB	CMC (1:1)	CIE94 (1:1:1)	CIEDE 2000 (1:1:1)
30	34.52	-1.87	4.49	-0.21	-29.65	1.71	2.54	2.27	2.00	1.72
31	34.56	-1.83	3.68	-1.02	-32.36	-1.00	2.32	1.79	2.02	1.96
32	34.93	-1.46	5.56	0.86	-30.91	0.45	1.75	1.80	1.59	1.50
33	37.81	1.42	3.70	-1.00	-30.47	0.89	1.95	2.35	1.59	1.29
34	37.86	1.47	4.31	-0.39	-27.88	3.48	3.80	1.86	2.06	2.01
35	38.03	1.64	4.69	-0.01	-30.44	0.92	1.88	1.45	1.68	1.47
36	37.41	1.02	3.94	-0.76	-32.50	-1.14	1.71	0.93	1.26	1.41
37	37.08	0.69	5.25	0.55	-32.08	-0.72	1.14	2.21	0.82	0.62
38	37.85	1.46	6.28	1.58	-30.31	1.05	2.39	1.52	1.90	2.13
39	37.25	0.86	6.09	1.39	-32.47	-1.11	1.98	1.80	1.30	0.98
40	34.82	-1.57	4.71	0.01	-32.35	-0.99	1.86	1.75	1.62	1.39
41	37.66	1.27	4.25	-0.45	-33.22	-1.86	2.30	1.59	1.54	1.64
42	36.75	0.36	4.57	-0.13	-28.23	3.13	3.15	0.46	1.35	1.59
43	36.63	0.24	4.51	-0.19	-32.00	-0.64	0.71	0.31	0.39	0.50
44	36.14	-0.25	4.55	-0.15	-31.14	0.22	0.37	1.99	0.28	0.22
45	36.85	0.46	5.00	0.30	-27.61	3.75	3.79	0.62	1.69	2.24
46	36.46	0.07	4.16	-0.54	-32.06	-0.70	0.89	0.15	0.50	0.75
47	36.51	0.12	4.77	0.07	-31.48	-0.12	0.18	0.49	0.14	0.11
48	36.50	0.11	5.04	0.34	-32.23	-0.87	0.94	0.87	0.42	0.28
49	37.16	0.77	4.82	0.12	-31.11	0.25	0.82	0.23	0.78	0.68
50	36.55	0.16	4.57	-0.13	-31.52	-0.16	0.26	1.32	0.20	0.22
51	36.63	0.24	5.97	1.27	-30.24	1.12	1.71	0.89	1.07	1.55
52	36.96	0.57	5.26	0.56	-30.65	0.71	1.07	0.83	0.77	0.91
53	36.54	0.15	5.67	0.97	-31.34	0.02	0.98	0.90	0.67	0.78
54	36.58	0.19	5.58	0.88	-32.60	-1.24	1.53	2.32	0.75	0.40
55	35.87	-0.52	7.41	2.71	-33.08	-1.72	3.25	3.03	1.90	1.47
56	37.38	0.99	7.74	3.04	-35.10	-3.74	4.92	3.24	2.54	1.45
57	37.78	1.39	7.87	3.17	-34.90	-3.54	4.95	2.43	2.74	1.73
58	35.82	-0.57	6.94	2.24	-35.04	-3.68	4.35	3.61	2.05	1.08
59	36.53	0.14	0.41	-4.29	-31.04	0.32	4.30	2.16	2.90	3.26

Appendix A (continued).

Samples	L*	DL*	a*	Da*	b*	Db*	CIELAB	CMC (1:1)	CIE94 (1:1:1)	CIEDE 2000 (1:1:1)
60	36.75	0.36	2.26	-2.44	-32.04	-0.68	2.56	1.12	1.74	2.22
61	36.25	-0.14	3.55	-1.15	-32.21	-0.85	1.44	0.46	0.90	1.28
62	36.58	0.19	4.73	0.03	-30.55	0.81	0.83	1.50	0.39	0.47
63	37.31	0.92	5.69	0.99	-30.18	1.18	1.79	2.51	1.28	1.55
64	36.94	0.55	3.43	-1.27	-26.56	4.80	5.00	1.10	2.14	1.84
65	36.96	0.57	4.18	-0.52	-29.62	1.74	1.90	0.57	0.95	0.77
66	35.94	-0.45	4.42	-0.28	-31.57	-0.21	0.57	2.90	0.50	0.49

Appendix B. The results of polynomial procedure using SAS to obtain statistically reliable polynomial equations for converting from gray scale to CIELAB, CIE94(1:1:1), CMC(1:1), and CIEDE2000(1:1:1) color difference, respectively.

Box on the numbers means there is statistically insignificant relationship with its equation at 5% of significant level (α=0.05).

The GLM Procedure

Dependent Variable: difference_cielab

Source	DF	Sum of Squares	Mean Square	F Value	Pr > F
Model	4	155.5511856	38.8877964	984.97	<.0001
Error	4	0.1579244	0.0394811		
Corrected Total	8	155.7091100			

R-Square	Coeff Var	Root MSE	difference_cielab Mean
0.998986	4.165609	0.198698	4.769974

Source	DF	Type I SS	Mean Square	F Value	Pr > F
grade	1	139.4054218	139.4054218	3530.94	<.0001
grade2	1	14.3076829	14.3076829	362.39	<.0001
grade3	1	1.7213133	1.7213133	43.60	0.0027
grade4	1	0.1167676	0.1167676	2.96	0.1606

Source	DF	Type III SS	Mean Square	F Value	Pr > F
grade	1	1.31618303	1.31618303	33.34	0.0045
grade2	1	0.42758819	0.42758819	10.83	0.0302
grade3	1	0.20353962	0.20353962	5.16	0.0857
grade4	1	0.11676762	0.11676762	2.96	0.1606

Parameter	Estimate	Standard Error	t Value	Pr > |t|
Intercept	28.55962490	2.08607129	13.69	0.0002
grade	-20.84850355	3.61086547	-5.77	0.0045
grade2	6.92033529	2.10285268	3.29	0.0302
grade3	-1.13334142	0.49914973	-2.27	0.0857
grade4	0.07127972	0.04144759	1.72	0.1606

A fourth-degree of polynomial equation for CIELAB.

Appendix B (continued).

The GLM Procedure

Dependent Variable: difference_cielab

Source	DF	Sum of Squares	Mean Square	F Value	Pr > F
Model	3	155.4344180	51.8114727	943.08	<.0001
Error	5	0.2746920	0.0549384		
Corrected Total	8	155.7091100			

R-Square	Coeff Var	Root MSE	difference_cielab Mean
0.998236	4.913851	0.234389	4.769974

Source	DF	Type I SS	Mean Square	F Value	Pr > F
grade	1	139.4054218	139.4054218	2537.49	<.0001
grade2	1	14.3076829	14.3076829	260.43	<.0001
grade3	1	1.7213133	1.7213133	31.33	0.0025

Source	DF	Type III SS	Mean Square	F Value	Pr > F
grade	1	7.96372011	7.96372011	144.96	<.0001
grade2	1	3.06818049	3.06818049	55.85	0.0007
grade3	1	1.72131328	1.72131328	31.33	0.0025

Parameter	Estimate	Standard Error	t Value	Pr > |t|
Intercept	25.28330368	1.00250877	25.22	<.0001
grade	-14.90683010	1.23812729	-12.04	<.0001
grade2	3.36398662	0.45014434	7.47	0.0007
grade3	-0.27798483	0.04966256	-5.60	0.0025

A third-degree of polynomial equation for CIELAB.

The GLM Procedure

Dependent Variable: difference_cie94

Source	DF	Sum of Squares	Mean Square	F Value	Pr > F
Model	4	155.5537406	38.8884351	981.11	<.0001
Error	4	0.1585487	0.0396372		
Corrected Total	8	155.7122893			

R-Square	Coeff Var	Root MSE	difference_cie94 Mean
0.998982	4.175442	0.199091	4.768138

Source	DF	Type I SS	Mean Square	F Value	Pr > F
grade	1	139.3940375	139.3940375	3516.75	<.0001
grade2	1	14.3251158	14.3251158	361.41	<.0001
grade3	1	1.7176696	1.7176696	43.33	0.0028
grade4	1	0.1169176	0.1169176	2.95	0.1610

Source	DF	Type III SS	Mean Square	F Value	Pr > F
grade	1	1.31615297	1.31615297	33.21	0.0045
grade2	1	0.42760791	0.42760791	10.79	0.0304
grade3	1	0.20363121	0.20363121	5.14	0.0861
grade4	1	0.11691765	0.11691765	2.95	0.1610

Parameter	Estimate	Standard Error	t Value	Pr > |t|
Intercept	28.55802726	2.09019085	13.66	0.0002
grade	-20.84826544	3.61799620	-5.76	0.0045
grade2	6.92049487	2.10700539	3.28	0.0304
grade3	-1.13359636	0.50013545	-2.27	0.0861
grade4	0.07132549	0.04152944	1.72	0.1610

A fourth-degree of polynomial equation for CIE94.

Appendix B (continued).

The GLM Procedure

Dependent Variable: difference_cie94

Source	DF	Sum of Squares	Mean Square	F Value	Pr > F
Model	3	155.4368229	51.8122743	940.45	<.0001
Error	5	0.2754664	0.0550933		
Corrected Total	8	155.7122893			

R-Square	Coeff Var	Root MSE	difference_cie94 Mean
0.998231	4.922667	0.234720	4.768138

Source	DF	Type I SS	Mean Square	F Value	Pr > F
grade	1	139.3940375	139.3940375	2530.15	<.0001
grade2	1	14.3251158	14.3251158	260.02	<.0001
grade3	1	1.7176696	1.7176696	31.18	0.0025

Source	DF	Type III SS	Mean Square	F Value	Pr > F
grade	1	7.95938926	7.95938926	144.47	<.0001
grade2	1	3.06430664	3.06430664	55.62	0.0007
grade3	1	1.71766958	1.71766958	31.18	0.0025

Parameter	Estimate	Standard Error	t Value	Pr > |t|
Intercept	25.27960197	1.00392085	25.18	<.0001
grade	-14.90277621	1.23987125	-12.02	<.0001
grade2	3.36186228	0.45077839	7.46	0.0007
grade3	-0.27769046	0.04973252	-5.58	0.0025

A third-degree of polynomial equation for CIE94.

The GLM Procedure

Dependent Variable: difference_cmc21

Source	DF	Sum of Squares	Mean Square	F Value	Pr > F
Model	4	39.13082562	9.78270640	1117.07	<.0001
Error	4	0.03503000	0.00875750		
Corrected Total	8	39.16585562			

R-Square	Coeff Var	Root MSE	difference_cmc21 Mean
0.999106	3.779880	0.093582	2.475780

Source	DF	Type I SS	Mean Square	F Value	Pr > F
grade	1	35.09405167	35.09405167	4007.31	<.0001
grade2	1	3.55513141	3.55513141	405.95	<.0001
grade3	1	0.43777972	0.43777972	49.99	0.0021
grade4	1	0.04386282	0.04386282	5.01	0.0888

Source	DF	Type III SS	Mean Square	F Value	Pr > F
grade	1	0.37452026	0.37452026	42.77	0.0028
grade2	1	0.13379755	0.13379755	15.28	0.0174
grade3	1	0.06995732	0.06995732	7.99	0.0475
grade4	1	0.04386282	0.04386282	5.01	0.0888

Parameter	Estimate	Standard Error	t Value	Pr > |t|
Intercept	14.76848874	0.98248209	15.03	0.0001
grade	-11.12127039	1.70061813	-6.54	0.0028
grade2	3.87113536	0.99038566	3.91	0.0174
grade3	-0.66443556	0.23508577	-2.83	0.0475
grade4	0.04368708	0.01952067	2.24	0.0888

A fourth-degree of polynomial equation for CMC.

Appendix B (continued).

The GLM Procedure

Dependent Variable: difference_cmc21

Source	DF	Sum of Squares	Mean Square	F Value	Pr > F
Model	3	39.08696280	13.02898760	825.74	<.0001
Error	5	0.07889281	0.01577856		
Corrected Total	8	39.16585562			

R-Square	Coeff Var	Root MSE	difference_cmc21 Mean
0.997986	5.073664	0.125613	2.475780

Source	DF	Type I SS	Mean Square	F Value	Pr > F
grade	1	35.09405167	35.09405167	2224.16	<.0001
grade2	1	3.55513141	3.55513141	225.31	<.0001
grade3	1	0.43777972	0.43777972	27.75	0.0033

Source	DF	Type III SS	Mean Square	F Value	Pr > F
grade	1	2.00496512	2.00496512	127.07	<.0001
grade2	1	0.77570571	0.77570571	49.16	0.0009
grade3	1	0.43777972	0.43777972	27.75	0.0033

Parameter	Estimate	Standard Error	t Value	Pr > |t|
Intercept	12.76044341	0.53725927	23.75	<.0001
grade	-7.47964039	0.66353071	-11.27	<.0001
grade2	1.69146222	0.24123901	7.01	0.0009
grade3	-0.14019062	0.02661490	-5.27	0.0033

A third-degree of polynomial equation for CMC.

The GLM Procedure

Dependent Variable: difference_cmc21

Source	DF	Sum of Squares	Mean Square	F Value	Pr > F
Model	4	153.9806192	38.4951548	994.59	<.0001
Error	4	0.1548179	0.0387045		
Corrected Total	8	154.1354371			

R-Square	Coeff Var	Root MSE	difference_cmc21 Mean
0.998996	4.267348	0.196735	4.610229

Source	DF	Type I SS	Mean Square	F Value	Pr > F
grade	1	135.7423924	135.7423924	3507.15	<.0001
grade2	1	16.0186006	16.0186006	413.87	<.0001
grade3	1	2.0579536	2.0579536	53.17	0.0019
grade4	1	0.1616726	0.1616726	4.18	0.1105

Source	DF	Type III SS	Mean Square	F Value	Pr > F
grade	1	1.57177602	1.57177602	40.61	0.0031
grade2	1	0.54773410	0.54773410	14.15	0.0197
grade3	1	0.27211765	0.27211765	7.03	0.0569
grade4	1	0.16167257	0.16167257	4.18	0.1105

Parameter	Estimate	Standard Error	t Value	Pr > |t|
Intercept	29.69646150	2.06545214	14.38	0.0001
grade	-22.78306100	3.57517495	-6.37	0.0031
grade2	7.83247779	2.08206766	3.76	0.0197
grade3	-1.31043244	0.49421603	-2.65	0.0569
grade4	0.08387314	0.04103792	2.04	0.1105

A fourth-degree of polynomial equation for CIEDE2000.

Appendix B (continued).

The GLM Procedure

Dependent Variable: difference_cmc21

Source	DF	Sum of Squares	Mean Square	F Value	Pr > F
Model	3	153.8189467	51.2729822	810.02	<.0001
Error	5	0.3164904	0.0632981		
Corrected Total	8	154.1354371			

R-Square	Coeff Var	Root MSE	difference_cmc21 Mean
0.997947	5.457237	0.251591	4.610229

Source	DF	Type I SS	Mean Square	F Value	Pr > F
grade	1	135.7423924	135.7423924	2144.49	<.0001
grade2	1	16.0186006	16.0186006	253.07	<.0001
grade3	1	2.0579536	2.0579536	32.51	0.0023

Source	DF	Type III SS	Mean Square	F Value	Pr > F
grade	1	8.93716165	8.93716165	141.19	<.0001
grade2	1	3.60774743	3.60774743	57.00	0.0006
grade3	1	2.05795363	2.05795363	32.51	0.0023

Parameter	Estimate	Standard Error	t Value	Pr > |t|
Intercept	25.84129249	1.07608230	24.01	<.0001
grade	-15.79163561	1.32899273	-11.88	<.0001
grade2	3.64780715	0.48318017	7.55	0.0006
grade3	-0.30395475	0.05330727	-5.70	0.0023

A third-degree of polynomial equation for CIEDE2000.

Appendix C. The table of the variability between each trial for an individual observer by paired t-test.

Observer No.	*Sex	*Nationality	Difference	DF	T-Statistic	P-value	Adoption	*R
1	M	O	Trial 1- Trail 2	65	-0.80	0.4279	H_0	
			Trial 2- Trail 3	65	1.26	0.2108	H_0	R
			Trial 1- Trail 3	65	0.21	0.8306	H_0	
2	M	O	Trial 1- Trail 2	65	-0.51	0.6129	H_0	
			Trial 2- Trail 3	65	-0.92	0.3603	H_0	R
			Trial 1- Trail 3	65	-1.42	0.1618	H_0	
3	M	K	Trial 1- Trail 2	65	1.29	0.2016	H_0	
			Trial 2- Trail 3	65	0.23	0.8160	H_0	R
			Trial 1- Trail 3	65	1.48	0.1426	H_0	
4	M	K	Trial 1- Trail 2	65	-2.57	0.0125	H_a	
			Trial 2- Trail 3	65	2.61	0.0111	H_a	
			Trial 1- Trail 3	65	-0.24	0.8095	H_0	
5	F	K	Trial 1- Trail 2	65	-0.35	0.7293	H_0	
			Trial 2- Trail 3	65	-3.59	0.0006	H_a	
			Trial 1- Trail 3	65	-4.22	<0.0001	H_a	
6	M	K	Trial 1- Trail 2	65	3.72	0.0004	H_a	
			Trial 2- Trail 3	65	0.42	0.6749	H_0	
			Trial 1- Trail 3	65	4.48	<0.0001	H_a	
7	M	K	Trial 1- Trail 2	65	-2.73	0.0081	H_a	
			Trial 2- Trail 3	65	2.78	0.0070	H_a	
			Trial 1- Trail 3	65	-0.35	0.7249	H_0	
8	M	O	Trial 1- Trail 2	65	0.43	0.6679	H_0	
			Trial 2- Trail 3	65	-4.02	0.0002	H_a	
			Trial 1- Trail 3	65	-2.86	0.0057	H_a	
9	M	K	Trial 1- Trail 2	65	-0.03	0.9744	H_0	
			Trial 2- Trail 3	65	-1.08	0.2846	H_0	R
			Trial 1- Trail 3	65	-1.06	0.2920	H_0	

*sex: M - male, F - female; *Nationality: K - Korean, O – Others; *R: Repeatability

Appendix C (continued).

Observer No.	*Sex	*Nationality	Difference	DF	T-Statistic	P-value	Adoption	*R
10	F	O	Trial 1- Trail 2	65	-1.77	0.0806	H_0	
			Trial 2- Trail 3	65	-0.52	0.6063	H_0	
			Trial 1- Trail 3	65	-2.51	0.0147	H_a	
11	M	K	Trial 1- Trail 2	65	-5.98	<0.0001	H_a	
			Trial 2- Trail 3	65	2.00	0.0495	H_0	
			Trial 1- Trail 3	65	-3.73	0.0004	H_a	
12	M	O	Trial 1- Trail 2	65	-0.76	0.4525	H_0	
			Trial 2- Trail 3	65	2.84	0.0061	H_a	
			Trial 1- Trail 3	65	1.57	0.1213	H_0	
13	F	O	Trial 1- Trail 2	65	2.60	0.0112	H_a	
			Trial 2- Trail 3	65	-1.78	0.0790	H_0	
			Trial 1- Trail 3	65	0.81	0.4221	H_0	
14	F	O	Trial 1- Trail 2	65	-2.37	0.0209	H_a	
			Trial 2- Trail 3	65	-1.30	0.1995	H_0	
			Trial 1- Trail 3	65	-3.51	0.0008	H_a	
15	M	O	Trial 1- Trail 2	65	-1.88	0.0652	H_0	
			Trial 2- Trail 3	65	0.86	0.3955	H_0	R
			Trial 1- Trail 3	65	-0.89	0.3784	H_0	
16	M	O	Trial 1- Trail 2	65	1.93	0.0581	H_0	
			Trial 2- Trail 3	65	0.22	0.8266	H_0	R
			Trial 1- Trail 3	65	1.79	0.0775	H_0	
17	F	O	Trial 1- Trail 2	65	-1.50	0.1396	H_0	
			Trial 2- Trail 3	65	-2.14	0.0358	H_a	
			Trial 1- Trail 3	65	-2.74	0.0078	H_a	
18	F	O	Trial 1- Trail 2	65	-0.86	0.3909	H_0	
			Trial 2- Trail 3	65	-0.57	0.5705	H_0	R
			Trial 1- Trail 3	65	-1.44	0.1559	H_0	
19	F	O	Trial 1- Trail 2	65	0.09	0.9275	H_0	
			Trial 2- Trail 3	65	-1.66	0.1018	H_0	R
			Trial 1- Trail 3	65	-1.60	0.1146	H_0	

*sex: M - male, F - female; *Nationality: K - Korean, O – Others; *R: Repeatability

Appendix C (continued).

Observer No.	*Sex	*Nationality	Difference	DF	T-Statistic	P-value	Adoption	*R
20	M	O	Trial 1- Trail 2	65	-3.41	0.0011	H_a	
			Trial 2- Trail 3	65	-0.22	0.8263	H_0	
			Trial 1- Trail 3	65	-2.35	0.0219	H_a	
21	F	K	Trial 1- Trail 2	65	-1.76	0.0828	H_0	
			Trial 2- Trail 3	65	-6.47	<0.0001	H_a	
			Trial 1- Trail 3	65	-7.24	<0.0001	H_a	
22	M	K	Trial 1- Trail 2	65	-1.32	0.1918	H_0	
			Trial 2- Trail 3	65	5.50	<0.0001	H_a	
			Trial 1- Trail 3	65	3.60	0.0006	H_a	
23	M	K	Trial 1- Trail 2	65	-1.96	0.0544	H_0	
			Trial 2- Trail 3	65	0.67	0.5038	H_0	R
			Trial 1- Trail 3	65	-1.27	0.2077	H_0	
24	M	K	Trial 1- Trail 2	65	2.62	0.0109	H_a	
			Trial 2- Trail 3	65	-1.36	0.1773	H_0	
			Trial 1- Trail 3	65	1.17	0.2463	H_0	
25	F	K	Trial 1- Trail 2	65	-1.26	0.2105	H_0	
			Trial 2- Trail 3	65	-5.77	<0.0001	H_a	
			Trial 1- Trail 3	65	-5.78	<0.0001	H_a	
26	F	K	Trial 1- Trail 2	65	3.98	0.0002	H_a	
			Trial 2- Trail 3	65	0.93	0.3579	H_0	
			Trial 1- Trail 3	65	4.53	<0.0001	H_a	

*sex: M - male, F - female; *Nationality: K - Korean, O – Others; *R: Repeatability

Appendix D. The table of the observer accuracy between responses given by an individual observer and mean group responses for each trial by paired t-test.

Observer No.	*Sex	*Nationality	Difference	DF	T-Statistic	P-value	Adoption	*R
1	M	O	Group1- Trail 1	65	-8.43	<0.0001	H_a	
			Group2- Trail 2	65	-11.21	<0.0001	H_a	
			Group3- Trail 3	65	-8.18	<0.0001	H_a	
			Group Mean – Trial Mean	65	-15.31	<0.0001	H_a	
2	M	O	Group1- Trail 1	65	-7.69	<0.0001	H_a	
			Group2- Trail 2	65	-8.36	<0.0001	H_a	
			Group3- Trail 3	65	-9.87	<0.0001	H_a	
			Group Mean – Trial Mean	65	-10.16	<0.0001	H_a	
3	M	K	Group1- Trail 1	65	4.42	<0.0001	H_a	
			Group2- Trail 2	65	6.82	<0.0001	H_a	
			Group3- Trail 3	65	9.99	<0.0001	H_a	
			Group Mean – Trial Mean	65	9.88	<0.0001	H_a	
4	M	K	Group1- Trail 1	65	1.94	0.0570	H_0	
			Group2- Trail 2	65	-0.44	0.6614	H_0	
			Group3- Trail 3	65	3.38	0.0012	H_a	
			Group Mean – Trial Mean	65	1.96	0.0541	H_0	
5	F	K	Group1- Trail 1	65	10.98	<0.0001	H_a	
			Group2- Trail 2	65	12.03	<0.0001	H_a	
			Group3- Trail 3	65	11.77	<0.0001	H_a	
			Group Mean – Trial Mean	65	12.34	<0.0001	H_a	

*sex: M - male, F - female; *Nationality: K - Korean, O – Others; *R: Repeatability

Appendix D (continued).

Observer No.	*Sex	*Nationality	Difference	DF	T-Statistic	P-value	Adoption	*R
6	M	K	Group1- Trail 1	65	1.01	0.3184	H_0	
			Group2- Trail 2	65	8.71	<0.0001	H_a	
			Group3- Trail 3	65	10.51	<0.0001	H_a	
			Group Mean – Trial Mean	65	7.59	<0.0001	H_a	
7	M	K	Group1- Trail 1	65	3.78	0.0003	H_a	
			Group2- Trail 2	65	1.89	0.0633	H_0	
			Group3- Trail 3	65	6.05	<0.0001	H_a	
			Group Mean – Trial Mean	65	6.08	<0.0001	H_a	
8	M	O	Group1- Trail 1	65	2.62	0.0108	H_a	
			Group2- Trail 2	65	4.79	<0.0001	H_a	
			Group3- Trail 3	65	0.81	0.4233	H_0	
			Group Mean – Trial Mean	65	4.70	<0.0001	H_a	
9	M	K	Group1- Trail 1	65	-2.24	0.0285	H_a	
			Group2- Trail 2	65	-2.61	0.0113	H_a	
			Group3- Trail 3	65	-3.51	0.0008	H_a	
			Group Mean – Trial Mean	65	-3.99	0.0002	H_a	
10	F	O	Group1- Trail 1	65	-0.09	0.9254	H_0	
			Group2- Trail 2	65	-1.68	0.0969	H_0	
			Group3- Trail 3	65	-2.18	0.0330	H_a	
			Group Mean – Trial Mean	65	-2.22	0.0302	H_a	
11	M	K	Group1- Trail 1	65	-1.71	0.0913	H_0	
			Group2- Trail 2	65	-7.69	<0.0001	H_a	
			Group3- Trail 3	65	-5.24	<0.0001	H_a	
			Group Mean – Trial Mean	65	-7.29	<0.0001	H_a	

*sex: M - male, F - female; *Nationality: K - Korean, O – Others; *R: Repeatability

Appendix D (continued).

Observer No.	*Sex	*Nationality	Difference	DF	T-Statistic	P-value	Adoption	*R
12	M	O	Group1- Trail 1	65	3.34	0.0014	H_a	
			Group2- Trail 2	65	4.02	0.0002	H_a	
			Group3- Trail 3	65	7.26	<0.0001	H_a	
			Group Mean – Trial Mean	65	5.39	<0.0001	H_a	
13	F	O	Group1- Trail 1	65	0.80	0.4245	H_0	
			Group2- Trail 2	65	4.69	<0.0001	H_a	
			Group3- Trail 3	65	3.40	0.0011	H_a	
			Group Mean – Trial Mean	65	3.80	0.0003	H_a	
14	F	O	Group1- Trail 1	65	-2.79	0.0069	H_a	
			Group2- Trail 2	65	-4.27	<0.0001	H_a	
			Group3- Trail 3	65	-6.52	<0.0001	H_a	
			Group Mean – Trial Mean	65	-5.99	<0.0001	H_a	
15	M	O	Group1- Trail 1	65	-5.92	<0.0001	H_a	
			Group2- Trail 2	65	-7.97	<0.0001	H_a	
			Group3- Trail 3	65	-6.69	<0.0001	H_a	
			Group Mean – Trial Mean	65	-9.00	<0.0001	H_a	
16	M	O	Group1- Trail 1	65	-4.51	<0.0001	H_a	
			Group2- Trail 2	65	-2.89	0.0053	H_a	
			Group3- Trail 3	65	-1.91	0.0603	H_0	
			Group Mean – Trial Mean	65	-5.03	<0.0001	H_a	
17	F	O	Group1- Trail 1	65	-2.41	0.0190	H_a	
			Group2- Trail 2	65	-5.61	<0.0001	H_a	
			Group3- Trail 3	65	-7.15	<0.0001	H_a	
			Group Mean – Trial Mean	65	-6.72	<0.0001	H_a	

*sex: M - male, F - female; *Nationality: K - Korean, O – Others; *R: Repeatability

Appendix D (continued).

Observer No.	*Sex	*Nationality	Difference	DF	T-Statistic	P-value	Adoption	*R
18	F	O	Group1- Trail 1	65	-4.60	<0.0001	H_a	
			Group2- Trail 2	65	-5.90	<0.0001	H_a	
			Group3- Trail 3	65	-6.31	<0.0001	H_a	
			Group Mean – Trial Mean	65	-8.42	<0.0001	H_a	
19	F	O	Group1- Trail 1	65	3.56	0.0007	H_a	
			Group2- Trail 2	65	6.26	<0.0001	H_a	
			Group3- Trail 3	65	3.79	0.0003	H_a	
			Group Mean – Trial Mean	65	7.84	<0.0001	H_a	
20	M	O	Group1- Trail 1	65	11.17	<0.0001	H_a	
			Group2- Trail 2	65	9.63	<0.0001	H_a	
			Group3- Trail 3	65	8.85	<0.0001	H_a	
			Group Mean – Trial Mean	65	14.20	<0.0001	H_a	
21	F	K	Group1- Trail 1	65	14.49	<0.0001	H_a	
			Group2- Trail 2	65	12.19	<0.0001	H_a	
			Group3- Trail 3	65	1.30	0.1989	H_0	
			Group Mean – Trial Mean	65	10.88	<0.0001	H_a	
22	M	K	Group1- Trail 1	65	0.29	0.7737	H_0	
			Group2- Trail 2	65	-0.85	0.3959	H_0	
			Group3- Trail 3	65	8.25	<0.0001	H_a	
			Group Mean – Trial Mean	65	2.53	0.0137	H_a	
23	M	K	Group1- Trail 1	65	3.25	0.0018	H_a	
			Group2- Trail 2	65	1.13	0.2628	H_0	
			Group3- Trail 3	65	2.74	0.0078	H_a	
			Group Mean – Trial Mean	65	3.82	0.0003	H_a	

*sex: M - male, F - female; *Nationality: K - Korean, O – Others; *R: Repeatability

Appendix D (continued).

Observer No.	*Sex	*Nationality	Difference	DF	T-Statistic	P-value	Adoption	*R
24	M	K	Group1- Trail 1	65	3.44	0.0010	H_a	
			Group2- Trail 2	65	9.66	<0.0001	H_a	
			Group3- Trail 3	65	6.83	<0.0001	H_a	
			Group Mean – Trial Mean	65	10.13	<0.0001	H_a	
25	F	K	Group1- Trail 1	65	11.01	<0.0001	H_a	
			Group2- Trail 2	65	11.88	<0.0001	H_a	
			Group3- Trail 3	65	7.73	<0.0001	H_a	
			Group Mean – Trial Mean	65	13.86	<0.0001	H_a	
26	F	K	Group1- Trail 1	65	2.52	0.0141	H_a	
			Group2- Trail 2	65	12.72	<0.0001	H_a	
			Group3- Trail 3	65	13.40	<0.0001	H_a	
			Group Mean – Trial Mean	65	12.40	<0.0001	H_a	

*sex: M - male, F - female; *Nationality: K - Korean, O – Others; *R: Repeatability

Appendix E. Computer programs.

```
% SEUNG GEOL LEE (2007)
% using MATLAB
% computes color difference
% using CIELAB formula
% lab1 and lab2 must be 3 by 1 or 1 by 3 matrices
% and contain L*, a* and b* values

clear all;
close all;
clear functions;
clc;

lab1 = [36.39 4.70 -31.36]; % lab1 = standard sample (L, a, b)
x = load('../work/data/blue.dat') % Batch samples loaded from blue.dat

Std=lab1;

for i = 1:1:size(x,1)
    lab2(i,:) = x(i,:);
    [de,dl,dc,dh] = cielabde(lab1, lab2(i,:));
       % function [de,dl,dc,dh] = cielabde(lab1,lab2)
    d(i,:) = [de];
    e(i,:) = [dl];
    f(i,:) = [dc];
    g(i,:) = [dh];
    c(i,:) = [x(i,:) d(i) e(i) f(i) g(i)];
end

Final = c
```

```
% This code was referred from
% Computational colour science using MATLAB
% Stephen Westland, Caterina Ripamonti
% Chichester, West Sussex, England; Hoboken, NJ : J. Wiley, c2004

function [de,dl,dc,dh] = cielabde(lab1,lab2)

% function [de,dl,dc,dh] = cielabde(lab1,lab2)
% computes colour difference from CIELAB values
% using CIELAB formula
% lab1 and lab2 must be 3 by 1 or 1 by 3 matrices
% and contain L*, a* and b* values

dim = size(lab1);
if (dim(1) == 1) | (dim(2) == 1)
   lab1 = lab1(:)'; % force to be a row matrix
else
   disp('lab1 must be a row matrix');
   return;
end
if (dim(2) ~= 3)
   disp('lab1 must be 3 by 1 or 1 by 3');
   return;
end

dim = size(lab2);
if (dim(1) == 1) | (dim(2) == 1)
   lab2 = lab2(:)'; % force to be a row matrix
else
   disp('lab2 must be a row matrix');
   return;
end
if (dim(2) ~= 3)
   disp('lab2 must be 3 by 1 or 1 by 3');
   return;
end
```

```
dl = lab2(1)-lab1(1);
dc = sqrt(lab2(2)^2 + lab2(3)^2) - sqrt(lab1(2)^2 + lab1(3)^2);
dh = sqrt((lab2(2)-lab1(2))^2 + (lab2(3)-lab1(3))^2 - dc^2);

% get the polarity of the dh term
dh = dh*dhpolarity(lab1,lab2);

de = sqrt((dl/1)^2 + dc^2 + dh^2);
```

```
% SEUNG GEOL LEE (2007)
% using MATLAB
% computes color difference
% using the CIE94 formula
% lab1 and lab2 must be 3 by 1 or 1 by 3 matrices
% and contain L*, a* and b* values

clear all;
close all;
clear functions;
clc;

lab1 = [36.39 4.70 -31.36]; % lab1 = standard sample (L, a, b)
x = load('../work/data/blue.dat') % Batch samples loaded from blue.dat

paral = 1; % Lightness weight
parac = 1; % Chroma weight
parah = 1; % Hue weight

Std=lab1

for i = 1:1:size(x,1)
    lab2(i,:) = x(i,:);
    [de,dl,dc,dh] = cie94de(lab1, lab2(i,:), paral, parac, parah);
        % function [de,dl,dc,dh] = cie94de(lab1,lab2)
    d(i,:) = [de];
    e(i,:) = [dl];
    f(i,:) = [dc];
    g(i,:) = [dh];
    c(i,:) = [x(i,:) d(i) e(i) f(i) g(i)];
end

Final = c
```

```
% This code was referred from
% Computational colour science using MATLAB
% Stephen Westland, Caterina Ripamonti
% Chichester, West Sussex, England; Hoboken, NJ : J. Wiley, c2004

function [de,dl,dc,dh] = cie94de(lab1,lab2,paral,parac,parah)

% function [de,dl,dc,dh] = cie94de(lab1,lab2,paral,parac,parah)
% computes colour difference from CIELAB values
% using the CIE94 formula
% lab1 and lab2 must be 3 by 1 or 1 by 3 matrices
% and contain L*, a* and b* values
% The dl, dc and dh components are CIE94 deltas

dim = size(lab1);
if (dim(1) == 1) | (dim(2) == 1)
   lab1 = lab1(:)'; % force to be a row matrix
else
   disp('lab1 must be a row matrix');
   return;
end
if (dim(2) ~= 3)
   disp('lab1 must be 3 by 1 or 1 by 3');
   return;
end

dim = size(lab2);
if (dim(1) == 1) | (dim(2) == 1)
   lab2 = lab2(:)'; % force to be a row matrix
else
   disp('lab2 must be a row matrix');
   return;
end
if (dim(2) ~= 3)
   disp('lab2 must be 3 by 1 or 1 by 3');
   return;
```

```
end

if (nargin<5)
   disp('using default values of parametric values')
   paral=1; parac=1; parah = 1;
end


dl = lab2(1)-lab1(1);
dc = sqrt(lab2(2)^2 + lab2(3)^2) - sqrt(lab1(2)^2 + lab1(3)^2);
dh = sqrt((lab2(2)-lab1(2))^2 + (lab2(3)-lab1(3))^2 - dc^2);

% get the polarity of the dh term
dh = dh*dhpolarity(lab1,lab2);

% need to compute the weights
Lweight = 1.0;
[c,h] = car2pol([lab1(2) lab1(3)]); % require C*ab and H*ab of standard
Cweight = 1.0 + 0.045*c;
Hweight = 1.0 + 0.015*c;

dl = dl/(Lweight*paral);
dc = dc/(Cweight*parac);
dh = dh/(Hweight*parah);

de = sqrt(dl^2 + dc^2 + dh^2);
```

```
% SEUNG GEOL LEE (2007)
% using MATLAB
% computes colour difference
% using CMC(l:c) formula
% lab1 and lab2 must be 3 by 1 or 1 by 3 matrices
% and contain L*, a* and b* values

clear all;
close all;
clear functions;
clc;

lab1 = [36.39 4.70 -31.36]; % lab1 = standard sample (L, a, b)
x = load('../work/data/blue.dat') % Batch samples loaded from blue.dat

paral = 1; % Lightness weight
parac = 1; % Chroma weight

Std=lab1

for i = 1:1:size(x,1)
    lab2(i,:) = x(i,:);
    [de,dl,dc,dh] = cmcde(lab1, lab2(i,:), paral, parac);
       % function cmcde [de, dl, dc, dh]
    d(i,:) = [de];
    e(i,:) = [dl];
    f(i,:) = [dc];
    g(i,:) = [dh];
    c(i,:) = [x(i,:) d(i) e(i) f(i) g(i)];

end

Final = c
```

```
% This code was referred from
% Computational colour science using MATLAB
% Stephen Westland, Caterina Ripamonti
% Chichester, West Sussex, England; Hoboken, NJ : J. Wiley, c2004

function [de,dl,dc,dh] = cmcde(lab1,lab2,paral,parac)

% function [de,dl,dc,dh] = cmcde(lab1,lab2,paral,parac)
% computes colour difference from CIELAB values
% using CMC(l:c) formula
% lab1 and lab2 must be 3 by 1 or 1 by 3 matrices
% and contain L*, a* and b* values
% The dl, dc and dh components are CMC deltas
% The defaults for paral and parac are 1

dim = size(lab1);
if (dim(1) == 1) | (dim(2) == 1)
   lab1 = lab1(:)'; % force to be a row matrix
else
   disp('lab1 must be a row matrix');
   return;
end
if (dim(2) ~= 3)
   disp('lab1 must be 3 by 1 or 1 by 3');
   return;
end

dim = size(lab2);
if (dim(1) == 1) | (dim(2) == 1)
   lab2 = lab2(:)'; % force to be a row matrix
else
   disp('lab2 must be a row matrix');
   return;
end
if (dim(2) ~= 3)
   disp('lab2 must be 3 by 1 or 1 by 3');
```

```
   return;
end

if (nargin<4)
   disp('using default values of l:c')
   paral=1; parac=1;
end

% first compute the CIELAB deltas
dl = lab2(1)-lab1(1);
dc = sqrt(lab2(2)^2 + lab2(3)^2) - sqrt(lab1(2)^2 + lab1(3)^2);
dh = sqrt((lab2(2)-lab1(2))^2 + (lab2(3)-lab1(3))^2 - dc^2);

% get the polarity of the dh term
dh = dh*dhpolarity(lab1,lab2);

% now compute the CMC weights
if (lab1(1)<16)
   Lweight = 0.511;
else
   Lweight = (0.040975*lab1(1))/(1 + 0.01765*lab1(1));
end
[c,h] = car2pol([lab1(2) lab1(3)]); % require C*ab and H*ab of standard
Cweight = 0.638 + (0.0638*c)/(1 + 0.0131*c);
if (164 < h & h < 345)
   k1 = 0.56; k2 = 0.20; k3 = 168;
else
   k1 = 0.36; k2 = 0.40; k3 = 35;
end
T = k1 + abs(k2*cos((h + k3)*pi/180));

F = sqrt((c^4)/(c^4 + 1900));
Hweight = Cweight*(T*F + 1 - F);

dl = dl/(Lweight*paral);
dc = dc/(Cweight*parac);
```

```
dh = dh/Hweight;

de = sqrt(dl^2 + dc^2 + dh^2);
```

```
% SEUNG GEOL LEE (2007)
% using MATLAB
% computes color difference
% using the CIEDE2000 formula
% lab1 and lab2 must be 3 by 1 or 1 by 3 matrices
% and contain L*, a* and b* values

clear all;
close all;
clear functions;
clc;

lab1 = [36.39 4.70 -31.36]; % lab1 = standard sample (L, a, b)
x = load('../work/data/blue.dat') % Batch samples loaded from blue.dat

paral = 1; % Lightness weight
parac = 1; % Chroma weight
parah = 1; % Hue weight

Std=lab1

for i = 1:1:size(x,1)
    lab2(i,:) = x(i,:);
    [de,dl,dc,dh] = cie00de(lab1, lab2(i,:), paral, parac, parah);
       % function [de,dl,dc,dh] = cie00de(lab1,lab2,paral,parac,parah)
    d(i,:) = [de];
    e(i,:) = [dl];
    f(i,:) = [dc];
    g(i,:) = [dh];
    c(i,:) = [x(i,:) d(i) e(i) f(i) g(i)];
end

Final = c
```

```
% This code was referred from
% Computational colour science using MATLAB
% Stephen Westland, Caterina Ripamonti
% Chichester, West Sussex, England; Hoboken, NJ : J. Wiley, c2004

function [de,dl,dc,dh] = cie00de(lab1,lab2,paral,parac,parah)

% function [de,dl,dc,dh] = cie00de(lab1,lab2,paral,parac,parah)
% computes colour difference from CIELAB values
% using the CIEDE2000 formula
% lab1 and lab2 must be 3 by 1 or 1 by 3 matrices
% and contain L*, a* and b* values
% The dl, dc and dh components are CIEDE2000 deltas
% The defaults for paral, parac and parah are 1

dim = size(lab1);
if (dim(1) == 1) | (dim(2) == 1)
   lab1 = lab1(:)'; % force to be a row matrix
else
   disp('lab1 must be a row matrix');
   return;
end
if (dim(2) ~= 3)
   disp('lab1 must be 3 by 1 or 1 by 3');
   return;
end

dim = size(lab2);
if (dim(1) == 1) | (dim(2) == 1)
   lab2 = lab2(:)'; % force to be a row matrix
else
   disp('lab2 must be a row matrix');
   return;
end
if (dim(2) ~= 3)
   disp('lab2 must be 3 by 1 or 1 by 3');
```

```
   return;
end

if (nargin<5)
   disp('using default values of parametric values')
   paral=1; parac=1; parah = 1;
end

% convert the cartesian a*b* to polar chroma and hue
[c1,h1] = car2pol([lab1(2) lab1(3)]);
[c2,h2] = car2pol([lab2(2) lab2(3)]);
meanC = (c2+c1)/2;

% compute the G factor using the arithmetic mean chroma
G = 0.5 - 0.5*sqrt((meanC^7)/(meanC^7 + 25^7));

% transform the a* values
lab1(2) = (1 + G)*lab1(2);
lab2(2) = (1 + G)*lab2(2);

disp('G a* a*')
disp([G lab1(2) lab2(2)])

% recompute the polar coordinates using the new a*
[c1,h1] = car2pol([lab1(2) lab1(3)]);
[c2,h2] = car2pol([lab2(2) lab2(3)]);
disp('new polar coordinates')
disp([c1 h1 c2 h2])

% compute the mean values for use later
meanC = (c2+c1)/2;
meanL = (lab2(1)+lab1(1))/2;
[a1,b1] = pol2car([1,h1]);
[a2,b2] = pol2car([1,h2]);
a = (a1+a2)/2;
b = (b1+b2)/2;
```

```
[c,meanH] = car2pol([a b]);

disp('Mean values')
disp([meanL (lab1(2)+lab2(2))/2 (lab1(3)+lab2(3))/2 meanC meanH])

% compute the basic delta values
dh = (h2-h1);
if (dh>180)
    dh = dh - 360;
end

dl = lab2(1)-lab1(1);
dc = c2-c1;
dh = 2*sqrt(c1*c2)*sin((dh/2)*pi/180);


disp('Delta values')
disp([dl dc dh])

T = 1 - 0.17*cos((meanH-30)*pi/180) + 0.24*cos((2*meanH)*pi/180);
T = T + 0.32*cos((3*meanH + 6)*pi/180) - 0.20*cos((4*meanH - 63)*pi/180);

dthe = 30*exp(-((meanH-275)/25)^2);
rc = 2*sqrt((meanC^7)/(meanC^7 + 25^7));
rt = -sin(2*dthe*pi/180)*rc;


disp('T dthe rc rt')
disp([T dthe rc rt])

Lweight = 1 + (0.015*(meanL-50)^2)/sqrt(20 + (meanL-50)^2);
Cweight = 1 + 0.045*meanC;
Hweight = 1 + 0.015*meanC*T;

disp('weights')
disp([Lweight Cweight Hweight])
```

```
dl = dl/(Lweight*paral);
dc = dc/(Cweight*parac);
dh = dh/(Hweight*parah);

de = sqrt(dl^2 + dc^2 + dh^2 + rt*dc*dh);
```

```
% This code was referred from
% Computational colour science using MATLAB
% Stephen Westland, Caterina Ripamonti
% Chichester, West Sussex, England; Hoboken, NJ : J. Wiley, c2004

function [p] = dhpolarity(lab1,lab2)

% function [p] = dhpolarity(lab1,lab2)
% computes polarity of hue difference
% lab1 and lab2 must be 3 by 1 or 1 by 3 matrices
% and contain L*, a* and b* values
% p is +1 if the hue of the trial (lab2) is anticlockwise
% from the standard (lab1) and -1 otherwise
% 10th June 2004 - the original code in the book was incomplete
% some polarity errors occured when the standard was in the
% 3rd or 4th quadrant
% this has been corrected by rotating the std and trial
% when the standard h > 180

[c1, h1] = car2pol([lab1(2) lab1(3)]);
[c2, h2] = car2pol([lab2(2) lab2(3)]);
if (h1>180)
    h1 = h1 - 180;
    h2 = h2 - 180;
    if (h2 < 0)
        h2 = h2 + 360;
    end
end
p = (h2-h1);
if (p==0)
    p = 1;
else
    if (p>180)
       p = p - 360;
    end
    p = p/abs(p);  end
```

```
% This code was referred from
% Computational colour science using MATLAB
% Stephen Westland, Caterina Ripamonti
% Chichester, West Sussex, England; Hoboken, NJ : J. Wiley, c2004

function [c,h] = car2pol(ab)

% function [c,h] = cartopol(ab)
% converts a*b* or u*v* into the polar coordinates
% of Chroma C and Hue H
% ab must be a row or column matrix 2 by 1 or 1 by 2
% see also pol2car

dim = size(ab);
if (dim(1) == 1) | (dim(2) == 1)
   ab = ab(:)'; % force to be a row matrix
else
   disp('ab must be a row matrix');
   return;
end
if (dim(2) ~= 2)
   disp('ab must be 2 by 1 or 1 by 2');
   return;
end

% compute the distance from the centre
c = sqrt(ab(1)*ab(1) + ab(2)*ab(2));

% compute the angular term
if (ab(1) == 0) & (ab(2) > 0)
   h = 90;
elseif (ab(1) == 0) & (ab(2) < 0)
   h = 270;
elseif (ab(1) < 0) & (ab(2) == 0)
   h = 180;
elseif (ab(1) > 0) & (ab(2) == 0)
```

```
   h = 0;
elseif (ab(1) == 0) & (ab(2) == 0)
   h = 0;
else
   h = atan(abs(ab(2))/abs(ab(1)));
   h = 180*h/pi; % convert from radians to degrees
   if ((ab(1) > 0) & (ab(2) > 0))
      h = h; % first quadrant
   elseif ((ab(1) < 0) & (ab(2) > 0))
      h = 180 - h; % second quadrant
   elseif ((ab(1) < 0) & (ab(2) < 0))
      h = 180 + h; % third quadrant
   else
      h = 360 - h; % fourth quadrant
   end
end
```

```
% This code was referred from
% Computational colour science using MATLAB
% Stephen Westland, Caterina Ripamonti
% Chichester, West Sussex, England; Hoboken, NJ : J. Wiley, c2004

function [a,b] = pol2car(ch)

% function [a,b] = pol2car(ch)
% converts the polar coordinates
% of Chroma C and Hue H
% ch must be a row or column matrix 2 by 1 or 1 by 2
% see also car2pol

dim = size(ch);
if (dim(1) == 1) | (dim(2) == 1)
   ch = ch(:)'; % force to be a row matrix
else
   disp('ch must be a row matrix');
   return;
end
if (dim(2) ~= 2)
   disp('ch must be 2 by 1 or 1 by 2');
   return;
end

C = ch(1);
H = ch(2);

fx = tan(H*pi/180);

a = sqrt(C*C/(1 + fx*fx));

b = a*fx;

if (H < 90.0)
    % first quadrant
```

```
    a = abs(a);
    b = abs(b);
elseif (H < 180)
    % second quadrant
    a = -abs(a);
    b = abs(b);
elseif (H < 270)
    % third quadrant
    a = -abs(a);
    b = -abs(b);
else
    % fourth quadrant
    a = abs(a);
    b = -abs(b);
end
```

```
% SEUNG GEOL LEE (2007)
% using MATLAB
% draw ellipsoids on CIELAB color space
% equation: DE = b11*Da^2 + b22*Db^2 + b33*DL^2 + b12*2*Da*Db + b13*2*Da*DL
% + b23*2*Db*DL
% Metric coefficients: b11, b22, b33, b12, b13, b23
% DE = 1 for tolerance

clear all;
close all;
clear functions;
clc;

% Create figure
figure1 = figure('PaperPosition',[0.6345 6.345 20.3
15.23],'PaperSize',[20.98 29.68]);

%% Create axes
axes1 = axes('Parent',figure1);
axis([-10 15 -40 -20 25 40])
title('a^* vs b^* vs L^*');
xlabel(axes1,'a^*');
ylabel(axes1,'b^*');
zlabel(axes1,'L^*');
grid(axes1,'on');
hold(axes1,'all');

[x, y, z] = meshgrid(-10:0.2:10); %[x, y, z] = [a, b, L];

% NCSU for CIE Blue
f1= 1.9567.*x.^2 + 0.6596.*y.^2 + 1.5713.*z.^2 +...
2.*0.7581.*x.*y + 2.*0.1724.*x.*z +2.*0.1410.*y.*z;
p1=patch(isosurface(x+(4.70), y+(-31.36), z+(36.39), f1, 1),
'facecolor','blue','edgecolor','none');
      % NCSU dataset, center a=4.70, b=-31.36, L=36.39
daspect([1 1 1]);
```

```
view(3);
camlight; lighting phong;
alpha(.1)

% RIT-Dupont for Moderate Blue
r1= 0.6609.*x.^2 + 0.2387.*y.^2 + 1.1973.*z.^2 + 2.*0.3080.*x.*y +...
2.*(-0.0144).*x.*z +2.*(-0.1315).*y.*z;
d1=patch(isosurface(x+(-1.403), y+(-27.810), z+(35.338), r1, 1),
'facecolor','blue','edgecolor','none');
      % RIT-Dupont dataset, center a=-1.403, b=-27.810, %L=35.338
daspect([1 1 1]);
view(3);
camlight; lighting phong;
alpha(0.3)

% RIT-Dupont for Dark Blue
r2= 0.7289.*x.^2 + 0.4255.*y.^2 + 0.9311.*z.^2 + 2.*0.5275.*x.*y +...
2.*0.0128.*x.*z +2.*0.0113.*y.*z;
d2=patch(isosurface(x+(6.826), y+(-31.146), z+(30.186), r2, 1),
'facecolor','blue','edgecolor','none');
      % RIT-Dupont dataset, center a=6.826, b=-31.146, %L=30.186
daspect([1 1 1]);
view(3);
camlight; lighting phong;
alpha(0.3)
```

```
% SEUNG GEOL LEE (2007)
% Convert Lab value to xyY value

clear all;
close all;
clear functions;
clc;

L=36.39; a=4.70; b=-31.36; % Lab value for converting procedure
var_Y = (L + 16 ) ./ 116
var_X = a ./ 500 + var_Y
var_Z = var_Y - b ./ 200

if ( var_Y.^3 > 0.008856 ) var_Y = var_Y.^3
else                       var_Y = ( var_Y - 16 ./ 116 ) ./ 7.787
end
if ( var_X.^3 > 0.008856 ) var_X = var_X.^3
else                       var_X = ( var_X - 16 ./ 116 ) ./ 7.787
end
if ( var_Z.^3 > 0.008856 ) var_Z = var_Z.^3
else                       var_Z = ( var_Z - 16 ./ 116 ) ./ 7.787
end

ref_X =  94.811; % Observer= 10 degree, Illuminant= D65
ref_Y = 100.000;
ref_Z = 107.304;

X = ref_X .* var_X;
Y = ref_Y .* var_Y;
Z = ref_Z .* var_Z;

Y = Y;
x = X ./ ( X + Y + Z );
y = Y ./ ( X + Y + Z );

final=[x y Y]
```

Appendix F. Raw data of gray scale evaluation of 66 sample pairs by 26 observers in 3 repetitions.

Repetition One

Pairs	Observers																									
	1	2	3	4	5	6	7	8	9	10	11	12	13	14	15	16	17	18	19	20	21	22	23	24	25	26
1	2.3	2.3	3.8	3.7	4.3	3.4	3.4	4.3	3.0	2.7	3.0	3.5	3.5	3.0	3.0	2.5	2.0	4.2	3.7	4.0	3.8	2.5	4.0	4.0	4.0	3.5
2	2.7	4.0	4.2	4.2	4.5	2.3	5.0	2.5	2.0	3.6	3.7	3.7	4.0	4.0	3.7	4.0	3.5	3.8	3.5	4.5	4.4	4.5	4.5	5.0	4.9	4.0
3	3.0	3.0	4.0	3.7	4.5	3.9	4.0	3.5	3.5	3.0	3.0	4.3	4.0	3.5	3.6	3.5	2.0	4.0	4.0	4.5	4.5	3.0	5.0	4.0	4.6	4.3
4	2.0	2.8	2.5	3.0	4.1	3.2	4.2	2.8	4.0	3.3	3.0	3.7	3.0	3.0	3.0	2.5	2.5	2.8	2.0	4.0	4.0	2.5	3.0	2.5	4.0	3.5
5	2.2	1.8	3.0	3.2	3.3	1.7	2.0	3.0	2.0	3.0	3.0	3.3	3.0	2.5	2.2	2.0	3.5	3.5	2.5	3.0	3.8	3.0	3.0	3.0	3.7	2.5
6	4.0	4.5	4.0	4.5	4.6	3.9	4.8	4.9	4.8	4.0	4.8	4.0	4.5	4.5	4.6	4.5	4.0	4.5	4.9	5.0	4.9	5.0	5.0	5.0	4.3	4.7
7	2.4	1.5	2.5	2.4	3.8	3.1	3.8	2.8	3.5	2.5	3.2	3.7	2.5	3.5	2.6	4.0	1.5	2.5	3.3	3.5	4.0	3.0	3.0	4.0	4.3	3.0
8	3.0	2.8	3.9	4.0	4.0	3.7	4.0	4.0	3.5	3.5	3.8	4.0	2.5	3.5	2.8	2.5	3.5	3.0	3.0	4.5	4.3	2.7	4.0	4.5	4.1	2.5
9	3.0	4.0	4.2	3.9	4.5	4.7	4.3	4.7	4.5	4.0	4.0	4.0	4.5	4.0	4.0	4.5	3.5	4.2	4.7	5.0	4.9	4.0	4.0	5.0	4.6	4.8
10	3.6	3.5	4.5	4.8	4.1	4.3	4.2	4.6	4.0	3.6	4.0	4.3	4.0	3.7	4.8	4.5	4.5	4.0	3.7	4.5	4.9	4.0	4.5	4.5	4.1	4.5
11	2.5	2.5	3.5	3.9	3.8	2.4	3.7	3.8	4.2	2.5	3.0	3.5	3.5	3.0	2.0	3.0	4.0	2.7	3.3	3.5	4.7	3.0	3.5	2.5	3.9	2.5
12	2.5	2.2	3.5	2.8	4.1	2.9	4.0	2.5	3.0	3.3	3.0	3.7	3.3	3.0	1.8	3.8	2.5	3.0	3.5	3.5	3.8	3.0	2.5	3.5	2.5	2.0
13	1.7	1.5	2.3	1.8	3.7	3.6	3.0	2.0	3.0	2.5	2.7	2.7	4.0	2.0	1.5	2.5	1.5	2.0	2.5	3.0	2.5	2.0	3.0	2.5	3.3	3.5
14	2.7	3.3	3.8	3.6	4.6	2.9	4.5	4.0	2.5	3.3	3.5	4.0	3.0	3.0	4.3	3.0	3.0	4.0	3.5	4.5	4.4	4.0	4.0	4.0	4.1	4.0
15	2.5	1.2	2.5	3.5	3.5	2.8	2.6	3.4	3.5	2.5	2.5	3.5	3.5	4.0	2.0	2.0	1.5	3.0	3.8	2.5	3.4	2.0	3.5	2.0	3.5	2.5
16	4.5	2.2	4.0	3.4	3.7	3.4	3.0	3.5	2.5	3.0	2.3	4.5	3.0	3.5	2.6	3.5	2.0	3.0	2.5	3.5	4.0	3.0	2.5	2.5	4.2	3.5
17	3.0	4.0	4.6	4.8	4.6	4.4	4.7	4.6	4.5	4.0	4.0	4.0	4.5	3.5	4.6	5.0	4.0	4.5	4.7	5.0	5.0	4.5	5.0	5.0	4.3	4.5
18	2.8	1.8	2.5	2.8	3.8	2.9	3.0	2.6	3.5	3.0	2.5	3.0	3.5	2.5	2.0	2.5	1.5	3.0	2.0	3.0	3.9	3.2	3.0	2.0	3.1	2.5
19	3.2	3.0	4.5	4.5	4.4	2.6	4.5	3.8	3.0	4.0	2.7	3.7	4.5	4.0	3.5	3.5	4.5	4.3	4.5	4.5	5.0	3.7	5.0	3.0	4.6	5.0

Appendix F (continued).

Pairs	Observers																									
	1	2	3	4	5	6	7	8	9	10	11	12	13	14	15	16	17	18	19	20	21	22	23	24	25	26
20	3.2	1.5	2.2	2.2	3.6	3.4	4.0	3.2	3.5	4.0	2.5	3.0	3.0	3.0	2.5	3.5	3.5	3.0	2.7	3.0	3.5	3.5	4.0	2.5	3.9	3.5
21	3.0	2.8	3.5	4.3	4.5	2.9	4.5	3.8	4.0	3.5	3.0	4.3	3.5	2.5	2.7	2.5	3.5	3.8	3.4	4.0	4.6	3.7	4.0	4.5	4.3	3.7
22	3.6	4.2	4.2	4.8	4.5	4.6	4.8	4.4	4.0	3.7	4.2	4.5	5.0	4.5	4.6	5.0	4.0	3.3	4.7	5.0	4.9	4.0	4.5	4.8	4.0	4.5
23	3.8	4.5	4.5	4.9	4.8	4.9	4.7	4.8	4.5	4.0	4.8	4.5	4.5	4.5	4.5	4.0	4.5	4.5	4.4	5.0	5.0	4.0	4.5	4.5	4.6	4.8
24	2.8	2.3	4.0	4.5	4.7	4.2	4.3	4.6	3.5	3.7	3.2	4.0	4.0	3.5	3.2	2.5	4.0	4.0	4.0	4.5	4.8	3.5	4.3	4.5	4.4	4.7
25	2.5	2.0	4.2	3.5	4.5	3.1	4.2	2.5	4.0	3.3	3.5	3.3	3.5	4.0	2.8	2.0	3.5	2.5	3.5	4.5	3.9	3.5	4.0	4.0	4.0	4.5
26	2.5	2.3	4.2	4.4	4.5	4.6	3.5	4.7	4.5	3.7	4.0	3.5	4.5	2.5	4.2	2.5	4.5	4.3	4.7	4.0	4.7	4.7	4.5	4.0	4.8	3.8
27	2.0	1.8	4.0	4.5	4.0	3.4	3.0	2.0	3.5	2.7	3.2	3.0	3.0	3.0	3.3	1.5	1.5	3.8	3.5	3.5	3.5	2.5	2.5	2.5	4.1	3.5
28	2.0	2.5	3.7	3.1	3.6	3.6	2.7	4.5	3.0	3.2	3.0	3.3	3.5	2.5	4.1	3.5	3.5	2.5	3.8	4.0	4.4	2.5	3.0	2.5	3.1	4.0
29	2.5	4.0	4.2	4.6	4.1	4.9	4.2	4.6	4.0	3.5	4.5	4.3	4.0	4.5	3.0	4.0	4.5	4.0	4.5	5.0	4.9	5.0	4.5	4.5	4.4	4.5
30	2.5	3.8	4.0	3.9	4.4	4.4	4.1	4.2	4.0	4.5	3.0	4.0	4.5	3.5	4.5	4.5	4.0	3.8	4.0	4.0	4.6	4.0	3.0	4.5	4.8	4.5
31	2.0	2.3	2.5	3.7	3.9	3.4	4.0	3.2	3.5	3.0	2.8	3.5	3.0	3.0	3.8	2.0	2.0	2.5	2.5	4.0	3.8	4.0	3.0	3.5	4.0	3.5
32	2.3	3.5	4.1	4.5	4.2	4.2	4.3	3.9	4.0	4.5	3.3	3.5	4.5	3.5	4.8	4.5	5.0	4.5	4.8	4.5	4.8	5.0	5.0	4.5	4.5	5.0
33	3.5	3.3	3.8	3.5	4.3	3.8	4.0	3.6	2.5	4.0	3.5	4.3	3.5	3.5	1.0	2.0	4.0	3.5	4.3	4.0	5.0	3.7	3.0	4.0	4.5	4.0
34	2.5	3.0	4.5	3.5	4.1	2.3	4.2	4.2	2.0	4.0	2.5	3.5	2.0	2.0	1.5	2.5	3.5	2.5	3.5	3.5	4.0	3.7	4.0	4.0	4.2	3.5
35	2.5	4.0	4.7	2.5	4.4	3.1	2.6	4.0	3.5	3.3	3.0	4.0	4.5	3.5	2.0	3.0	4.0	2.5	4.0	4.5	4.4	3.7	4.0	4.7	4.6	4.5
36	2.6	2.8	4.2	2.5	4.2	4.3	3.6	4.0	3.0	2.5	3.5	3.7	3.5	3.5	2.0	3.5	3.5	2.2	4.0	4.0	4.3	3.7	3.5	3.0	4.0	3.8
37	2.7	4.3	4.4	4.0	4.7	4.8	4.4	4.3	4.0	5.0	4.7	4.5	4.0	4.5	3.5	4.5	4.0	3.8	5.0	5.0	4.9	5.0	4.8	4.5	4.7	4.5
38	2.7	2.2	3.8	3.8	4.1	4.2	3.0	4.2	2.5	2.5	2.5	3.5	3.0	2.5	2.5	2.5	3.5	3.0	3.3	3.5	3.7	3.0	3.0	4.0	4.1	2.5
39	4.0	2.5	4.1	3.5	4.4	3.2	3.3	4.2	2.5	3.5	3.0	3.5	4.5	4.5	2.8	3.0	3.5	3.0	4.7	4.0	4.2	4.5	2.5	3.5	4.2	3.8
40	3.7	3.0	3.7	3.0	4.2	3.5	3.6	4.0	4.5	3.3	3.7	4.5	4.0	4.0	3.8	2.5	3.5	3.2	4.0	4.5	4.3	3.5	4.3	4.0	4.5	3.5

Appendix F (continued).

Pairs	Observers																									
	1	2	3	4	5	6	7	8	9	10	11	12	13	14	15	16	17	18	19	20	21	22	23	24	25	26
41	3.0	1.8	4.3	2.5	4.2	3.7	3.7	3.5	3.0	3.5	3.0	3.0	3.0	3.5	1.5	3.0	3.0	2.0	4.0	4.0	3.9	2.5	3.0	4.0	4.2	3.5
42	3.2	2.0	4.3	3.5	4.3	2.9	3.8	4.2	3.0	4.0	2.7	3.0	2.5	3.0	2.3	2.5	3.5	3.0	4.0	3.5	4.0	4.0	4.0	3.7	4.4	3.5
43	3.0	3.8	4.8	4.2	4.6	4.4	3.9	4.7	3.5	4.7	4.0	4.3	3.5	3.5	2.2	4.5	4.0	4.0	4.5	4.0	4.4	5.0	4.5	4.3	4.8	4.5
44	4.0	4.5	4.2	5.0	4.8	4.7	4.4	4.9	4.0	4.3	4.7	4.5	5.0	4.5	4.7	4.5	4.0	4.5	4.6	5.0	4.8	4.0	4.7	4.8	4.8	4.5
45	2.5	1.8	4.3	3.5	4.2	3.5	3.2	3.9	4.0	3.0	4.0	3.8	3.0	2.0	2.1	2.0	3.5	2.5	2.7	2.5	3.8	2.5	4.0	4.0	4.1	2.5
46	4.0	3.3	4.4	4.0	4.5	3.8	4.3	4.3	4.0	4.5	4.7	4.3	4.0	3.5	3.6	4.0	4.5	3.8	4.5	4.0	4.6	4.5	3.0	4.7	4.8	4.0
47	3.5	4.0	4.6	4.3	4.6	4.8	4.7	4.6	4.5	4.7	4.3	4.5	4.0	4.5	3.2	4.0	4.5	3.0	4.9	5.0	4.7	5.0	4.0	4.5	4.6	4.0
48	4.0	4.7	4.6	5.0	4.6	4.8	4.5	4.8	3.5	4.5	4.0	4.8	4.0	4.0	4.5	4.0	4.0	4.0	5.0	5.0	5.0	4.5	4.5	5.0	4.9	5.0
49	4.0	4.8	4.6	4.5	4.6	4.4	4.6	4.1	3.5	4.5	4.0	4.0	4.0	4.5	4.7	5.0	4.0	4.0	4.8	5.0	4.9	4.0	3.0	4.8	4.6	4.5
50	4.5	5.0	4.8	4.7	4.6	4.6	4.0	4.3	4.5	4.5	3.9	4.3	3.5	5.0	4.0	4.5	4.5	3.2	4.7	5.0	4.7	4.5	4.5	4.9	4.8	4.5
51	3.7	2.5	4.1	3.8	4.4	3.9	4.4	3.8	3.5	4.0	3.2	3.0	3.5	2.5	3.0	3.5	3.5	3.0	3.5	3.5	4.5	4.5	4.5	4.0	4.3	4.3
52	3.5	4.2	3.9	4.5	4.7	4.4	4.4	4.0	4.0	4.5	3.2	4.0	4.5	3.0	3.6	3.4	4.0	3.5	4.7	4.5	4.9	4.5	3.5	4.5	4.7	5.0
53	3.5	4.0	4.9	4.5	4.7	3.7	4.7	4.5	4.0	4.5	3.5	4.3	4.5	3.5	4.8	4.0	4.0	4.2	4.0	5.0	4.9	5.0	5.0	4.7	4.9	5.0
54	3.5	4.5	5.0	4.7	4.6	4.9	4.5	4.5	4.0	3.7	4.9	4.5	4.5	4.5	3.8	4.5	4.0	3.5	4.9	5.0	4.7	5.0	4.5	4.5	4.9	4.0
55	3.5	2.3	4.2	2.7	4.4	3.7	3.4	4.0	1.5	3.0	2.5	3.0	3.0	3.0	2.2	2.5	3.5	2.5	3.5	3.5	3.9	3.5	3.5	2.5	4.4	3.5
56	3.0	2.2	3.8	3.3	3.8	2.8	3.4	2.4	2.5	3.5	3.0	3.5	4.0	3.0	2.0	3.0	3.0	2.5	3.5	4.0	3.6	3.0	3.0	4.5	4.6	3.0
57	2.5	1.8	3.7	2.2	3.5	3.1	3.4	2.8	2.5	2.5	3.5	2.8	2.5	2.5	1.5	2.5	3.0	2.2	3.0	3.0	2.3	4.0	4.0	3.0	3.9	2.5
58	3.0	2.5	3.5	3.7	4.0	3.9	2.6	3.0	4.0	3.5	3.8	3.0	4.0	3.5	2.6	3.0	3.5	3.2	3.5	4.0	4.1	3.7	4.0	4.5	4.3	3.0
59	1.8	2.0	2.0	3.7	3.7	2.2	3.2	2.5	1.5	2.5	2.5	3.5	2.3	2.0	1.5	1.0	1.5	1.5	2.5	2.5	2.5	1.5	2.0	2.0	2.8	2.5
60	2.0	1.5	2.5	3.5	4.0	2.2	3.0	2.3	2.0	2.7	3.0	2.8	2.5	2.0	1.0	1.0	3.5	2.0	3.0	3.0	3.6	2.5	3.5	3.5	3.9	2.0
61	2.7	2.2	4.0	3.0	4.3	4.1	3.8	3.0	3.0	2.7	3.7	3.5	2.5	3.0	1.5	2.0	3.5	3.5	4.5	4.0	4.0	4.0	3.5	4.0	4.3	3.8

Appendix F (continued).

Pairs	Observers																								
	1	2	3	4	5	6	7	8	9	10	11	12	13	14	15	16	17	18	19	20	21	22	23	24	25	26
62	3.7	4.5	4.7	4.8	4.8	4.8	4.7	4.8	4.5	4.7	4.8	4.0	4.5	4.5	4.3	4.0	4.5	4.0	4.8	4.5	5.0	4.5	5.0	4.5	5.0	4.8
63	2.5	3.0	3.9	3.7	4.4	4.3	3.0	4.5	3.0	3.0	3.5	3.3	3.0	4.0	2.0	2.5	3.5	3.0	3.8	3.0	4.4	3.7	3.5	4.5	3.8	3.5
64	2.7	2.8	3.3	3.0	4.1	3.7	3.0	4.0	2.5	3.5	3.4	3.0	3.5	3.0	1.8	2.5	3.5	2.0	4.0	3.5	3.5	2.0	3.5	4.0	4.1	3.5
65	4.0	3.5	4.8	4.7	4.5	4.3	4.6	4.6	4.5	4.3	4.0	4.0	3.5	4.0	2.5	4.0	4.0	3.5	4.5	4.5	4.6	4.0	5.0	4.5	4.8	4.3
66	4.5	4.0	4.9	4.5	4.6	4.2	3.6	4.5	4.5	4.5	3.7	3.5	4.5	4.0	4.2	4.0	4.5	4.0	4.5	4.5	4.3	4.0	4.0	4.5	4.5	4.0

Repetition Two

Pairs	Observers																								
	1	2	3	4	5	6	7	8	9	10	11	12	13	14	15	16	17	18	19	20	21	22	23	24	25	26
1	3.0	2.8	2.8	2.3	4.7	3.7	3.5	4.0	3.0	3.0	2.2	3.8	4.0	3.0	2.7	3.0	2.0	2.8	3.9	4.5	3.9	3.2	3.0	4.5	4.1	3.5
2	3.0	2.5	4.4	4.0	4.3	4.0	4.0	3.8	3.5	4.3	3.5	3.8	3.6	3.5	3.0	3.0	3.5	3.5	3.7	4.0	4.8	4.0	4.5	4.8	4.6	4.5
3	3.8	2.5	4.3	3.0	4.4	3.4	3.9	4.2	3.0	3.7	3.7	4.0	4.0	2.5	2.6	2.5	2.5	3.8	4.5	4.0	4.1	4.0	4.5	4.8	4.7	3.8
4	2.0	2.5	4.2	3.0	4.0	4.3	2.6	4.0	3.0	2.7	2.7	3.5	3.5	3.0	2.0	2.5	3.5	2.8	3.5	4.0	4.6	2.0	2.5	3.5	4.0	4.0
5	2.0	1.5	3.8	3.8	4.0	2.4	2.6	3.5	2.5	2.5	2.3	3.0	3.5	1.5	1.5	2.0	2.5	2.5	3.5	3.0	2.6	2.5	2.5	4.0	3.1	2.5
6	3.5	3.8	4.3	4.0	4.6	4.6	4.4	4.8	3.5	4.3	3.7	4.0	4.5	4.5	4.0	4.5	4.0	4.5	4.9	5.0	4.9	4.0	4.7	4.7	4.5	5.0
7	2.2	1.5	3.9	3.0	4.2	2.7	2.4	3.0	3.0	2.7	3.0	3.5	3.5	2.5	2.0	2.0	2.0	2.5	3.5	3.0	3.5	2.0	3.0	4.0	4.2	3.8
8	2.2	2.3	4.2	3.5	4.2	3.2	3.7	3.8	4.0	3.5	2.6	4.0	3.5	2.5	1.5	3.5	2.5	2.5	4.0	4.0	4.0	2.5	3.0	4.0	4.3	3.2
9	3.9	3.5	4.7	3.7	4.5	4.8	4.5	4.7	3.5	4.0	3.3	3.8	4.5	4.0	3.5	4.5	3.5	4.0	4.9	5.0	4.9	4.0	4.3	4.5	4.0	4.9
10	3.2	4.3	4.2	4.5	4.2	3.9	4.0	4.2	2.5	5.0	3.7	4.5	4.5	4.0	3.2	4.0	4.0	3.5	4.0	4.0	4.8	4.2	4.5	4.7	4.5	4.5
11	2.2	2.5	3.5	2.5	4.0	3.9	3.4	3.8	3.0	2.7	2.3	3.0	3.7	2.5	2.5	3.5	2.5	3.0	3.5	3.5	3.9	3.0	3.5	3.0	3.7	3.5

Appendix F (continued).

Pairs	Observers																									
	1	2	3	4	5	6	7	8	9	10	11	12	13	14	15	16	17	18	19	20	21	22	23	24	25	26
12	2.5	2.0	3.1	3.5	4.7	3.4	3.0	3.7	3.5	3.0	2.7	3.8	4.0	3.5	1.5	3.0	2.5	1.8	3.5	3.5	3.0	2.5	2.5	4.0	3.7	3.2
13	2.0	1.8	3.5	2.0	3.6	3.4	2.7	3.5	2.5	2.3	2.5	2.8	4.0	1.5	2.2	1.5	2.0	2.0	2.5	2.5	2.0	1.5	2.5	3.0	3.3	2.8
14	2.3	3.5	4.0	3.8	4.4	4.8	3.8	4.0	3.0	3.6	3.2	4.0	4.0	3.0	3.8	4.0	3.0	2.8	3.9	4.5	4.3	2.5	3.0	4.5	4.1	4.5
15	2.5	2.2	3.8	2.0	3.5	2.7	2.5	4.0	3.0	2.5	3.0	3.0	3.5	2.5	1.0	2.0	2.0	1.8	2.0	2.5	2.5	3.0	2.0	2.5	3.8	3.5
16	2.5	2.0	4.0	3.5	3.5	3.9	3.3	3.8	2.5	4.0	2.2	3.3	4.0	3.0	1.5	3.0	2.5	2.8	3.7	3.0	3.0	3.0	2.5	3.5	4.4	3.5
17	3.5	3.5	4.4	4.7	4.6	4.9	4.3	4.6	4.0	4.5	2.7	4.0	4.5	4.0	4.2	4.0	4.0	4.0	4.7	5.0	4.9	4.5	4.9	4.7	4.6	5.0
18	2.5	1.8	3.2	3.3	3.6	3.8	2.5	3.0	3.0	2.5	2.2	3.3	3.5	2.5	1.5	2.5	2.5	2.5	3.0	3.0	3.3	3.7	3.5	3.5	3.8	3.2
19	2.5	2.5	4.0	3.7	4.2	4.3	4.0	4.0	4.5	4.0	3.7	3.5	4.5	2.5	3.5	3.5	4.5	4.0	3.9	4.0	4.6	2.5	4.3	4.5	4.5	4.0
20	2.0	1.8	3.3	2.5	3.6	2.9	3.3	3.5	2.5	2.5	2.0	3.5	3.0	2.0	2.0	3.5	2.5	2.5	2.5	3.0	2.8	3.5	3.5	3.5	3.1	3.8
21	2.5	2.0	4.5	3.5	4.4	3.9	3.6	4.0	3.5	3.0	3.0	3.8	4.5	3.0	3.2	4.5	3.5	3.2	4.2	4.0	4.9	3.5	4.5	4.0	4.0	4.5
22	3.4	4.8	4.3	3.8	4.4	4.0	3.8	4.5	4.0	4.5	3.5	4.5	5.0	4.5	4.5	4.5	4.0	3.2	4.7	4.5	4.9	4.0	4.0	4.7	4.5	4.8
23	3.0	4.8	4.1	4.0	4.6	4.8	4.3	4.5	4.5	4.5	4.8	4.8	4.5	4.5	3.9	4.5	4.5	4.2	4.7	5.0	5.0	4.5	4.0	4.5	4.6	5.0
24	2.5	3.2	4.5	4.0	4.4	4.4	4.1	4.5	4.0	3.7	3.5	4.0	4.0	2.5	2.8	4.0	2.5	3.8	4.2	4.0	4.7	4.0	3.5	3.5	4.3	4.5
25	2.5	2.2	3.4	3.0	4.1	4.2	3.0	3.5	3.0	3.0	2.2	4.0	4.0	3.0	1.8	2.0	3.0	2.8	3.9	3.5	3.8	2.0	3.5	4.0	3.7	3.8
26	3.5	2.8	4.1	3.0	4.2	4.3	3.3	4.0	4.5	4.3	3.5	3.5	4.5	3.5	3.5	4.0	4.5	4.2	4.5	4.0	4.9	4.5	4.5	4.5	4.7	4.9
27	2.2	2.5	3.9	2.5	3.3	2.6	3.0	3.0	2.0	2.5	2.7	3.5	2.5	3.5	3.4	3.5	2.5	2.2	2.5	4.0	3.8	2.0	2.0	3.5	3.5	4.3
28	3.0	2.3	2.5	2.5	4.0	4.1	3.8	3.8	3.5	3.5	2.3	3.5	4.0	3.5	2.4	3.5	3.5	3.0	3.0	3.5	4.5	2.5	3.5	4.0	4.2	3.0
29	4.0	4.0	3.6	3.8	4.3	4.7	4.7	4.5	4.5	3.7	4.0	4.8	4.5	3.5	4.5	4.0	3.0	3.8	4.9	5.0	5.0	3.7	4.0	4.5	4.6	4.3
30	3.3	3.5	4.6	4.0	4.6	4.6	4.1	4.5	3.5	4.0	3.7	4.0	4.5	3.5	2.5	3.0	3.0	3.8	4.0	3.5	4.3	3.5	3.5	4.5	4.5	4.9
31	3.0	2.2	3.2	2.3	4.2	3.5	3.9	4.1	3.5	2.7	3.5	4.0	3.5	2.0	2.0	2.5	2.0	2.0	3.5	3.5	3.8	3.5	2.5	4.0	3.8	4.0
32	3.3	2.8	4.5	4.5	4.6	4.3	4.0	4.6	4.0	4.5	4.0	3.5	4.0	3.0	3.0	4.5	4.0	3.8	4.5	4.5	5.0	4.0	4.7	4.8	4.5	5.0

Appendix F (continued).

Pairs	Observers																									
	1	2	3	4	5	6	7	8	9	10	11	12	13	14	15	16	17	18	19	20	21	22	23	24	25	26
33	2.0	3.8	4.2	3.0	4.4	4.7	4.2	4.0	4.0	3.7	2.5	4.0	3.0	4.0	3.3	4.0	4.0	3.8	4.6	4.0	4.8	3.0	2.0	4.5	3.8	4.3
34	2.5	2.0	3.4	2.7	3.6	3.3	2.9	2.5	3.5	2.5	2.5	2.8	3.5	2.5	2.5	2.5	2.0	2.5	2.5	3.0	2.5	2.5	3.0	4.0	3.5	3.2
35	2.7	4.0	3.8	3.3	3.9	4.4	3.3	3.0	4.0	3.5	2.2	3.8	3.0	2.5	2.3	3.0	3.0	2.8	3.5	3.5	4.7	4.0	3.5	4.0	4.0	4.3
36	3.0	3.2	3.9	3.5	4.4	4.2	3.7	4.0	3.5	3.0	3.5	4.0	3.5	3.5	2.6	3.0	4.0	2.5	4.0	4.0	4.2	4.0	3.5	3.5	4.2	3.8
37	3.5	2.5	4.6	4.3	4.6	4.2	4.2	4.2	3.5	4.3	3.3	4.0	3.0	4.5	3.0	4.0	4.5	3.5	4.5	4.5	4.9	5.0	4.7	4.3	4.9	4.7
38	2.2	1.8	3.7	3.5	3.9	3.4	2.9	3.0	2.5	2.5	2.2	3.0	3.5	2.5	1.5	2.3	3.0	3.5	3.5	3.5	2.8	3.0	4.0	3.5	4.0	3.5
39	3.2	2.3	4.1	3.3	4.4	3.3	4.0	3.7	2.5	3.5	3.0	3.3	3.5	4.0	2.6	4.5	3.0	3.5	4.0	4.5	4.2	3.7	4.5	4.0	4.1	4.0
40	2.5	3.8	4.3	3.5	4.3	4.3	4.5	3.0	4.0	3.7	3.0	4.0	3.5	4.0	3.0	3.0	3.0	3.5	4.0	4.0	4.3	3.7	3.0	4.5	4.4	4.3
41	2.5	2.5	3.8	2.7	4.1	3.4	2.9	4.0	3.5	3.5	2.3	3.5	3.5	3.0	1.2	4.0	3.0	3.0	3.5	3.5	4.8	3.5	4.0	3.5	4.1	4.5
42	2.6	2.7	4.1	3.8	4.1	3.6	3.2	3.5	3.0	2.5	2.7	3.3	3.5	2.5	2.3	3.0	2.5	3.5	3.0	3.5	4.4	3.7	3.5	3.8	4.0	3.5
43	3.7	3.7	4.3	3.8	4.7	3.9	4.4	4.7	3.5	4.5	3.8	4.0	4.0	3.8	3.8	4.5	4.5	4.0	4.8	4.0	4.9	4.0	4.3	4.0	4.7	4.9
44	4.0	4.8	4.2	4.7	4.8	4.9	4.8	4.5	4.5	4.5	4.0	4.5	4.5	4.8	4.8	4.5	4.5	3.5	4.7	5.0	5.0	5.0	4.5	4.8	4.8	4.8
45	2.5	2.0	3.9	3.5	3.6	3.6	3.2	3.7	3.0	3.0	3.0	3.5	3.0	2.0	2.0	3.5	2.0	2.5	3.0	2.5	4.0	3.5	4.5	4.3	4.0	3.8
46	2.8	3.2	4.0	4.3	4.6	4.3	4.0	3.8	4.0	4.3	3.8	4.3	3.5	4.0	3.0	3.5	3.5	3.2	4.0	4.0	4.8	4.2	4.3	3.7	4.5	4.0
47	3.8	4.0	4.3	3.4	4.6	4.7	4.2	4.2	4.0	4.5	4.0	3.8	4.0	4.8	4.0	3.5	4.0	4.5	4.8	4.5	4.8	4.5	4.5	4.3	4.4	4.8
48	3.4	4.8	4.7	4.8	4.8	4.7	4.7	4.5	4.0	4.0	4.0	4.5	4.5	4.0	3.0	4.5	4.5	4.0	4.8	5.0	5.0	4.5	4.3	4.7	4.6	4.7
49	3.0	4.7	4.3	4.5	4.5	4.6	4.3	4.0	3.5	4.3	3.3	3.5	4.5	4.5	3.5	4.5	4.0	3.5	4.5	4.5	4.9	4.0	4.0	3.3	4.5	4.8
50	3.5	4.5	4.6	4.4	4.8	4.5	4.2	4.8	4.5	4.5	4.0	4.8	4.0	4.5	3.6	4.5	4.0	4.5	4.8	5.0	5.0	4.0	4.5	4.8	4.8	4.9
51	3.8	2.8	3.8	3.7	4.0	4.5	3.6	3.5	3.0	2.5	3.0	3.8	4.0	2.5	2.2	2.5	4.5	3.8	3.7	4.0	4.8	4.0	4.3	4.0	4.1	4.0
52	3.0	4.2	4.2	4.7	4.6	4.7	4.3	3.5	3.5	4.0	3.5	3.5	4.0	3.0	3.5	4.5	4.5	3.8	4.0	4.5	4.9	4.0	4.7	4.3	4.6	4.5
53	3.8	3.2	4.7	4.7	4.8	4.2	4.6	4.5	4.0	4.0	3.3	3.5	4.0	3.5	4.5	4.5	4.5	4.0	4.7	4.5	4.9	5.0	4.3	4.8	4.5	4.9

Appendix F (continued).

Pairs	Observers																									
	1	2	3	4	5	6	7	8	9	10	11	12	13	14	15	16	17	18	19	20	21	22	23	24	25	26
54	3.5	4.0	4.4	4.3	4.8	4.9	4.0	4.7	3.5	5.0	3.8	4.0	4.0	4.5	4.0	3.5	4.0	3.8	4.7	4.5	4.4	4.5	4.3	4.8	4.5	4.5
55	3.2	1.8	4.0	3.5	3.7	3.9	2.1	2.8	3.0	3.0	2.2	3.8	4.0	3.5	2.8	3.5	3.5	2.8	3.5	4.0	3.7	3.5	4.0	4.0	3.5	3.5
56	2.3	1.8	3.8	2.3	4.1	3.2	3.2	3.0	2.5	2.5	2.7	3.0	3.5	3.0	2.3	3.0	2.5	3.5	3.7	3.5	3.8	2.5	3.5	4.3	4.3	3.5
57	2.6	1.5	4.1	2.0	4.1	4.2	3.1	2.8	2.0	2.0	2.3	2.8	3.0	3.5	1.7	2.0	3.0	2.0	3.0	3.5	3.2	3.5	2.0	4.3	4.2	3.8
58	2.7	2.8	4.2	3.5	4.2	4.1	3.6	3.0	3.5	3.7	3.5	3.0	4.0	3.0	2.5	3.0	2.5	3.0	4.0	4.0	3.8	3.7	3.0	4.3	4.2	3.8
59	2.5	1.5	2.0	3.5	3.8	2.6	2.3	2.0	1.5	2.0	2.0	3.0	3.0	2.0	1.0	1.5	2.0	2.0	2.0	2.5	2.3	3.2	2.5	2.8	3.8	2.5
60	2.2	2.3	3.5	3.3	3.9	3.9	2.7	3.0	2.5	2.5	2.5	3.0	3.0	2.0	1.0	2.0	2.0	2.2	3.0	3.0	3.5	2.5	3.0	2.5	3.0	3.2
61	2.7	2.2	4.2	3.8	4.4	4.2	3.1	3.0	3.0	2.7	3.3	3.0	3.0	3.0	2.0	3.5	2.5	4.0	3.7	3.5	4.0	3.7	4.0	4.5	4.1	3.5
62	4.0	4.5	4.2	4.5	4.4	4.6	4.3	4.5	4.0	5.0	4.0	4.5	4.5	4.5	4.2	4.0	4.0	4.0	4.8	5.0	4.9	4.5	4.5	4.6	4.8	4.6
63	2.7	2.3	3.8	3.7	4.1	4.1	3.6	3.5	3.0	2.5	2.3	3.5	3.0	3.0	2.5	3.5	2.5	2.5	3.5	3.5	3.4	3.7	4.0	4.3	4.0	3.2
64	2.5	2.0	3.9	3.3	4.3	3.8	3.0	3.0	3.5	3.5	2.7	3.3	3.5	3.5	2.0	3.0	2.0	2.5	3.0	3.5	3.9	3.0	3.0	3.7	4.1	3.8
65	3.5	3.7	4.6	4.5	4.3	4.2	4.2	4.0	4.0	4.0	3.8	4.0	4.0	3.5	3.8	4.0	3.5	3.5	4.5	4.0	4.4	4.0	4.7	4.3	4.3	4.2
66	3.8	4.5	4.3	3.7	4.7	4.6	4.4	4.0	4.0	4.5	3.7	4.0	4.0	4.5	3.5	4.5	4.0	4.0	4.2	4.5	4.8	4.5	4.5	4.7	4.5	4.9

Repetition Three

Pairs	Observers																									
	1	2	3	4	5	6	7	8	9	10	11	12	13	14	15	16	17	18	19	20	21	22	23	24	25	26
1	3.2	2.0	3.2	3.5	4.6	3.6	4.1	3.0	3.5	3.5	3.5	3.5	4.5	3.5	4.0	3.0	2.0	4.0	3.5	4.0	3.5	4.0	4.0	3.5	3.8	4.3
2	3.0	2.7	3.9	3.0	4.3	3.1	4.3	4.0	3.5	4.0	2.5	3.8	3.5	3.5	2.5	3.0	3.5	3.5	4.5	4.0	3.7	4.5	4.5	4.0	4.0	4.2
3	3.5	2.5	4.1	3.7	4.2	3.7	4.2	3.5	3.5	3.5	3.0	3.5	3.5	3.0	3.0	3.5	3.0	3.8	4.0	4.0	3.8	3.5	4.7	4.5	4.4	4.4

Appendix F (continued).

Pairs	Observers																									
	1	2	3	4	5	6	7	8	9	10	11	12	13	14	15	16	17	18	19	20	21	22	23	24	25	26
4	2.3	1.5	3.6	2.5	3.5	4.0	2.7	3.0	2.0	3.0	3.0	3.5	3.0	2.8	1.3	2.0	3.0	2.5	2.5	3.5	3.5	3.0	4.3	2.0	3.5	3.8
5	2.5	1.8	2.7	3.5	3.5	2.7	3.4	3.0	2.0	2.3	2.3	2.8	2.5	2.0	1.5	3.0	1.5	2.0	2.0	2.5	2.2	3.5	3.3	4.3	2.5	3.0
6	3.7	3.5	4.7	4.5	4.5	4.7	4.1	3.8	4.0	4.5	3.5	4.5	4.0	4.0	3.0	5.0	3.5	4.2	4.8	4.5	4.8	5.0	4.5	4.8	4.5	4.7
7	2.5	1.8	3.5	3.0	3.9	3.6	3.2	3.0	3.5	2.5	2.5	3.8	2.5	2.0	1.0	2.5	2.5	2.5	3.5	3.0	3.5	3.5	3.0	4.2	3.0	3.8
8	2.7	2.5	3.9	2.5	4.0	4.2	3.9	3.0	3.5	2.5	3.2	3.8	3.0	3.5	2.0	3.0	2.5	2.5	3.5	4.0	3.8	3.5	3.5	3.8	2.7	3.5
9	3.0	4.0	4.5	3.8	4.5	4.2	3.6	4.0	4.0	4.5	3.7	4.0	4.5	4.0	4.0	3.5	3.5	4.0	4.8	4.5	4.9	4.5	4.0	4.3	4.2	4.5
10	3.0	3.5	4.6	4.5	4.0	4.1	3.4	3.7	3.5	4.0	3.3	4.5	4.0	3.5	4.7	4.0	4.5	4.5	4.5	4.5	4.7	5.0	4.5	4.7	4.0	4.3
11	3.0	1.8	3.8	3.0	3.5	3.9	3.2	3.0	3.0	2.5	2.7	3.5	2.5	2.0	2.0	3.0	2.0	2.5	3.0	3.0	3.8	3.7	3.5	4.2	2.5	3.5
12	2.5	2.2	3.0	2.5	3.6	3.6	3.8	3.0	3.0	2.7	2.8	3.5	3.5	2.5	1.0	3.5	2.5	2.5	2.5	3.0	2.7	3.5	3.0	3.7	3.5	3.3
13	2.0	1.5	3.2	2.0	2.9	3.3	2.3	2.5	2.5	2.5	2.4	3.3	3.0	2.0	1.5	2.0	1.5	2.0	2.0	2.0	1.8	2.5	3.3	2.5	2.3	3.5
14	2.7	3.2	4.2	4.0	4.0	3.4	3.3	3.5	3.0	3.5	3.2	4.0	3.5	3.0	3.2	4.0	2.5	3.5	4.3	4.5	2.9	3.7	4.0	4.5	3.0	3.9
15	2.2	1.5	3.0	3.2	3.5	2.9	2.9	2.5	3.0	2.5	3.0	3.5	2.5	2.0	1.8	2.0	2.0	2.2	2.5	2.5	2.0	3.5	3.5	3.5	3.0	3.2
16	2.5	1.5	3.2	3.0	3.6	3.4	3.3	2.7	2.0	3.0	2.7	3.0	3.5	2.5	2.0	2.5	2.0	2.8	2.7	3.5	3.3	3.7	3.5	4.0	3.3	3.2
17	2.8	3.2	4.3	4.2	3.9	4.4	4.3	4.0	4.0	3.7	3.8	4.0	4.0	3.0	2.8	4.5	3.5	3.5	4.0	4.5	5.0	4.5	4.0	4.8	4.4	4.5
18	3.5	2.0	3.4	3.3	3.0	3.6	3.4	3.0	2.5	3.0	2.4	3.5	2.5	2.0	2.2	2.5	3.5	2.5	2.7	3.0	3.3	3.0	3.5	3.0	3.0	3.5
19	2.5	2.5	4.3	3.7	4.6	4.2	3.3	3.5	3.0	4.0	2.8	3.8	4.0	2.5	3.1	4.0	3.5	3.8	4.0	4.0	4.4	4.5	4.5	4.3	4.3	4.8
20	3.0	1.8	3.0	3.0	3.7	3.3	3.1	2.9	2.5	2.5	2.5	3.0	3.0	1.5	1.8	3.0	2.5	2.5	3.0	3.0	3.2	3.5	3.5	4.5	2.7	3.8
21	3.0	2.0	4.6	3.0	4.1	4.1	4.1	3.0	4.0	3.0	2.2	4.0	4.0	3.0	1.5	4.0	2.5	3.2	3.7	4.5	4.0	3.7	4.0	4.0	3.5	3.9
22	2.5	4.7	4.0	4.5	4.5	3.7	4.2	4.3	4.0	4.0	3.8	4.5	4.5	3.5	4.2	4.0	4.0	4.0	4.5	5.0	4.9	4.0	4.3	4.4	4.3	3.5
23	3.0	3.8	4.7	4.5	4.5	4.5	4.2	4.0	4.0	3.5	4.0	4.5	5.0	4.0	4.5	4.0	3.0	4.0	4.7	5.0	5.0	4.0	4.5	4.7	4.7	4.9
24	3.5	3.0	4.1	4.3	4.2	4.2	4.5	3.8	3.5	3.5	3.3	4.3	4.0	3.0	3.0	4.0	3.0	3.5	3.7	4.0	3.5	4.0	4.7	4.4	4.3	4.5

Appendix F (continued).

Pairs	Observers																									
	1	2	3	4	5	6	7	8	9	10	11	12	13	14	15	16	17	18	19	20	21	22	23	24	25	26
25	2.7	2.0	3.4	3.8	4.2	3.3	3.5	3.0	3.5	3.0	2.3	4.0	4.0	3.0	2.3	4.0	2.5	3.5	3.0	3.0	3.4	3.0	3.5	4.3	3.5	4.2
26	2.8	2.5	4.3	4.0	4.1	4.3	4.2	4.0	3.5	3.7	3.2	3.5	4.0	3.0	3.5	3.5	4.0	2.5	3.5	4.0	4.7	4.5	3.7	4.5	4.2	4.3
27	2.0	2.5	3.5	3.5	3.7	3.3	3.5	2.8	3.5	3.0	2.5	3.8	3.5	2.5	2.5	3.5	2.5	2.0	3.0	3.5	2.8	2.5	3.0	3.0	2.5	3.8
28	3.5	2.2	3.5	2.5	3.8	4.1	2.6	2.8	3.0	3.3	3.5	3.3	4.0	2.5	1.7	1.5	2.0	2.5	3.5	4.0	3.0	2.5	3.5	4.0	3.0	4.3
29	3.4	4.3	3.8	4.0	4.2	4.6	4.5	4.0	4.0	3.7	4.0	4.3	4.0	3.8	3.5	4.5	3.0	3.5	4.5	5.0	4.0	4.5	4.0	4.3	4.5	4.5
30	2.5	4.5	4.4	4.0	4.3	4.3	3.7	4.0	4.0	3.7	3.7	4.0	4.5	4.0	4.0	2.5	3.0	4.0	3.7	4.5	4.3	4.0	4.5	3.0	4.3	4.8
31	3.0	2.0	3.8	3.7	4.8	3.2	3.4	3.0	2.5	2.5	3.2	4.0	3.5	3.0	2.0	1.5	2.0	2.5	3.3	4.0	2.9	3.7	4.0	4.0	3.5	4.0
32	3.5	2.5	4.3	3.8	4.2	4.4	4.1	4.0	3.5	4.0	3.7	3.5	4.5	2.5	3.8	4.0	4.0	3.2	3.7	4.0	4.6	3.7	4.3	4.2	4.5	4.5
33	2.7	3.3	4.2	3.0	4.0	3.8	4.0	3.8	3.5	3.5	2.8	3.5	3.5	3.8	3.3	3.5	3.0	2.8	4.3	4.0	4.5	4.0	4.3	4.0	4.0	4.0
34	3.0	2.3	3.2	3.0	4.0	3.4	2.6	3.5	1.5	2.5	2.8	3.0	2.5	2.5	2.5	2.5	2.5	3.2	3.0	3.0	2.6	4.5	3.0	2.5	3.3	4.3
35	3.5	3.5	4.1	3.0	4.0	4.1	3.2	3.8	3.0	3.5	3.6	3.8	3.5	3.5	3.6	4.0	3.5	2.5	3.7	4.0	3.8	4.0	3.0	3.2	4.0	3.9
36	2.5	2.5	3.7	4.0	4.0	4.2	4.0	3.0	3.5	3.0	2.8	4.0	4.0	3.0	1.5	3.5	2.5	2.8	4.0	4.0	3.6	3.5	3.0	3.5	4.0	3.3
37	3.0	3.7	4.8	4.8	4.5	4.4	4.1	4.0	3.0	3.7	3.7	4.0	4.0	4.0	3.0	4.0	4.0	4.0	4.5	4.0	4.3	5.0	4.5	4.7	4.5	4.6
38	3.2	2.2	4.8	4.0	3.9	3.8	2.7	3.2	2.0	3.0	2.8	3.5	3.0	2.5	2.2	3.5	2.5	3.0	2.5	3.5	2.7	3.7	2.0	3.7	3.5	4.2
39	3.5	2.8	4.0	3.2	4.2	3.4	4.3	3.8	3.0	3.5	3.0	3.8	4.0	3.5	3.0	4.0	4.5	3.5	4.0	4.5	3.0	4.0	3.5	4.2	4.5	4.3
40	3.0	2.8	4.2	4.2	4.0	4.4	4.3	3.5	3.5	3.0	3.5	4.0	4.0	4.0	3.8	2.5	3.0	3.0	4.0	4.5	3.0	4.2	4.0	3.8	3.8	4.3
41	3.5	1.8	4.5	3.3	4.2	4.3	3.5	3.7	3.5	3.5	3.8	3.5	4.0	3.0	2.0	4.0	3.5	2.8	3.5	3.5	3.2	3.5	3.0	4.0	3.8	3.8
42	2.7	2.5	3.5	4.2	4.3	4.1	4.0	3.5	2.5	4.0	3.2	3.5	3.5	2.5	1.5	3.0	3.0	3.0	3.5	3.5	2.9	4.0	4.0	4.0	3.8	4.5
43	3.0	3.8	4.0	4.3	4.2	4.8	4.5	4.0	4.0	4.0	3.7	4.5	4.0	4.3	3.9	3.5	4.5	4.0	4.8	4.5	4.7	4.2	4.0	4.7	4.2	4.7
44	4.0	4.5	4.7	4.8	4.6	5.0	4.8	4.5	4.0	4.5	4.0	4.5	4.0	4.5	4.5	4.0	4.0	3.8	4.7	5.0	4.9	5.0	4.5	4.7	4.8	4.7
45	2.5	2.2	3.9	3.5	4.0	4.0	3.6	3.2	2.5	4.0	3.7	3.3	2.5	2.0	2.5	2.0	2.5	2.5	2.8	3.5	3.2	3.7	3.5	4.3	3.0	4.3

Appendix F (continued).

Pairs	Observers																									
	1	2	3	4	5	6	7	8	9	10	11	12	13	14	15	16	17	18	19	20	21	22	23	24	25	26
46	2.2	3.5	4.2	4.7	4.5	4.2	4.5	4.0	4.0	3.5	3.5	4.5	4.0	3.5	3.5	4.0	3.5	3.8	4.0	4.5	4.6	4.5	4.3	4.5	4.3	4.8
47	3.2	2.8	4.0	4.0	4.3	4.8	4.2	4.0	4.0	4.0	3.8	4.0	4.0	4.5	2.8	4.0	3.5	3.5	4.8	4.0	4.9	4.5	4.0	4.2	4.4	4.5
48	3.5	4.5	4.3	3.0	4.5	5.0	4.8	4.0	4.0	4.5	3.8	4.5	5.0	4.0	3.5	5.0	4.5	3.5	4.8	5.0	4.9	5.0	4.7	4.3	4.8	4.9
49	3.6	4.2	4.3	4.7	4.6	4.4	4.6	4.5	3.5	4.3	3.9	4.3	4.0	3.5	5.0	3.0	3.5	4.0	4.6	5.0	4.9	4.0	3.5	4.0	4.8	4.7
50	2.8	4.5	4.6	4.5	4.6	4.9	4.7	4.7	4.0	4.0	4.0	4.5	4.5	4.0	4.8	4.5	4.5	3.8	4.8	5.0	4.7	4.5	4.0	4.8	4.9	4.8
51	3.0	2.7	4.2	4.3	4.4	4.3	3.9	3.5	3.0	3.0	3.0	4.0	3.0	2.5	3.5	3.0	3.5	4.5	3.5	4.0	3.5	4.5	3.5	4.0	3.8	3.8
52	3.5	3.2	4.7	4.7	4.2	4.7	3.7	3.0	3.5	4.5	3.3	3.8	3.5	3.0	4.2	4.7	4.0	3.0	3.5	4.5	5.0	4.5	3.5	4.3	4.8	4.6
53	3.5	3.3	4.6	4.6	4.6	3.9	4.6	4.0	3.5	3.7	3.0	4.5	4.0	3.0	4.0	3.5	4.0	3.8	4.7	4.5	4.8	5.0	4.5	4.7	4.5	4.9
54	3.0	4.0	3.8	4.8	4.3	4.9	4.6	4.0	3.0	4.0	2.9	4.0	4.5	4.0	4.2	4.5	4.0	3.0	4.8	5.0	4.5	4.5	4.3	4.5	4.5	4.7
55	3.0	2.0	3.4	4.5	4.1	3.8	2.9	3.0	2.5	2.7	2.3	3.5	3.5	2.5	3.2	3.5	2.5	2.5	3.3	4.0	2.7	3.5	3.5	4.0	3.5	3.8
56	2.5	2.7	4.0	3.0	4.1	3.1	4.0	2.8	2.5	3.0	2.6	3.0	4.0	3.0	3.5	3.5	2.5	2.0	3.6	3.5	3.0	4.0	2.5	2.7	4.2	3.8
57	2.2	2.0	3.8	2.5	3.8	3.2	2.7	3.0	2.5	2.5	2.5	3.0	3.0	2.5	2.8	3.0	2.0	2.5	3.5	3.5	2.3	4.2	3.0	3.5	3.8	3.5
58	2.5	2.2	4.0	4.0	4.2	4.4	4.1	3.0	4.0	3.5	3.2	4.0	4.0	4.0	3.0	3.5	3.0	3.2	4.0	4.0	3.3	3.0	3.0	4.3	4.3	4.3
59	2.5	1.8	3.2	3.0	3.6	2.9	3.2	2.5	3.0	2.5	3.0	3.5	3.5	2.0	1.0	2.0	1.5	1.5	2.0	2.0	1.5	3.0	2.0	3.2	2.8	3.2
60	2.0	2.2	3.3	3.5	3.7	3.4	3.5	3.0	3.5	2.5	2.6	3.3	3.5	2.5	1.5	2.5	1.5	2.5	2.5	2.5	2.8	3.5	2.0	2.5	2.5	3.2
61	2.5	2.5	4.3	3.5	4.4	4.2	4.3	3.8	4.5	3.0	2.9	4.3	4.0	3.0	2.5	4.0	2.5	3.0	4.0	4.0	2.8	4.0	4.0	4.3	4.0	3.5
62	4.0	4.0	4.5	4.5	4.5	4.7	4.3	4.0	3.0	4.0	3.8	4.5	4.5	4.0	4.0	3.0	4.0	4.0	4.7	5.0	4.9	5.0	4.5	4.8	4.9	4.7
63	3.5	2.3	4.1	4.3	4.2	4.1	4.4	3.0	2.5	4.0	2.9	3.5	3.0	3.0	2.5	4.0	2.5	3.5	3.5	4.0	3.4	3.5	2.5	3.7	4.0	4.0
64	2.7	2.7	3.3	3.5	3.9	3.9	3.6	3.2	2.5	2.5	3.0	3.5	3.5	3.0	2.0	4.0	2.5	2.5	3.5	3.5	2.0	4.0	3.5	3.7	3.8	3.3
65	3.2	4.2	4.7	4.7	4.6	4.5	4.3	4.0	3.5	4.0	3.8	4.5	3.5	4.0	2.5	3.5	3.5	3.5	4.8	4.0	4.7	4.2	4.3	4.5	4.2	4.7
66	3.7	3.2	4.3	4.2	4.4	4.6	4.2	4.5	3.5	4.0	3.8	4.0	4.0	4.5	2.2	3.5	3.5	4.2	4.8	4.0	4.2	4.5	4.0	4.3	4.4	4.5